Further Assessment of the LET Theory

Mark Filipiak

Doctor of Philosophy

The University of Edinburgh

1992

Declaration

The work presented in this thesis is my own or was carried out in collaboration with Dr. W. D. McComb, except where otherwise stated. I have composed this thesis by myself.

A paper including some of the work presented in Chapter 2 has been submitted to the *Journal of Fluid Mechanics* [44].

Acknowledgements

Rosie comes first in any acknowledgements: she has supported and encouraged me throughout my PhD studies, especially during the writing of the thesis.

I acknowledge with thanks the sound advice and direction given by my supervisor, Dr. W.D. McComb. Dr. V. Shanmugasundaram wrote the programs for the LET calculations of the velocity field and the work in Chapters 2 and 4 is built on these solid foundations. He has always been very helpful with questions on numerics or programming. I would also like to thank Professor J.A. Domaradzki for providing unpublished results on energy transfer for comparison with LET (Chapter 4). Finally, life as a PhD student would have been rather dull without the *esprit de corps* generated by Bill Roberts and Alex Watt (and others).

I gratefully acknowledge the financial support of the SERC.

Abstract

This thesis extends and analyses the Local Energy Transfer (LET) approximation for turbulence. LET is a two-point two-time second moment closure for the Navier-Stokes equations, developed using renormalised perturbation theory in an Eulerian coordinate system. Analytical and numerical calculations of LET for the velocity field have been made in previous work.

This thesis consists of three parts

1. The LET approximation is extended to treat the transport of a passive scalar. The LET equations for passive scalar transport are derived and used in numerical calculations at a range of Reynolds and Prandtl numbers. The evolution in time of the scalar energy, dissipation and transfer spectra is calculated, and these spectra are shown to become self-similar under convective or Kolmogorov scaling. The scalar energy, dissipation and transfer spectra at $R_\lambda \sim 40$ compare well with experiment. The two-time scalar correlation is calculated and the relevant scaling for the time separation is shown to be convective at small Reynolds number and Kolmogorov (i.e. inertial) at large Reynolds number. The effect of the ratio of the velocity energy spectrum peak wavenumber to the scalar energy peak wavenumber on the thermal to mechanical time-scale ratio is compared with experiment. At large Reynolds number the scalar energy spectrum is shown to have a $k^{-5/3}$ inertial-convective range at $Pr = 0.5$, with a value of 1.13 for the Obukhov-Corrsin constant β. The scalar energy balance is calculated at several Reynolds numbers and at large Reynolds number shows a clear separation in wavenumber of the production (in fact the energy peak in decaying turbulence) and dissipation ranges. The dependence of the velocity-scalar cross derivative skewness on the Reynolds and Prandtl numbers is compared with direct numerical simulation and experiment. The magnitude and the Reynolds number dependence of the skewness is in fair agreement with the simulation, but the Prandtl number dependence is reversed.

2. The Galilean transformation properties of the Navier-Stokes equations, velocity moment equations, perturbation expansion and LET are investigated.

The perturbation expansion (used to derive LET) is shown to be invariant under a Galilean transformation, term by term, thus any truncation well be Galilean invariant. The LET equations are also shown to be Galilean invariant. The concept of Random Galilean Transformation (RGT) is analysed. The RGT was developed by Kraichnan to model the convective effects of the large scales in turbulence. Invariance under a RGT is violated by Eulerian renormalised perturbation theories—this led to the development of quasi-Lagrangian theories. The RGT is shown to be a change of ensemble rather than a symmetry transformation. This change of ensemble makes the derivation of an Eulerian renormalised perturbation theory impossible as the zero-order solution is no longer Gaussian and the zero-order propagator/response function becomes a random variable.

3. The details of the energy transfer in low Reynolds number ($R_\lambda = 14$) turbulence have recently been investigated using a direct numerical simulation. LET is compared with these results, using the same numerical conditions. The agreement between LET and the simulation is very good. The main conclusion is that (at least at low Reynolds number) energy transfer is local in wavenumber but arises from non-local triads of modes, with one mode near the peak of the energy spectrum.

Contents

Chapter 1

Introduction

Turbulent flow is characterised by random variation in time and space of the velocity, making deterministic calculations impossible—a statistical approach is required. Less apparent is the existence of strong dissipation in turbulence, mediated by the transfer of energy from large to small scales where there is strong viscous dissipation. The energy transfer is due to non-linear mixing of modes and leads to excited modes over a continuum of length and time scales. The flow of energy from large to small scales arises because energy is being supplied at large scales by the driving forces and is being dissipated at small scales.

Thus the turbulence problem requires statistical methods for its (approximate) solution. For incompressible flow these approximations are based on the Navier-Stokes equations for the velocity field and generally provide information on averaged quantities, such as the turbulent energy.

1.1 The Local Energy Transfer (LET) approximation for turbulence

The Local Energy Transfer (LET) approximation [42] is a two-point, two-time closure for the Navier-Stokes equations, and calculates double moments (e.g. the kinetic energy) for turbulent flows. Results for LET calculations of the velocity field give good agreement with experiment [45, 46]. LET is derived in an Eulerian coordinate system but, unlike the Direct Interaction Approximation [27], it

gives the experimentally verified Kolmogorov energy spectrum (in wavenumber) at large Reynolds number.

1.2 Turbulent flows and statistical methods

LET models turbulence for an incompressible fluid. The basic equations for the flow of an incompressible, Newtonian fluid are the Navier-Stokes equations, the balance of momentum equation

$$\frac{\partial \mathbf{U}(\mathbf{x},t)}{\partial t} + \mathbf{U}.\nabla\mathbf{U}(\mathbf{x},t) = -\frac{1}{\rho}\nabla P(\mathbf{x},t) + \frac{1}{\rho}\mathbf{F}(\mathbf{x},t) - \nu\nabla^2\mathbf{U}(\mathbf{x},t) \quad (1.1)$$

and the incompressibility condition

$$\nabla.\mathbf{U}(\mathbf{x},t) = 0; \quad (1.2)$$

(see e.g. [5]). The LHS of Equation 1.1 is the material derivative of the velocity and on the RHS are the viscous damping and pressure and body forces. For a sufficiently large ratio of inertial effects (the convective derivative $\mathbf{U}.\nabla\mathbf{U}(\mathbf{x},t)$ and the pressure gradient $\frac{1}{\rho}\nabla P(\mathbf{x},t)$) to viscous effects, we find that the flow is turbulent, with random variation of velocity in time and space. More precisely, the velocity field is excited over a continuum of length and time scales, from the large scales of external forcing to the smallest scales where viscous decay will dominate, and there is a 'flow' of energy from large scales to small scales. The large range of scales arises because of the mode mixing caused by the non-linear terms $\mathbf{U}.\nabla\mathbf{U}(\mathbf{x},t)$ and $\frac{1}{\rho}\nabla P(\mathbf{x},t)$ (the incompressibility constraint relates the pressure gradient to the convective derivative).

The existence of random variations indicates the need for statistical methods, with turbulence treated as a fluctuation about the mean flow. Writing the velocity $\mathbf{U}(\mathbf{x},t)$ as the sum of a mean $\overline{\mathbf{U}}(\mathbf{x},t)$ and a fluctuation $\mathbf{u}(\mathbf{x},t)$

$$\mathbf{U}(\mathbf{x},t) = \overline{\mathbf{U}}(\mathbf{x},t) + \mathbf{u}(\mathbf{x},t) \quad (1.3)$$

and then averaging Equation 1.1, we get the equation for the average velocity

$$\begin{aligned}
&\frac{\partial \overline{U}_\alpha(\mathbf{x},t)}{\partial t} + \overline{U}_\beta \frac{\partial}{\partial x_\beta}\overline{U}_\alpha(\mathbf{x},t) + \frac{\partial}{\partial x_\beta}\langle u_\alpha(\mathbf{x},t)u_\beta(\mathbf{x},t)\rangle \\
&= -\frac{1}{\rho}\frac{\partial}{\partial x_\alpha}\overline{P}(\mathbf{x},t) + \frac{1}{\rho}\overline{F}(\mathbf{x},t) - \nu\frac{\partial^2}{\partial x_\beta \partial x_\beta}\overline{U}_\alpha(\mathbf{x},t),
\end{aligned} \tag{1.4}$$

where $\langle\rangle$ denotes averaging. We have used the incompressibility condition to write $\mathbf{U}.\nabla\mathbf{U}$ as $\nabla.(\mathbf{UU})$ and have used suffix notation to clarify the form of $\nabla.(\mathbf{uu})$. This has the same form as the Navier-Stokes momentum equation, for averaged quantities, with the addition of an extra term $\partial/\partial x_\beta\langle u_\alpha(\mathbf{x},t)u_\beta(\mathbf{x},t)\rangle$. The quantity $\langle u_\alpha(\mathbf{x},t)u_\beta(\mathbf{x},t)\rangle$ is called the Reynolds stress and couples the fluctuations to the averaged quantities. The Reynolds stress is effectively the quantity that is modelled (directly or indirectly) by any approximation for turbulence.

Subtracting Equation 1.4 from Equation 1.1 gives us the equation for the fluctuating velocity $\mathbf{u}(\mathbf{x},t)$

$$\begin{aligned}
&\frac{\partial u_\alpha(\mathbf{x},t)}{\partial t} + \frac{\partial}{\partial x_\beta}\overline{U}_\alpha(\mathbf{x},t)u_\beta(\mathbf{x},t) + \frac{\partial}{\partial x_\beta}u_\alpha(\mathbf{x},t)\overline{U}_\beta(\mathbf{x},t) \\
&+\frac{\partial}{\partial x_\beta}u_\alpha(\mathbf{x},t)u_\beta(\mathbf{x},t) - \frac{\partial}{\partial x_\beta}\langle u_\alpha(\mathbf{x},t)u_\beta(\mathbf{x},t)\rangle \\
&= -\frac{1}{\rho}\frac{\partial}{\partial x_\alpha}p(\mathbf{x},t) + \frac{1}{\rho}f_\alpha(\mathbf{x},t) - \nu\frac{\partial^2}{\partial x_\beta \partial x_\beta}u_\alpha(\mathbf{x},t),
\end{aligned} \tag{1.5}$$

where p and $\mathbf{f}$ are the fluctuating pressure and velocity. We can multiply this by $\mathbf{u}(\mathbf{x}',t')$ and average to get the equation for the two-point, two-time correlation:

$$\begin{aligned}
&\frac{\partial\langle u_\alpha(\mathbf{x},t)u_\delta(\mathbf{x}',t')\rangle}{\partial t} + \frac{\partial}{\partial x_\beta}\langle u_\alpha(\mathbf{x},t)u_\beta(\mathbf{x},t)u_\delta(\mathbf{x}',t')\rangle \\
&+\frac{\partial}{\partial x_\beta}\overline{U}_\alpha(\mathbf{x},t)\langle u_\beta(\mathbf{x},t)u_\delta(\mathbf{x}',t')\rangle + \frac{\partial}{\partial x_\beta}\overline{U}_\beta(\mathbf{x},t)\langle u_\alpha(\mathbf{x},t)u_\delta(\mathbf{x}',t')\rangle \\
&= -\frac{1}{\rho}\frac{\partial}{\partial x_\alpha}\langle p(\mathbf{x},t)u_\delta(\mathbf{x}',t')\rangle + \frac{1}{\rho}\langle f_\alpha(\mathbf{x},t)u_\delta(\mathbf{x}',t')\rangle \\
&\quad -\nu\frac{\partial^2}{\partial x_\beta \partial x_\beta}\langle u_\alpha(\mathbf{x},t)u_\delta(\mathbf{x}',t')\rangle,
\end{aligned} \tag{1.6}$$

or (taking care with the time derivative) by $\mathbf{u}(\mathbf{x},t)$ to get the single-point, single-time correlation.

The approximations for the Reynolds stress can be divided into two types. Engineering problems require solutions for mean velocities in complicated flows and result in direct models for the Reynolds stress (e.g. mixing length theories, eddy viscosities) or approximate equations for the single-point, single-time moments (e.g. $k-\epsilon$ models). The models all require some parameters to be determined empirically. See [21, 43] for more details of this approach. The more fundamental approach is to approximate Equation 1.6, which relates $\langle \mathbf{uu} \rangle$ to $\langle \mathbf{uuu} \rangle$, with no empirical constants. We can get an equation for $\langle \mathbf{uuu} \rangle$ by multiplying Equation 1.4 by $\mathbf{uu}$ and averaging—this leads to an equation for $\langle \mathbf{uuu} \rangle$ in terms of $\langle \mathbf{uuuu} \rangle$. We can continue this process for higher moments, but we will always get an equation for the nth moment in terms of the $n+1$th moment—this is the moment closure problem. Most, if not all, of the approximations for turbulence close this hierarchy of moment equations by approximating the triple moment $\langle \mathbf{uuu} \rangle$ as some function of the double moments $\langle \mathbf{uu} \rangle$.

The LET theory [42] is of the 'fundamental approach' type and is in the class of Eulerian renormalised perturbation theories, developed in the late 1950's and early 1960's by Kraichnan, Edwards, Herring and others (see [43] for a discussion of these theories). Renormalised perturbation theories have generally studied the simplest possible flows in order to concentrate on the turbulence problem itself, rather than any complications of flow geometry. Thus they deal with homogeneous, isotropic flows, with zero mean velocity and are developed in wavenumber space. The Navier-Stokes equations in wavenumber space are

$$\left(\frac{\partial}{\partial t}+\nu k^2\right) u_\alpha(\mathbf{k},t) \;=\; M_{\alpha\beta\gamma}(\mathbf{k}) \int d^3j\, u_\beta(\mathbf{k}-\mathbf{j},t) u_\gamma(\mathbf{j},t) + f_\alpha(\mathbf{k},t) \quad (1.7)$$

and

$$k_\alpha u_\alpha(\mathbf{k},t) \;=\; 0, \quad (1.8)$$

where

$$M_{\alpha\beta\gamma}(\mathbf{k}) \;=\; (1/2i)\left[k_\beta D_{\alpha\gamma}(\mathbf{k}) + k_\gamma D_{\alpha\beta}(\mathbf{k})\right] \quad (1.9)$$

and the projection operator $D_{\alpha\beta}(\mathbf{k})$ is

$$D_{\alpha\beta}(\mathbf{k}) = \delta_{\alpha\beta} - \frac{k_\alpha k_\beta}{k^2} \tag{1.10}$$

and we write $\mathbf{u}$ for $\mathbf{U}$ since the mean velocity is taken to be zero. These equations are the Fourier transforms of Equations 1.1 and 1.2, with the pressure term eliminated by using the incompressibility constraint. (For the derivation of these equations from the Navier-Stokes $\mathbf{x}$-space equations and for general reference, see [43]). The 2nd moment equation is now

$$\begin{aligned}&\left(\frac{\partial}{\partial t} + \nu k^2\right) \langle u_\alpha(\mathbf{k},t) u_\delta(\mathbf{k}',t')\rangle \\ &= M_{\alpha\beta\gamma}(\mathbf{k}) \int d^3j \, \langle u_\beta(\mathbf{k}-\mathbf{j},t) u_\gamma(\mathbf{j},t) u_\delta(\mathbf{k}',t')\rangle + f_\alpha(\mathbf{k},t).\end{aligned} \tag{1.11}$$

The basic method is to treat the non-linear term on the RHS of Equation 1.7 as a perturbation and expand the velocity field about the zero order solution. The RHS of Equations 1.7 and 1.11 are similarly expanded in terms of $\mathbf{u}^{(0)}$ and $H^{(0)}$. Of course, such expansions are effectively in powers of the Reynolds number, which is large, and thus the series will be divergent. However, we will see later that by renormalising the expansion we can (perhaps) remove the divergence.

The zero order velocity $u_\alpha^{(0)}(\mathbf{k},t)$ is given by

$$\begin{aligned}u_\alpha^{(0)}(\mathbf{k},t) &= \left(\frac{\partial}{\partial t} + \nu k^2\right)^{-1} f_\alpha(\mathbf{k},t) \\ &= H^{(0)}(\mathbf{k},t) f_\alpha(\mathbf{k},t),\end{aligned} \tag{1.12}$$

defining the zero order (viscous) propagator $H^{(0)}(\mathbf{k},t)$. We assume that the forcing has a Gaussian probability distribution, thus the zero order fields are Gaussian. This assumption is required to enable us to factor the zero order velocity moments and is valid since the non-linear terms will introduce the required non-Gaussianity.

The next step is to postulate that the effect of the non-linear terms can be described by an effective propagator, corresponding to the renormalisation of $H^{(0)}$ (the renormalisation of $\langle \mathbf{u}^{(0)}\mathbf{u}^{(0)}\rangle$ is $\langle \mathbf{uu}\rangle$). It is possible to show [37, 43, 60] that

the expanded RHS of the $\langle \mathbf{uu} \rangle$ equation can be re-ordered and then partially summed into a series of terms containing the renormalised propagator H and $\langle \mathbf{uu} \rangle$ only. This expansion (which has unknown convergence properties) is then truncated at the lowest non-trivial term to form the particular approximation.

There are differences between various approximations due to different choices of definitions of $H^{(0)}$ (the Direct Interaction Approximation (DIA) and LET) and some theories (Edwards-Fokker-Planck and Self Consistent Field) have a very different approach but retain the concept of the renormalisation of the propagator by the non-linear term. Questions about the validity of the DIA theory led to the development of a quasi-Lagrangian approximation (LHDIA) which is a renormalised perturbation theory developed in mixed Eulerian-Lagrangian coordinates. See [43] for more details of these theories.

In the following chapters the LET theory is extended and analysed. In Chapter 2 LET is extended to treat the convection of a passive scalar. Chapter 3 deals with the problem of non-invariance of Eulerian renormalised perturbation theories under Random Galilean Transformations. Finally, in Chapter 4 the detailed energy dynamics of LET are investigated.

Chapter 2

Passive Scalar Transport

2.1 Introduction

Previous work using similar closures is discussed, then the LET equations for scalar transport are derived. The conversions required from the velocity code are described, including a discussion of the numerical differences between two formally equivalent schemes. Computational results (time evolution of integral parameters, wavenumber spectra, normalised spectra, two-time correlations) for a range of Reynolds and Prandtl numbers are plotted, analysed and compared with direct numerical simulations and experiments.

2.2 Background

Fluid flows can transport scalar quantities, e.g. temperature, salinity, dye concentration. In general, these scalars have an effect on the flow—in a gravitational field temperature or salinity differences give rise to buoyancy effects because of the associated density differences. In addition the scalars may be reacting. However, the simplest case to treat is that of a passive scalar which is convected by the flow but has no effect on the flow. In this case the conservation equation which describes the time evolution of the scalar only has terms corresponding to

molecular diffusion and the convective transport by the flow. This equation is

$$\frac{\partial\theta(\mathbf{x},t)}{\partial t}+\left(u_\beta(\mathbf{x},t)\frac{\partial}{\partial x_\beta}\right)\theta(\mathbf{x},t) \;=\; \kappa\nabla^2\theta(\mathbf{x},t)+\chi(\mathbf{x},t), \qquad (2.1)$$

where θ is the passive scalar density, u is the total velocity, κ is the scalar diffusivity (for temperature this is conductivity divided by fluid mass density) and χ is any applied source of the scalar θ. The LHS of Equation (2.1) is the material derivative of the scalar field. The similarity parameters for scalar transport are the Reynolds number and the Prandtl (temperature) or Schmidt (concentration) number, $Pr=\nu/\kappa$. Since we are going to deal with initial value problems only, with some initial distribution of θ and no sources, we can ignore the χ term. Since LET is formulated most easily in wavenumber space, Equation (2.1) is Fourier transformed to

$$\frac{\partial\theta(\mathbf{k},t)}{\partial t}+ik_\beta\int d^3j\, u_\beta(\mathbf{k}-\mathbf{j},t)\theta(\mathbf{j},t) \;=\; -\kappa k^2\theta(\mathbf{k},t). \qquad (2.2)$$

Rearranging Equation (2.2) gives

$$\left(\frac{\partial}{\partial t}+\kappa k^2\right)\theta(\mathbf{k},t). \;=\; -ik_\beta\int d^3j\, u_\beta(\mathbf{k}-\mathbf{j},t)\theta(\mathbf{j},t) \qquad (2.3)$$

and this will be the basis for the LET theory.

The scalar transport equation is linear in θ but its solution requires knowledge of the velocity field and, since the velocity field in turbulent flow is excited on many scales, the treatment of many wavenumber modes. These two requirements make the use of statistical methods necessary for the theoretical calculation of scalar transport by turbulent flows. Statistical methods can be divided into closures, and mode elimination methods using renormalisation group methods. Second order closures approximate the convective term in the scalar energy or two-time correlation equations derived from Equation (2.3) in order to get an equation in terms of these second order moments only. The closures that have the most 'fundamental' character are the renormalised perturbation theories, described in Chapter 1. Various RPTs have been extended to scalar transport.

The DIA family (DIA, LHDIA, ALHDIA, SBLHDIA) have all been formulated for scalar transport and some calculations have been performed. DIA was formally extended to scalar transport by Kraichnan [29] and was applied to diffusion by Roberts [52]. A comparison of scalar DIA and a direct numerical simulation was carried out by Herring and Kerr (see below) [18], with DIA giving qualitatively good results at $R_\lambda \approx 6$, and DIA for the scalar with the velocity field energy spectrum and correlations specified has been calculated by Lee [36]. The LHDIA and ALHDIA closures have been applied to a scalar by Kraichnan [33, 32]. The analytic results give the various power law ranges (see below) and the numerical calculations give qualitatively good results but at high R_λ the values of the Obukhov-Corrsin constant is 0.2 compared with the experimental value of 0.67 and the eddy Prandtl number is 0.1 compared with 0.7 to 0.8.

TFM for passive scalar transport has been developed by Newman and Herring [48]. It has been compared to a direct numerical simulation at low Reynolds number in Herring and Kerr [18] but gives poorer results (Θ spectrum and velocity-scalar skewness $S_{u\theta}$) than DIA. It has been used at high Reynolds number by Larcheveque *et al.* [35] and Herring *et al.* [19] and gives (with suitable adjustment of its free parameters) good quantitative agreement with experiment. In the same papers the EDQNM closure was tested at high Reynolds number and also gave good agreement with experiment. Finally, Kaneda [22] has done analytic calculations using his LRA closure to get a value of 0.34 for the Obukhov-Corrsin constant.

In the subsequent sections of this chapter the LET theory is extended to treat scalar transport, at variety of Reynolds numbers and Prandtl numbers.

The LET results can be compared with a wide range of experimental and full numerical simulation data. At low to medium Reynolds number there are several experiments, giving scalar energy, dissipation and transfer spectra, two-time correlations for the scalar, and scalar energy decay. Yeh and van Atta [61] have performed measurements on grid generated turbulence with a heated grid to generate temperature fluctuations at $R_\lambda = 35$ (grid Reynolds number 10500) and give details of the scalar energy, dissipation and transfer spectra and

scalar energy decay. Lin and Lin [40] have performed similar experiments with higher overheats at $R_\lambda = 150$. Warhaft and Lumley [58] use a separate grid to generate the temperature fluctuations at $R_\lambda = 45$ (grid Reynolds number 10000) and measure the scalar energy and dissipation spectra and scalar energy decay, producing more consistent results for the decay exponents than Yeh and van Atta or Lin and Lin. Sreenivasan *et al.* [57] extended Warhaft and Lumley's work. Sepri [53] has also measured two-point and two-time Θ correlations in grid generated turbulence at $R_\lambda = 35$.

At high Reynolds number, there have been many experiments: temperature and humidity fluctuations in air [1, 2, 7, 8, 51, 59] and temperature and salinity fluctuations in water [13, 14, 15].

At high Reynolds number, for $Pr \sim 1$, Kolmogorov's dimensional analysis can be extended to scalar transport [4, 6]. Then the scalar energy spectrum can be normalised by the Kolmogorov scales $k_d \equiv (\epsilon/\nu^3)^{1/4}$ and $\theta_d \equiv \epsilon_\theta(\nu^5/\epsilon^3)^{1/4}$, and there will be a range of wavenumbers, the inertial-convective range, where the effects of viscosity and conductivity are negligible and the scalar energy E_θ takes the form

$$E_\theta(k) = \beta\epsilon_\theta\epsilon^{-1/3}k^{-5/3}, \tag{2.4}$$

where ϵ is the velocity dissipation and ϵ_θ is the scalar dissipation, and β is the Obukhov-Corrsin constant. The inertial-convective range is k such that $k_\theta \ll k \ll k_d$, where k_θ is the wavenumber characterising the θ-energy containing scales.

At very low Prandtl number Obukhov-Corrsin scaling [4, 6] must be used as well, with scales $k_{O-C} \equiv (\epsilon/\kappa^3)^{1/4}$ and $\Theta_{O-C} \equiv \epsilon_\theta(\kappa^5/\epsilon^3)^{1/4}$. In this case there will be an inertial-convective range below k_{O-C} and, according to Batchelor, Howells and Townsend, an inertial diffusive range between k_{O-C} and k_d with scalar energy spectrum

$$E_\theta(k) = (1/3)\alpha\epsilon_\theta\kappa^{-3}\epsilon^{2/3}k^{-17/3}, \tag{2.5}$$

where α is the Kolmogorov constant. Gibson [12] predicts that Equation (2.5)

will be valid only between k_B (see below) and k_d and that between k_{O-C} and k_B the scalar energy spectrum will be proportional to k^{-3}. At very high Prandtl number Batchelor scaling [4, 6] must be used, with scales $k_B \equiv (\epsilon/\nu\kappa^2)^{1/4}$ and $\theta_B \equiv \epsilon_\theta((\nu\kappa^2)^{5/3}/\epsilon^3)^{1/4}$. Then there is the usual inertial-convective range below k_d and a viscous-convective range between k_d and k_B with $E_\theta(k)$ proportional to k^{-1}. For all values of the Prandtl number the dissipation range, where both viscosity and scalar diffusion dominate, is generally expected to have $E_\theta(k)$ decaying exponentially with k. Gibson [12] predicts that in the dissipation range Batchelor scaling will hold at all Prandtl numbers—scalar dissipation scaled by $\epsilon_\theta(\nu/\epsilon)^{1/2}k_B$ will be independent of Prandtl number.

The $k^{-5/3}$ inertial-convective range has been observed in all of the high Reynolds number experiments cited above, with a best estimate for β of 0.67–0.83 and the k^{-1} viscous-convective range has been observed by Gibson and Schwarz [13] and Grant *et al.* [15]

Complementing the experimental data direct numerical simulations of scalar transport have been performed by Herring and Kerr [18], Kerr [23, 24, 25], Eswaran and Pope [11] and Shirani, Ferziger and Reynolds [56], in which the Navier-Stokes equations and the scalar transport equations are solved numerically. The Reynolds numbers are low to medium, rising to $R_\lambda = 83$ in Kerr [25] where a small inertial range is seen, but the advantage of numerical simulations over experiments is that higher order moments, including the scalar-velocity derivative skewness, can be 'measured'.

2.3 The LET equations

In this section we derive in detail the LET equations for the velocity and scalar fields.

The basic equations are the solenoidal Navier-Stokes equations and the scalar transport equations, for decaying turbulence (i.e. no forcing terms) in wavenum-

ber space,

$$\left(\frac{\partial}{\partial t}+\nu k^2\right) u_\alpha(\mathbf{k},t) \;=\; M_{\alpha\beta\gamma}(\mathbf{k}) \int d^3j\, u_\beta(\mathbf{k}-\mathbf{j},t) u_\gamma(\mathbf{j},t) \tag{2.6}$$

and

$$\left(\frac{\partial}{\partial t}+\kappa k^2\right) \theta(\mathbf{k},t) \;=\; -ik_\beta \int d^3j\, u_\beta(\mathbf{k}-\mathbf{j},t)\theta(\mathbf{j},t), \tag{2.7}$$

where

$$M_{\alpha\beta\gamma}(\mathbf{k}) \;=\; (1/2i)\left[k_\beta D_{\alpha\gamma}(\mathbf{k}) + k_\gamma D_{\alpha\beta}(\mathbf{k})\right] \tag{2.8}$$

and the projection operator $D_{\alpha\beta}(\mathbf{k})$ is

$$D_{\alpha\beta}(\mathbf{k}) \;=\; \delta_{\alpha\beta} - \frac{k_\alpha k_\beta}{k^2}. \tag{2.9}$$

These equations are supplemented by the values of the velocity and scalar fields at some initial time t_0. (For the derivation of these equations from the Navier-Stokes equations and for general reference, see [43]). The LET theory is a closure for the velocity and scalar fluctuations about a mean rather than for the mean values themselves and approximates the equations for the two-time, two-point moments $\langle u_\alpha(\mathbf{k},t) u_\beta(\mathbf{k}',t')\rangle$ and $\langle \theta(\mathbf{k},t)\theta(\mathbf{k}',t')\rangle$ The problem of the diffusion of a scalar could be treated by LET, as it has been by DIA [52], but the present work deals exclusively with the scalar fluctuations, which are important for flux estimation [8].

Without loss of generality, we assume the means are zero in order to simplify the treatment. So

$$\langle \mathbf{u}(\mathbf{k},t)\rangle \;=\; \mathbf{0}, \tag{2.10}$$

$$\langle \theta(\mathbf{k},t)\rangle \;=\; 0, \tag{2.11}$$

where $\langle\rangle$ denotes an ensemble average and the u and θ are now the fluctuating quantities. The equations for the two-time moments of the velocity and scalar

are formed by multiplying Equations (2.6) and (2.7) by $\mathbf{u}(\mathbf{k}',t')$ or $\theta(\mathbf{k}',t')$ and then averaging:

$$\left(\frac{\partial}{\partial t}+\nu k^2\right)\langle u_\alpha(\mathbf{k},t)u_\delta(\mathbf{k}',t')\rangle = M_{\alpha\beta\gamma}(\mathbf{k})\int d^3j\,\langle u_\beta(\mathbf{k}-\mathbf{j},t)u_\gamma(\mathbf{j},t)u_\delta(\mathbf{k}',t')\rangle, \quad (2.12)$$

$$\left(\frac{\partial}{\partial t}+\kappa k^2\right)\langle \theta(\mathbf{k},t)u_\delta(\mathbf{k}',t')\rangle = -ik_\beta\int d^3j\,\langle u_\beta(\mathbf{k}-\mathbf{j},t)\theta(\mathbf{j},t)u_\delta(\mathbf{k}',t')\rangle, \quad (2.13)$$

$$\left(\frac{\partial}{\partial t}+\nu k^2\right)\langle u_\alpha(\mathbf{k},t)\theta(\mathbf{k}',t')\rangle = M_{\alpha\beta\gamma}(\mathbf{k})\int d^3j\,\langle u_\beta(\mathbf{k}-\mathbf{j},t)u_\gamma(\mathbf{j},t)\theta(\mathbf{k}',t')\rangle, \quad (2.14)$$

$$\left(\frac{\partial}{\partial t}+\kappa k^2\right)\langle \theta(\mathbf{k},t)\theta(\mathbf{k}',t')\rangle = -ik_\beta\int d^3j\,\langle u_\beta(\mathbf{k}-\mathbf{j},t)\theta(\mathbf{j},t)\theta(\mathbf{k}',t')\rangle. \quad (2.15)$$

The energy equation (strictly $1/4\pi\times$ the energy equation) is formed by multiplying Equation (2.6) by $\mathbf{u}(\mathbf{k}',t)$, multiplying Equation (2.6) for $(\mathbf{k}',t)$ by $\mathbf{u}(\mathbf{k},t)$, adding the resulting equations together, using

$$\frac{\partial}{\partial t}[u_\alpha(\mathbf{k},t)u_\delta(\mathbf{k}',t)] = u_\alpha(\mathbf{k},t)\frac{\partial}{\partial t}u_\delta(\mathbf{k}',t)+[\frac{\partial}{\partial t}u_\alpha(\mathbf{k},t)]u_\delta(\mathbf{k}',t) \quad (2.16)$$

and finally averaging to get

$$\left(\frac{\partial}{\partial t}+2\nu k^2\right)\langle u_\alpha(\mathbf{k},t)u_\delta(\mathbf{k}',t)\rangle = M_{\alpha\beta\gamma}(\mathbf{k})\int d^3j\,\langle u_\beta(\mathbf{k}-\mathbf{j},t)u_\gamma(\mathbf{j},t)u_\delta(\mathbf{k}',t)\rangle + M_{\delta\beta\gamma}(\mathbf{k}')\int d^3j\,\langle u_\beta(\mathbf{k}'-\mathbf{j},t)u_\gamma(\mathbf{j},t)u_\alpha(\mathbf{k},t)\rangle. \quad (2.17)$$

The θ single-time moment equation is formed similarly:

$$\left(\frac{\partial}{\partial t} + 2\kappa k^2\right) \langle \theta(\mathbf{k},t)\theta(\mathbf{k}',t)\rangle$$
$$= -ik_\beta \int d^3j \, \langle u_\beta(\mathbf{k}-\mathbf{j},t)\theta(\mathbf{j},t)\theta(\mathbf{k}',t)\rangle$$
$$-ik'_\beta \int d^3j \, \langle u_\beta(\mathbf{k}'-\mathbf{j},t)\theta(\mathbf{j},t)\theta(\mathbf{k},t)\rangle. \qquad (2.18)$$

All of these equations relate the rate of change of double moments to an integral of triple moments and the object of any second order (moment) closure, LET, DIA, whatever, is to approximate the triple moment by some product of the double moments to get a closed set of equations.

The basic postulate of LET for the velocity field has been stated in Chapter 1, and is that the time evolution of the two-time moments can be described by a simple propagator, the renormalised equivalent of the zero order (viscous) propagator $(\partial/\partial t + \nu k^2)^{-1}$. Assuming a homogeneous flow we have

$$\langle u_\alpha(\mathbf{k},t)u_\beta(\mathbf{k}',t')\rangle = Q_{\alpha\beta}(\mathbf{k};t,t')\delta^3(\mathbf{k}+\mathbf{k}'), \qquad (2.19)$$

which defines Q—the two-time moment, and the LET postulate is that

$$Q_{\alpha\beta}(\mathbf{k};t,t') = H_{\alpha\gamma}(\mathbf{k};t,t')Q_{\gamma\beta}(\mathbf{k};t',t'). \qquad (2.20)$$

H is the renormalised propagator derived in the renormalised perturbation theory (see below) and Equation (2.20) can be regarded as a type of fluctuation-dissipation theorem. Alternatively, and more pragmatically, Equation (2.20) can be regarded as the definition of H.

The corresponding postulate for the scalar field is that

$$\Theta(\mathbf{k};t,t') = H^{\theta\theta}(\mathbf{k};t,t')\Theta(\mathbf{k};t',t'), \qquad (2.21)$$

where

$$\langle \theta(\mathbf{k},t)\theta(\mathbf{k}',t')\rangle = \Theta(\mathbf{k};t,t')\delta^3(\mathbf{k}+\mathbf{k}'). \qquad (2.22)$$

In isotropic flow (the only flow we will treat) the correlation function Q and the propagator H can be specified as follows:

$$Q_{\alpha\beta}(\mathbf{k};t,t') = D_{\alpha\beta}(\mathbf{k})Q(k;t,t'), \tag{2.23}$$

$$H_{\alpha\beta}(\mathbf{k};t,t') = D_{\alpha\beta}(\mathbf{k})H(k;t,t'), \tag{2.24}$$

$$\Theta(\mathbf{k};t,t') = \Theta(k;t,t'), \tag{2.25}$$

$$H^{\theta\theta}(\mathbf{k};t,t') = H^{\theta\theta}(k;t,t'). \tag{2.26}$$

The LET postulates become

$$Q(k;t,t') = H(k;t,t')Q(k;t',t') \tag{2.27}$$

and

$$\Theta(k;t,t') = H^{\theta\theta}(k;t,t')\Theta(k;t',t'). \tag{2.28}$$

The cross moments and propagators also have to be considered. $H^{u\theta}$ must be zero since the scalar is passive, i.e. it has no effect on the velocity field. $H^{\theta u}$ is obviously zero when there is no scalar field, otherwise it could create scalar fluctuations, but it could be non-zero when there is a scalar field since a fluctuation in velocity can cause a fluctuation in the scalar field. Thus $H^{\theta u}$ would measure in some way the direct effect of the velocity field on the scalar field. However, $H^{\theta\theta}$ will depend on the velocity field and thus the velocity field will affect the scalar field indirectly through this propagator. In any case, we will sidestep these issues since we treat homogeneous isotropic incompressible turbulence only, where $H^{\theta u}_{\beta}(\mathbf{k};t,t') \sim k_\beta$ from symmetry considerations and thus $H^{\theta u}_{\beta}(\mathbf{k};t,t')Q_{\beta\gamma}(\mathbf{k};t',t') \sim k_\beta D_{\beta\gamma}(\mathbf{k}) = 0$ since, in isotropic incompressible flow, $Q_{\beta\gamma}(\mathbf{k};t,t') = D_{\beta\gamma}(\mathbf{k})Q(k;t,t')$. We similarly avoid deriving an LET closure for $Q^{\theta u}$ and $Q^{u\theta}$ by treating homogeneous isotropic incompressible turbulence where $Q^{\theta u}$ and $Q^{u\theta}$ are zero from symmetry and incompressibility.

We now derive the LET equations for the velocity and scalar fields. We expand the Navier-Stokes and the scalar transport equations in parallel.

In the Navier-Stokes equation we multiply the non-linear term by an expansion parameter λ_u and in the scalar transport equation we multiply the convection term by the expansion parameter λ_θ. The velocity and scalar fields are then expanded in powers of the relevant expansion parameter. Both expansion parameters will be set to 1 eventually. Thus we have

$$\left(\frac{\partial}{\partial t}+\nu k^2\right) u_\alpha(\mathbf{k},t) = \lambda_u M_{\alpha\beta\gamma}(\mathbf{k}) \int d^3j\, u_\beta(\mathbf{k}-\mathbf{j},t) u_\gamma(\mathbf{j},t), \quad (2.29)$$

$$\left(\frac{\partial}{\partial t}+\kappa k^2\right) \theta(\mathbf{k},t) = -i\lambda_\theta k_\beta \int d^3j\, u_\beta(\mathbf{k}-\mathbf{j},t)\theta(\mathbf{j},t), \quad (2.30)$$

and

$$\mathbf{u}(\mathbf{k},t) = \mathbf{u}^{(0)}(\mathbf{k},t)+\lambda_u \mathbf{u}^{(1)}(\mathbf{k},t)+\lambda_u^2\mathbf{u}^{(2)}(\mathbf{k},t)+\ldots, \quad (2.31)$$

$$\theta(\mathbf{k},t) = \theta^{(0)}(\mathbf{k},t)+\lambda_\theta \theta^{(1)}(\mathbf{k},t)+\lambda_\theta^2\theta^{(2)}(\mathbf{k},t)+\ldots \quad (2.32)$$

Now substitute the expansions for the exact velocity and scalar fields in Equations (2.29) and (2.30) and equate powers of the expansion parameters, taking $\lambda_u \equiv \lambda_\theta$:

$$\begin{aligned}
&\left(\frac{\partial}{\partial t}+\nu k^2\right)\left[u_\alpha^{(0)}(\mathbf{k},t)+\lambda_u u_\alpha^{(1)}(\mathbf{k},t)+\lambda_u^2 u_\alpha^{(2)}(\mathbf{k},t)+\ldots\right] \\
&= \lambda_u M_{\alpha\beta\gamma}(\mathbf{k}) \int d^3j \\
&\quad \times \left[u_\beta^{(0)}(\mathbf{k}-\mathbf{j},t)+\lambda_u u_\beta^{(1)}(\mathbf{k}-\mathbf{j},t)+\lambda_u^2 u_\beta^{(2)}(\mathbf{k}-\mathbf{j},t)+\ldots\right] \\
&\quad \times \left[u_\gamma^{(0)}(\mathbf{j},t)+\lambda_u u_\gamma^{(1)}(\mathbf{j},t)+\lambda_u^2 u_\gamma^{(2)}(\mathbf{j},t)+\ldots\right], \quad (2.33)
\end{aligned}$$

$$\begin{aligned}
&\left(\frac{\partial}{\partial t}+\kappa k^2\right)\left[\theta^{(0)}(\mathbf{k},t)+\lambda_\theta \theta^{(1)}(\mathbf{k},t)+\lambda_\theta^2\theta^{(2)}(\mathbf{k},t)+\ldots\right] \\
&= -i\lambda_\theta k_\beta \int d^3j \\
&\quad \times \left[u_\beta^{(0)}(\mathbf{k}-\mathbf{j},t)+\lambda_u u_\beta^{(1)}(\mathbf{k}-\mathbf{j},t)+\lambda_u^2 u_\beta^{(2)}(\mathbf{k}-\mathbf{j},t)+\ldots\right] \\
&\quad \times \left[\theta^{(0)}(\mathbf{j},t)+\lambda_\theta \theta^{(1)}(\mathbf{j},t)+\lambda_\theta^2\theta^{(2)}(\mathbf{j},t)+\ldots\right] \quad (2.34)
\end{aligned}$$

The zero-order solution velocity and scalar are solutions of Equations (2.29) and (2.30) with the expansion parameters set to zero, i.e. with no non-linear or

convection terms:

$$\left(\frac{\partial}{\partial t}+\nu k^2\right) u_\alpha^{(0)}(\mathbf{k},t) = 0 \tag{2.35}$$

$$\left(\frac{\partial}{\partial t}+\kappa k^2\right) \theta^{(0)}(\mathbf{k},t) = 0 \tag{2.36}$$

These zero-order equations can be solved easily to give

$$u_\alpha^{(0)}(\mathbf{k},t) = e^{-\nu k^2(t-t_0)}\, u_\alpha^{(0)}(\mathbf{k},t_0), \tag{2.37}$$

$$\theta^{(0)}(\mathbf{k},t) = e^{-\kappa k^2(t-t_0)}\, \theta^{(0)}(\mathbf{k},t_0). \tag{2.38}$$

We also assume that the fields at t_0 are Gaussian and so can identify $u(t_0)$ and $u^{(0)}(t_0)$, and $\theta(t_0)$ and $\theta^{(0)}(t_0)$. The zero-order propagators are just

$$\begin{aligned} H_{\alpha\beta}^{(0)}(\mathbf{k};t,s) &= D_{\alpha\beta}(\mathbf{k})\left(\frac{\partial}{\partial t}+\nu k^2\right)^{-1} \\ &= D_{\alpha\beta}(\mathbf{k}) e^{-\nu k^2(t-s)}, \end{aligned} \tag{2.39}$$

where the projection operator is inserted to ensure that the result of applying the velocity propagator is a solenoidal field, and

$$\begin{aligned} H^{\theta\theta(0)}(\mathbf{k};t,s) &= \left(\frac{\partial}{\partial t}+\kappa k^2\right)^{-1} \\ &= e^{-\kappa k^2(t-s)}. \end{aligned} \tag{2.40}$$

The first order corrections are given by

$$\left(\frac{\partial}{\partial t}+\nu k^2\right) u_\alpha^{(1)}(\mathbf{k},t) = M_{\alpha\beta\gamma}(\mathbf{k}) \int d^3j\, u_\beta^{(0)}(\mathbf{k}-\mathbf{j},t) u_\gamma^{(0)}(\mathbf{j},t) \tag{2.41}$$

with solution

$$\begin{aligned} u_\alpha^{(1)}(\mathbf{k},t) &= \int_{t_0}^{t} ds\, e^{-\nu k^2(t-s)}\, M_{\alpha\beta\gamma}(\mathbf{k}) \int d^3j\, u_\beta^{(0)}(\mathbf{k}-\mathbf{j},s) u_\gamma^{(0)}(\mathbf{j},s) \\ &= \int_{t_0}^{t} ds\, H_{\alpha\beta}^{(0)}(\mathbf{k};t,s) M_{\alpha\beta\gamma}(\mathbf{k}) \int d^3j\, u_\beta^{(0)}(\mathbf{k}-\mathbf{j},s) u_\gamma^{(0)}(\mathbf{j},s), \end{aligned} \tag{2.42}$$

and

$$\left(\frac{\partial}{\partial t}+\kappa k^2\right)\theta^{(1)}(\mathbf{k},t) \;=\; -ik_\beta\int d^3j\, u^{(0)}_\beta(\mathbf{k}-\mathbf{j},t)\theta^{(0)}(\mathbf{j},t) \qquad (2.43)$$

with solution

$$\begin{aligned}\theta^{(1)}(\mathbf{k},t) &= \int_{t_0}^{t} ds\, e^{-\kappa k^2(t-s)}\,(-i)k_\beta\int d^3j\, u^{(0)}_\beta(\mathbf{k}-\mathbf{j},s)\theta^{(0)}(\mathbf{j},s)\\ &= \int_{t_0}^{t} ds\, H^{\theta\theta(0)}(\mathbf{k};t,s)(-i)k_\beta\int d^3j\, u^{(0)}_\beta(\mathbf{k}-\mathbf{j},s)\theta^{(0)}(\mathbf{j},s). \qquad (2.44)\end{aligned}$$

The higher order corrections are formed similarly.

We are now in a position to find the LET approximations for Equations (2.12) and (2.15).

For the velocity fluctuation correlation Q, expand the RHS of Equation (2.12) using Equations (2.31) and (2.42),

$$\begin{aligned}&\left(\frac{\partial}{\partial t}+\nu k^2\right)\langle u_\alpha(\mathbf{k},t)u_\delta(\mathbf{k}',t')\rangle\\ &= \lambda_u M_{\alpha\beta\gamma}(\mathbf{k})\int d^3j\,\Big[\langle u^{(0)}_\beta(\mathbf{j},t)u^{(0)}_\gamma(\mathbf{k}-\mathbf{j},t)u^{(0)}_\delta(\mathbf{k}',t')\rangle\\ &\quad+\lambda_u\langle u^{(0)}_\beta(\mathbf{j},t)u^{(0)}_\gamma(\mathbf{k}-\mathbf{j},t)u^{(1)}_\delta(\mathbf{k}',t')\rangle\\ &\quad+2\lambda_u\langle u^{(1)}_\beta(\mathbf{j},t)u^{(0)}_\gamma(\mathbf{k}-\mathbf{j},t)u^{(0)}_\delta(\mathbf{k}',t')\rangle\\ &\quad+O(\lambda_u^2)\Big] \qquad (2.45)\\ &= \lambda_u M_{\alpha\beta\gamma}(\mathbf{k})\int d^3j\,\Big[\langle u^{(0)}_\beta(\mathbf{j},t)u^{(0)}_\gamma(\mathbf{k}-\mathbf{j},t)u^{(0)}_\delta(\mathbf{k}',t')\rangle\\ &\quad+\lambda_u\langle u^{(0)}_\beta(\mathbf{j},t)u^{(0)}_\gamma(\mathbf{k}-\mathbf{j},t)\\ &\quad\times\int_{t_0}^{t'} ds\, H^{(0)}_{\delta\sigma}(\mathbf{k}';t',s)M_{\sigma\omega\phi}(\mathbf{k}')\int d^3l\, u^{(0)}_\omega(\mathbf{l},s)u^{(0)}_\phi(\mathbf{k}'-\mathbf{l},s)\rangle\\ &\quad+2\lambda_u\langle\int_{t_0}^{t} ds\, H^{(0)}_{\beta\sigma}(\mathbf{j};t,s)M_{\sigma\omega\phi}(\mathbf{j})\int d^3l\, u^{(0)}_\omega(\mathbf{l},s)u^{(0)}_\phi(\mathbf{j}-\mathbf{l},s)\\ &\quad\times u^{(0)}_\gamma(\mathbf{k}-\mathbf{j},t)u^{(0)}_\delta(\mathbf{k}',t')\rangle\\ &\quad+O(\lambda_u^2)\Big], \qquad (2.46)\end{aligned}$$

where the symmetry of the $\int d^3j$ integral under $\mathbf{k}-\mathbf{j}\leftrightarrow\mathbf{j}$ and of $M_{\alpha\beta\gamma}$ under $\beta\leftrightarrow\gamma$ are used to simplify the RHS. Because $\mathbf{u}^{(0)}$ is Gaussian, the triple moment on the RHS is zero and the quadruple moments can be factorised into products

of double moments as follows:

$$\begin{aligned}
&\langle u_\beta^{(0)}(\mathbf{j},t)u_\gamma^{(0)}(\mathbf{k}-\mathbf{j},t)u_\omega^{(0)}(\mathbf{l},s)u_\phi^{(0)}(\mathbf{k}'-\mathbf{l},s)\rangle \\
&= \langle u_\beta^{(0)}(\mathbf{j},t)u_\gamma^{(0)}(\mathbf{k}-\mathbf{j},t)\rangle\langle u_\omega^{(0)}(\mathbf{l},s)u_\phi^{(0)}(\mathbf{k}'-\mathbf{l},s)\rangle \\
&\quad +\langle u_\beta^{(0)}(\mathbf{j},t)u_\omega^{(0)}(\mathbf{l},s)\rangle\langle u_\gamma^{(0)}(\mathbf{k}-\mathbf{j},t)u_\phi^{(0)}(\mathbf{k}'-\mathbf{l},s)\rangle \\
&\quad +\langle u_\beta^{(0)}(\mathbf{j},t)u_\phi^{(0)}(\mathbf{k}'-\mathbf{l},s)\rangle\langle u_\gamma^{(0)}(\mathbf{k}-\mathbf{j},t)u_\omega^{(0)}(\mathbf{l},s)\rangle, \qquad (2.47)
\end{aligned}$$

$$\begin{aligned}
&\langle u_\omega^{(0)}(\mathbf{l},s)u_\phi^{(0)}(\mathbf{j}-\mathbf{l},s)u_\gamma^{(0)}(\mathbf{k}-\mathbf{j},t)u_\delta^{(0)}(\mathbf{k}',t')\rangle \\
&= \langle u_\omega^{(0)}(\mathbf{l},s)u_\phi^{(0)}(\mathbf{j}-\mathbf{l},s)\rangle\langle u_\gamma^{(0)}(\mathbf{k}-\mathbf{j},t)u_\delta^{(0)}(\mathbf{k}',t')\rangle \\
&\quad +\langle u_\omega^{(0)}(\mathbf{l},s)u_\gamma^{(0)}(\mathbf{k}-\mathbf{j},t)\rangle\langle u_\phi^{(0)}(\mathbf{j}-\mathbf{l},s)u_\delta^{(0)}(\mathbf{k}',t')\rangle \\
&\quad +\langle u_\omega^{(0)}(\mathbf{l},s)u_\delta^{(0)}(\mathbf{k}',t')\rangle\langle u_\phi^{(0)}(\mathbf{j}-\mathbf{l},s)u_\gamma^{(0)}(\mathbf{k}-\mathbf{j},t)\rangle. \qquad (2.48)
\end{aligned}$$

Then for homogeneous turbulence, we use Equation (2.19) to write Equations (2.47) and (2.48) as

$$\begin{aligned}
&\langle u_\beta^{(0)}(\mathbf{j},t)u_\gamma^{(0)}(\mathbf{k}-\mathbf{j},t)u_\omega^{(0)}(\mathbf{l},s)u_\phi^{(0)}(\mathbf{k}'-\mathbf{l},s)\rangle \\
&= \delta^3(\mathbf{k})Q_{\beta\gamma}^{(0)}(\mathbf{j};t,t)\delta^3(\mathbf{k}')Q_{\omega\phi}^{(0)}(\mathbf{l};s,s) \\
&\quad +\delta^3(\mathbf{j}+\mathbf{l})Q_{\beta\omega}^{(0)}(\mathbf{j};t,s)\delta^3((\mathbf{k}+\mathbf{k}')-(\mathbf{j}+\mathbf{l}))Q_{\gamma\phi}^{(0)}(\mathbf{k}-\mathbf{j};t,s) \\
&\quad +\delta^3(\mathbf{j}+\mathbf{k}'-\mathbf{l})Q_{\beta\phi}^{(0)}(\mathbf{j};t,s)\delta^3(\mathbf{k}-\mathbf{j}+\mathbf{l})Q_{\gamma\omega}^{(0)}(\mathbf{k}-\mathbf{j};t,s), \qquad (2.49)
\end{aligned}$$

$$\begin{aligned}
&\langle u_\omega^{(0)}(\mathbf{l},s)u_\phi^{(0)}(\mathbf{j}-\mathbf{l},s),u_\gamma^{(0)}(\mathbf{k}-\mathbf{j},t)u_\delta^{(0)}(\mathbf{k}',t')\rangle \\
&= \delta^3(\mathbf{j})Q_{\omega\phi}^{(0)}(\mathbf{l};s,s),\delta^3((\mathbf{k}+\mathbf{k}')-\mathbf{j})Q_{\gamma\delta}^{(0)}(\mathbf{k}-\mathbf{j};t,t') \\
&\quad +\delta^3(\mathbf{l}+\mathbf{k}-\mathbf{j})Q_{\omega\gamma}^{(0)}(\mathbf{l};s,t)\delta^3(\mathbf{j}-\mathbf{l}+\mathbf{k}')Q_{\phi\delta}^{(0)}(\mathbf{j}-\mathbf{l};s,t') \\
&\quad +\delta^3(\mathbf{l}+\mathbf{k}')Q_{\omega\delta}^{(0)}(\mathbf{l};s,t')\delta^3(\mathbf{k}-\mathbf{l})Q_{\phi\gamma}^{(0)}(\mathbf{j}-\mathbf{l};s,t). \qquad (2.50)
\end{aligned}$$

Substituting these results into Equation (2.46), using Equation (2.19) to write the LHS in terms of Q, integrating over $\mathbf{l}$ and $\mathbf{k}'$ to get rid of the δ-functions and

using the identity

$$M_{\alpha\beta\gamma}(\mathbf{k})\delta^3(\mathbf{k}) \;=\; 0, \tag{2.51}$$

we get:

$$\begin{aligned}
&\left(\frac{\partial}{\partial t}+\nu k^2\right) Q_{\alpha\delta}(\mathbf{k};t,t') \\
&= \lambda_u M_{\alpha\beta\gamma}(\mathbf{k}) \int d^3j \\
&\quad \times \Bigg[\lambda_u \int_{t_0}^{t'} ds\, H^{(0)}_{\delta\sigma}(-\mathbf{k};t',s) M_{\sigma\omega\phi}(-\mathbf{k}) \\
&\quad \times \left\{Q^{(0)}_{\beta\omega}(\mathbf{j};t,s) Q^{(0)}_{\gamma\phi}(\mathbf{k}-\mathbf{j};t,s) + Q^{(0)}_{\beta\phi}(\mathbf{j};t,s) Q^{(0)}_{\gamma\omega}(\mathbf{k}-\mathbf{j};t,s)\right\} \\
&\quad +2\lambda_u \int_{t_0}^{t} ds\, H^{(0)}_{\beta\sigma}(\mathbf{j};t,s) M_{\sigma\omega\phi}(\mathbf{j}) \\
&\quad \times \left\{Q^{(0)}_{\gamma\omega}(\mathbf{k}-\mathbf{j};t,s) Q^{(0)}_{\phi\delta}(\mathbf{k};s,t') + Q^{(0)}_{\omega\delta}(\mathbf{k};s,t') Q^{(0)}_{\gamma\phi}(\mathbf{k}-\mathbf{j};t,s)\right\} \\
&\quad +O(\lambda_u^2)\Bigg].
\end{aligned} \tag{2.52}$$

Now set $\lambda_u = 1$ and renormalise the series on the RHS. This leads to a new series with the first term on the RHS as shown in Equation (2.52) but with $H^{(0)}$ replaced by the renormalised propagator H and the zero-order moment $Q^{(0)}$ replaced by Q (the details of the renormalisation are given in [43, 42]). The renormalised expansion on the RHS is truncated at the first term to give

$$\begin{aligned}
&\left(\frac{\partial}{\partial t}+\nu k^2\right) Q_{\alpha\delta}(\mathbf{k};t,t') \\
&= M_{\alpha\beta\gamma}(\mathbf{k}) \int d^3j \\
&\quad \times \Bigg[2\int_{t_0}^{t'} ds\, H_{\delta\sigma}(-\mathbf{k};t',s) M_{\sigma\omega\phi}(-\mathbf{k}) Q_{\beta\omega}(\mathbf{j};t,s) Q_{\gamma\phi}(\mathbf{k}-\mathbf{j};t,s) \\
&\quad +4\int_{t_0}^{t} ds\, H_{\beta\sigma}(\mathbf{j};t,s) M_{\sigma\omega\phi}(\mathbf{j}) Q_{\gamma\omega}(\mathbf{k}-\mathbf{j};t,s) Q_{\phi\delta}(\mathbf{k};s,t')\Bigg],
\end{aligned} \tag{2.53}$$

where we have used the symmetry properties of M to simplify the terms. Equation (2.53) with Equation (2.20)

$$Q_{\alpha\beta}(\mathbf{k};t,t') \;=\; H_{\alpha\gamma}(\mathbf{k};t,t') Q_{\gamma\beta}(\mathbf{k};t',t'). \tag{2.54}$$

relating the propagator H to the correlation Q, are the LET equations for the velocity fluctuations. As it stands, the equation is still too difficult to solve numerically, so we specialise further to isotropic turbulence. Using the definitions of H and Q in isotropic turbulence (Equation (2.23) and (2.24)) we get

$$\begin{aligned}
&\left(\frac{\partial}{\partial t}+\nu k^2\right) D_{\alpha\delta}(\mathbf{k})Q(k;t,t') \\
&= M_{\alpha\beta\gamma}(\mathbf{k})\int d^3j \\
&\quad \times\left[2\int_{t_0}^{t'} ds\, D_{\delta\sigma}(-\mathbf{k})H(k;t',s)M_{\sigma\omega\phi}(-\mathbf{k})\right. \\
&\quad \times D_{\beta\omega}(\mathbf{j})Q(j;t,s)D_{\gamma\phi}(\mathbf{k}-\mathbf{j})Q(|\mathbf{k}-\mathbf{j}|;t,s) \\
&\quad +4\int_{t_0}^{t} ds\, D_{\beta\sigma}(\mathbf{j})H(j;t,s)M_{\sigma\omega\phi}(\mathbf{j}) \\
&\quad \left.\times D_{\gamma\omega}(\mathbf{k}-\mathbf{j})Q(|\mathbf{k}-\mathbf{j}|;t,s)D_{\phi\delta}(\mathbf{k})Q(k;s,t')\right]. \qquad (2.55)
\end{aligned}$$

Contracting the indices α and δ and reducing the product of M's and D's we get

$$\begin{aligned}
&\left(\frac{\partial}{\partial t}+\nu k^2\right) Q(k;t,t') \\
&= \int d^3j\, L(\mathbf{k},\mathbf{j})\left[\int_{t_0}^{t'} ds\, H(k;t',s)Q(j;t,s)Q(|\mathbf{k}-\mathbf{j}|;t,s)\right. \\
&\quad \left.-\int_{t_0}^{t} ds\, H(j;t,s)Q(|\mathbf{k}-\mathbf{j}|;t,s)Q(k;s,t')\right], \qquad (2.56)
\end{aligned}$$

where

$$L(\mathbf{k},\mathbf{j}) = \frac{[\mu(k^2+j^2)-kj(1+2\mu^2)](1-\mu^2)kj}{k^2+j^2-2kj\mu} \qquad (2.57)$$

and μ is the cosine of the angle between the vectors $\mathbf{k}$ and $\mathbf{j}$ (for details of the derivation of $L(\mathbf{k},\mathbf{j})$ see [43]).

The LET equation for the velocity single-time moment is derived from Equation (2.17) in exactly the same way to give

$$\begin{aligned}
&\left(\frac{\partial}{\partial t}+2\nu k^2\right) Q(k;t,t) \\
&= 2\int d^3j\, L(\mathbf{k},\mathbf{j})\int_{t_0}^{t} ds\, [H(k;t,s)Q(j;t,s)Q(|\mathbf{k}-\mathbf{j}|;t,s) \\
&\quad -H(j;t,s)Q(|\mathbf{k}-\mathbf{j}|;t,s)Q(k;s,t)]. \qquad (2.58)
\end{aligned}$$

Equations (2.56), (2.58) and (2.27)

$$Q(k;t,t') = H(k;t,t')Q(k;t',t') \tag{2.59}$$

form the basis for the numerical calculations of the velocity field.

For the scalar fluctuation correlation Θ, expand the RHS of Equation (2.15) using Equations (2.31), (2.32), (2.42) and (2.44),

$$\begin{aligned}
&\left(\frac{\partial}{\partial t}+\kappa k^2\right)\langle\theta(\mathbf{k},t)\theta(\mathbf{k}',t')\rangle \\
&= -i\lambda_\theta k_\alpha \int d^3j \,\Big[\langle u_\alpha^{(0)}(\mathbf{k}-\mathbf{j},t)\theta^{(0)}(\mathbf{j},t)\theta^{(0)}(\mathbf{k}',t')\rangle \\
&\quad +\lambda_u\langle u_\alpha^{(1)}(\mathbf{k}-\mathbf{j},t)\theta^{(0)}(\mathbf{j},t)\theta^{(0)}(\mathbf{k}',t')\rangle \\
&\quad +\lambda_\theta\langle u_\alpha^{(0)}(\mathbf{k}-\mathbf{j},t)\theta^{(1)}(\mathbf{j},t)\theta^{(0)}(\mathbf{k}',t')\rangle \\
&\quad +\lambda_\theta\langle u_\alpha^{(0)}(\mathbf{k}-\mathbf{j},t)\theta^{(0)}(\mathbf{j},t)\theta^{(1)}(\mathbf{k}',t')\rangle \\
&\quad +O(\lambda^2)\Big] \qquad (2.60)\\
&= -i\lambda_\theta k_\alpha \int d^3j \,\Big[\langle u_\alpha^{(0)}(\mathbf{k}-\mathbf{j},t)\theta^{(0)}(\mathbf{j},t)\theta^{(0)}(\mathbf{k}',t')\rangle \\
&\quad +\lambda_u\langle\int_{t_0}^{t} ds\, H_{\alpha\sigma}^{(0)}(\mathbf{k}-\mathbf{j};t,s)M_{\sigma\beta\gamma}(\mathbf{k}-\mathbf{j})\int d^3l\, u_\beta^{(0)}(\mathbf{k}-\mathbf{j}-\mathbf{l},s)u_\gamma^{(0)}(\mathbf{l},s) \\
&\quad \times\theta^{(0)}(\mathbf{j},t)\theta^{(0)}(\mathbf{k}',t')\rangle \\
&\quad +\lambda_\theta\langle u_\alpha^{(0)}(\mathbf{k}-\mathbf{j},t) \\
&\quad \times\int_{t_0}^{t} ds\, H^{\theta\theta(0)}(\mathbf{j};t,s)(-ij_\beta)\int d^3l\, u_\beta^{(0)}(\mathbf{j}-\mathbf{l},s)\theta^{(0)}(\mathbf{l},s) \\
&\quad \times\theta^{(0)}(\mathbf{k}',t')\rangle \\
&\quad +\lambda_\theta\langle u_\alpha^{(0)}(\mathbf{k}-\mathbf{j},t)\theta^{(0)}(\mathbf{j},t) \\
&\quad \times\int_{t_0}^{t'} ds\, H^{\theta\theta(0)}(\mathbf{k}';t',s)(-ik'_\beta)\int d^3l\, u_\beta^{(0)}(\mathbf{k}'-\mathbf{l},s)\theta^{(0)}(\mathbf{l},s)\rangle \\
&\quad +O(\lambda^2)\Big]. \qquad (2.61)
\end{aligned}$$

Because $\mathbf{u}^{(0)}$ and $\theta^{(0)}$ are Gaussian, the triple moment on the RHS is zero and the quadruple moments can be factorised into products of double moments as follows:

$$\begin{aligned}
&\langle u_\beta^{(0)}(\mathbf{k}-\mathbf{j}-\mathbf{l},s)u_\gamma^{(0)}(\mathbf{l},s)\theta^{(0)}(\mathbf{j},t)\theta^{(0)}(\mathbf{k}',t')\rangle \\
&\quad = \langle u_\beta^{(0)}(\mathbf{k}-\mathbf{j}-\mathbf{l},s)u_\gamma^{(0)}(\mathbf{l},s)\rangle\langle\theta^{(0)}(\mathbf{j},t)\theta^{(0)}(\mathbf{k}',t')\rangle +
\end{aligned}$$

$$+\langle u_\beta^{(0)}(\mathbf{k}-\mathbf{j}-\mathbf{l},s)\theta^{(0)}(\mathbf{j},t)\rangle\langle u_\gamma^{(0)}(\mathbf{l},s)\theta^{(0)}(\mathbf{k}',t')\rangle$$
$$+\langle u_\beta^{(0)}(\mathbf{k}-\mathbf{j}-\mathbf{l},s)\theta^{(0)}(\mathbf{k}',t')\rangle\langle u_\gamma^{(0)}(\mathbf{l},s)\theta^{(0)}(\mathbf{j},t)\rangle, \tag{2.62}$$

$$\begin{aligned}&\langle u_\alpha^{(0)}(\mathbf{k}-\mathbf{j},t)u_\beta^{(0)}(\mathbf{j}-\mathbf{l},s)\theta^{(0)}(\mathbf{l},s)\theta^{(0)}(\mathbf{k}',t')\rangle\\ &= \langle u_\alpha^{(0)}(\mathbf{k}-\mathbf{j},t)u_\beta^{(0)}(\mathbf{j}-\mathbf{l},s)\rangle\langle\theta^{(0)}(\mathbf{l},s)\theta^{(0)}(\mathbf{k}',t')\rangle\\ &\quad+\langle u_\alpha^{(0)}(\mathbf{k}-\mathbf{j},t)\theta^{(0)}(\mathbf{l},s)\rangle\langle u_\beta^{(0)}(\mathbf{j}-\mathbf{l},s)\theta^{(0)}(\mathbf{k}',t')\rangle\\ &\quad+\langle u_\alpha^{(0)}(\mathbf{k}-\mathbf{j},t)\theta^{(0)}(\mathbf{k}',t')\rangle\langle u_\beta^{(0)}(\mathbf{j}-\mathbf{l},s)\theta^{(0)}(\mathbf{l},s)\rangle,\end{aligned} \tag{2.63}$$

$$\begin{aligned}&\langle u_\alpha^{(0)}(\mathbf{k}-\mathbf{j},t)\theta^{(0)}(\mathbf{j},t)u_\beta^{(0)}(\mathbf{k}'-\mathbf{l},s)\theta^{(0)}(\mathbf{l},s)\rangle\\ &= \langle u_\alpha^{(0)}(\mathbf{k}-\mathbf{j},t)\theta^{(0)}(\mathbf{j},t)\rangle\langle u_\beta^{(0)}(\mathbf{k}'-\mathbf{l},s)\theta^{(0)}(\mathbf{l},s)\rangle\\ &\quad+\langle u_\alpha^{(0)}(\mathbf{k}-\mathbf{j},t)u_\beta^{(0)}(\mathbf{k}'-\mathbf{l},s)\rangle\langle\theta^{(0)}(\mathbf{j},t)\theta^{(0)}(\mathbf{l},s)\rangle\\ &\quad+\langle u_\alpha^{(0)}(\mathbf{k}-\mathbf{j},t)\theta^{(0)}(\mathbf{l},s)\rangle\langle\theta^{(0)}(\mathbf{j},t)u_\beta^{(0)}(\mathbf{k}'-\mathbf{l},s)\rangle\end{aligned} \tag{2.64}$$

To simplify the derivation, we specialise to homogeneous isotropic turbulence, where all the $\langle u\theta\rangle$ correlations are zero and we can use Equations (2.19), (2.22), (2.23), (2.24), (2.25) and (2.26) to write Equations (2.62), (2.63) and (2.64) as

$$\begin{aligned}&\langle u_\beta^{(0)}(\mathbf{k}-\mathbf{j}-\mathbf{l},s)u_\gamma^{(0)}(\mathbf{l},s)\theta^{(0)}(\mathbf{j},t)\theta^{(0)}(\mathbf{k}',t')\rangle\\ &= \delta^3(\mathbf{k}-\mathbf{j})D_{\beta\gamma}(\mathbf{k}-\mathbf{j}-\mathbf{l})Q^{(0)}(|\mathbf{k}-\mathbf{j}-\mathbf{l}|;s,s)\\ &\quad\times\delta^3(\mathbf{j}+\mathbf{k}')\Theta^{(0)}(j;t,t'),\end{aligned} \tag{2.65}$$

$$\begin{aligned}&\langle u_\alpha^{(0)}(\mathbf{k}-\mathbf{j},t)u_\beta^{(0)}(\mathbf{j}-\mathbf{l},s)\theta^{(0)}(\mathbf{l},s)\theta^{(0)}(\mathbf{k}',t')\rangle\\ &= \delta^3(\mathbf{k}-\mathbf{l})D_{\alpha\beta}(\mathbf{k}-\mathbf{j})Q^{(0)}(|\mathbf{k}-\mathbf{j}|;t,s)\\ &\quad\times\delta^3(\mathbf{l}+\mathbf{k}')\Theta^{(0)}(l;s,t'),\end{aligned} \tag{2.66}$$

$$\begin{aligned}&\langle u_\alpha^{(0)}(\mathbf{k}-\mathbf{j},t)\theta^{(0)}(\mathbf{j},t)u_\beta^{(0)}(\mathbf{k}'-\mathbf{l},s)\theta^{(0)}(\mathbf{l},s)\rangle\\ &= \delta^3(\mathbf{k}-\mathbf{j}+\mathbf{k}'-\mathbf{l})D_{\alpha\beta}(\mathbf{k}-\mathbf{j})Q^{(0)}(|\mathbf{k}-\mathbf{j}|;t,s)\times\end{aligned}$$

$$\times\delta^3(\mathbf{j}+\mathbf{l})\Theta^{(0)}(j;t,s). \tag{2.67}$$

To get the isotropic version of Equation (2.61) we substitute these results, writing the LHS in terms of $\Theta(k;t,t')$, integrating over $\mathbf{l}$ and $\mathbf{k}'$ to get rid of the δ-functions, thus changing $\mathbf{k}'$ to $-\mathbf{k}$, using the isotropic forms of $H^{(0)}$ and $H^{\theta\theta(0)}$ and using the identity

$$M_{\alpha\beta\gamma}(\mathbf{k})\delta^3(\mathbf{k}) \;=\; 0 \tag{2.68}$$

to get rid of the first λ^2 term on the RHS of Equation (2.61). We eventually get:

$$\begin{aligned}
&\left(\frac{\partial}{\partial t}+\kappa k^2\right)\Theta(k;t,t') \\
&= -ik_\alpha\int d^3j\,\Big[\lambda_\theta\int_{t_0}^{t} ds\,H^{\theta\theta(0)}(j;t,s)(-ij_\beta) \\
&\quad\times D_{\alpha\beta}(\mathbf{k}-\mathbf{j})Q^{(0)}(|\mathbf{k}-\mathbf{j}|;t,s)\Theta^{(0)}(k;s,t') \\
&\quad+\lambda_\theta\int_{t_0}^{t'} ds\,H^{\theta\theta(0)}(k;t',s)(ik_\beta) \\
&\quad\times D_{\alpha\beta}(\mathbf{k}-\mathbf{j})Q^{(0)}(|\mathbf{k}-\mathbf{j}|;t,s)\Theta^{(0)}(j;t,s) \\
&\quad+O(\lambda^2)\Big].
\end{aligned} \tag{2.69}$$

We can reduce the geometrical factors in the two terms on the RHS as follows:

$$\begin{aligned}
&-ik_\alpha(i)k_\beta D_{\alpha\beta}(\mathbf{k}-\mathbf{j}) \\
&= k_\alpha k_\beta\left[\delta_{\alpha\beta}-\frac{(k_\alpha-j_\alpha)(k_\beta-j_\beta)}{(\mathbf{k}-\mathbf{j}).(\mathbf{k}-\mathbf{j})}\right] \\
&= k^2-\frac{(k^2-\mathbf{j}.\mathbf{k})(k^2-\mathbf{j}.\mathbf{k})}{k^2+j^2-2\mathbf{j}.\mathbf{k}} \\
&= k^2-\frac{(k^2-jk\mu)(k^2-jk\mu)}{k^2+j^2-2jk\mu} \\
&= \frac{(k^4+k^2j^2-2jk^3\mu)-(k^4-2jk^3\mu+j^2k^2\mu^2)}{k^2+j^2-2jk\mu} \\
&= \frac{k^2j^2-j^2k^2\mu^2}{k^2+j^2-2jk\mu} \\
&= \frac{k^2j^2(1-\mu^2)}{k^2+j^2-2jk\mu} \\
&\equiv N(\mathbf{k},\mathbf{k}-\mathbf{j}),
\end{aligned} \tag{2.70}$$

where μ is the cosine of the angle between the vectors $\mathbf{k}$ and $\mathbf{j}$, and

$$\begin{aligned} -ik_\alpha(-i)j_\beta D_{\alpha\beta}(\mathbf{k}-\mathbf{j}) &= -ik_\alpha(-i)k_\beta D_{\alpha\beta}(\mathbf{k}-\mathbf{j}) \\ &= -\frac{k^2j^2(1-\mu^2)}{k^2+j^2-2jk\mu} \\ &\equiv -N(\mathbf{k},\mathbf{k}-\mathbf{j}), \end{aligned} \tag{2.71}$$

since

$$D_{\alpha\beta}(\mathbf{k}-\mathbf{j})(k_\beta - j_\beta) = 0. \tag{2.72}$$

We now set $\lambda_u = 1$ and $\lambda_\theta = 1$ and renormalise the expansion on the RHS of Equation (2.69), effectively substituting H for $H^{(0)}$, Q for $Q^{(0)}$, $H^{\theta\theta}$ for $H^{\theta\theta(0)}$ and Θ for $\Theta^{(0)}$. We then truncate the expansion on the RHS to get the LET equation for the scalar correlation,

$$\begin{aligned} &\left(\frac{\partial}{\partial t}+\kappa k^2\right)\Theta(k;t,t') \\ &= \int d^3j\, N(\mathbf{k},\mathbf{k}-\mathbf{j}) \times \\ &\quad \left[-\int_{t_0}^{t} ds\, H^{\theta\theta}(j;t,s)Q(|\mathbf{k}-\mathbf{j}|;t,s)\Theta(k;s,t') \right. \\ &\quad \left. +\int_{t_0}^{t'} ds\, H^{\theta\theta}(k;t',s)Q(|\mathbf{k}-\mathbf{j}|;t,s)\Theta(j;t,s)\right]. \end{aligned} \tag{2.73}$$

The LET equation for the scalar single-time moment is derived from Equation (2.18) in exactly the same way to give

$$\begin{aligned} &\left(\frac{\partial}{\partial t}+2\kappa k^2\right)\Theta(k;t,t) \\ &= 2\int d^3j\, N(\mathbf{k},\mathbf{k}-\mathbf{j}) \times \\ &\quad \int_{t_0}^{t} ds\, \left[-H^{\theta\theta}(j;t,s)Q(|\mathbf{k}-\mathbf{j}|;t,s)\Theta(k;s,t)\right. \\ &\quad \left. +H^{\theta\theta}(k;t,s)Q(|\mathbf{k}-\mathbf{j}|;t,s)\Theta(j;t,s)\right]. \end{aligned} \tag{2.74}$$

Equations (2.73) and (2.74), with Equation (2.28) relating the propagator $H^{\theta\theta}$ to the correlation Θ, form the LET equations for the scalar fluctuations, in the case of homogeneous, isotropic turbulence.

Equation (2.73) can re-written with $\mathbf{k}-\mathbf{j}$ and $\mathbf{j}$ transposed since the integral over $\mathbf{j}$ is symmetrical in $\mathbf{k}-\mathbf{j}$ and $\mathbf{j}$; this gives

$$\begin{aligned}
&\left(\frac{\partial}{\partial t}+\kappa k^2\right)\Theta(k;t,t') \\
&= \int d^3j\, N(\mathbf{k},\mathbf{j}) \times \\
&\quad \Big[-\int_{t_0}^{t} ds\, H^{\theta\theta}(|\mathbf{k}-\mathbf{j}|;t,s)Q(j|;t,s)\Theta(k;s,t') \\
&\quad +\int_{t_0}^{t'} ds\, H^{\theta\theta}(k;t',s)Q(j|;t,s)\Theta(|\mathbf{k}-\mathbf{j}|;t,s)\Big], \qquad (2.75)
\end{aligned}$$

where

$$N(\mathbf{k},\mathbf{j}) = k^2(1-\mu^2). \qquad (2.76)$$

Equation (2.75) is formally equivalent to Equation (2.73) and was the formulation originally used in the numerical calculations, but it did not conserve Θ (see Section 2.5 for details).

2.4 Numerical analysis

We now have the LET equations for the velocity and scalar fields in homogeneous, isotropic, decaying turbulence

$$Q(k;t,t') = H(k;t,t')Q(k;t',t'), \qquad (2.77)$$

$$\begin{aligned}
&\left(\frac{\partial}{\partial t}+\nu k^2\right)Q(k;t,t') \\
&= \int d^3j\, L(\mathbf{k},\mathbf{j})\Big[\int_{t_0}^{t'} ds\, H(k;t',s)Q(j;t,s)Q(|\mathbf{k}-\mathbf{j}|;t,s) \\
&\quad -\int_{t_0}^{t} ds\, H(j;t,s)Q(|\mathbf{k}-\mathbf{j}|;t,s)Q(k;s,t')\Big] \qquad (2.78)
\end{aligned}$$

$$\left(\frac{\partial}{\partial t}+2\nu k^2\right)Q(k;t,t) =$$

$$= 2\int d^3j\, L(\mathbf{k},\mathbf{j}) \int_{t_0}^{t} ds\, [H(k;t,s)Q(j;t,s)Q(|\mathbf{k}-\mathbf{j}|;t,s) - H(j;t,s)Q(|\mathbf{k}-\mathbf{j}|;t,s)Q(k;s,t)] \quad (2.79)$$

and

$$\Theta(k;t,t') = H^{\theta\theta}(k;t,t')\Theta(k;t',t'), \quad (2.80)$$

$$\left(\frac{\partial}{\partial t} + \kappa k^2\right)\Theta(k;t,t') = \int d^3j\, N(\mathbf{k},\mathbf{k}-\mathbf{j}) \times \left[-\int_{t_0}^{t} ds\, H^{\theta\theta}(j;t,s)Q(|\mathbf{k}-\mathbf{j}|;t,s)\Theta(k;s,t') + \int_{t_0}^{t'} ds\, H^{\theta\theta}(k;t',s)Q(|\mathbf{k}-\mathbf{j}|;t,s)\Theta(j;t,s)\right], \quad (2.81)$$

$$\left(\frac{\partial}{\partial t} + 2\kappa k^2\right)\Theta(k;t,t) = 2\int d^3j\, N(\mathbf{k},\mathbf{k}-\mathbf{j}) \times \int_{t_0}^{t} ds\, \left[-H^{\theta\theta}(j;t,s)Q(|\mathbf{k}-\mathbf{j}|;t,s)\Theta(k;s,t) + H^{\theta\theta}(k;t,s)Q(|\mathbf{k}-\mathbf{j}|;t,s)\Theta(j;t,s)\right], \quad (2.82)$$

and we have to integrate these evolution equations forward in time from the initial conditions. These initial conditions are specified by the energy and scalar energy spectra at $t = 0$. The numerical method used is exactly that described in [45]. Indeed the FORTRAN code used for the LET scalar calculation is a slight modification of Dr. V. Shanmugasundaram's LET velocity code. The velocity code is run first, to get values for Q and H, and then the scalar code is run using these data to get values for Θ and $H^{\theta\theta}$.

Wavenumber discretisation and integration

The wavenumbers k and j are restricted to the finite range (k_{bot}, k_{top}). There are constraints on k_{bot} and k_{top} and these are discussed in Section 2.5. This

wavenumber range is divided into N constant logarithmic intervals Δk_n, with n increasing with wavenumber. In each interval we choose a centre value k_n, calculated as the geometric mean of the limits of the interval. Thus we have

$$\begin{aligned} k_1 &= 2^{\Delta(Octave)/2} k_{bot} \\ k_{n+1} &= 2^{\Delta(Octave)} k_n, \end{aligned}$$

where $\Delta(Octave) = 0.25$ or 0.33 for all the calculations. The variable μ, the cosine of the angle between the vectors $\mathbf{k}$ and $\mathbf{j}$, lies in the range $(+1, -1)$ and we divide this into M constant linear intervals of size $\Delta\mu_m$. The integral $\int d^3j$ is written as $\int dj\, 2\pi j^2 \int d\mu$. We now write down the wavenumber discretised versions of Equations (2.77), (2.78), (2.79), (2.80), (2.81) and (2.82):

$$Q(k_n; t, t') = H(k_n; t, t') Q(k_n; t', t'), \tag{2.83}$$

$$\begin{aligned} &\left(\frac{\partial}{\partial t} + \nu k_n^2\right) Q(k_n; t, t') \\ &= \sum_{p=1}^{N} \sum_{m=1}^{M} \mathcal{L}_{npm} \left[\int_{t_0}^{t'} ds\, H(k_n; t', s) Q(k_p; t, s) Q(k_{npm}; t, s) \right. \\ &\quad \left. - \int_{t_0}^{t} ds\, H(k_p; t, s) Q(k_{npm}; t, s) Q(k_n; s, t') \right] \\ &\equiv A_n(t, t') \end{aligned} \tag{2.84}$$

$$\begin{aligned} &\left(\frac{\partial}{\partial t} + 2\nu k_n^2\right) Q(k_n; t, t) \\ &= 2 \sum_{p=1}^{N} \sum_{m=1}^{M} \mathcal{L}_{npm} \int_{t_0}^{t} ds\, [H(k_n; t, s) Q(k_p; t, s) Q(k_{npm}; t, s) \\ &\quad - H(k_p; t, s) Q(k_{npm}; t, s) Q(k_n; s, t)] \\ &\equiv B_n(t, t') \end{aligned} \tag{2.85}$$

and

$$\Theta(k_n; t, t') = H^{\theta\theta}(k_n; t, t') \Theta(k_n; t', t'), \tag{2.86}$$

$$\left(\frac{\partial}{\partial t}+\kappa k_n^2\right)\Theta(k_n;t,t')$$
$$= \sum_{p=1}^{N}\sum_{m=1}^{M}\mathcal{N}_{npm}$$
$$\left[-\int_{t_0}^{t} ds\, H^{\theta\theta}(k_p;t,s)Q(k_{npm};t,s)\Theta(k_n;s,t')\right.$$
$$\left.+\int_{t_0}^{t'} ds\, H^{\theta\theta}(k_n;t',s)Q(k_{npm};t,s)\Theta(k_p;t,s)\right] \qquad (2.87)$$
$$\equiv C_n(t,t'),$$

$$\left(\frac{\partial}{\partial t}+2\kappa k_n^2\right)\Theta(k_n;t,t)$$
$$= 2\sum_{p=1}^{N}\sum_{m=1}^{M}\mathcal{N}_{npm}$$
$$\int_{t_0}^{t} ds\,\left[-H^{\theta\theta}(k_p;t,s)Q(k_{npm};t,s)\Theta(k_n;s,t)\right.$$
$$\left.+H^{\theta\theta}(k_n;t,s)Q(k_{npm};t,s)\Theta(k_p;t,s)\right] \qquad (2.88)$$
$$\equiv D_n(t,t'),$$

where

$$\mathcal{L}_{npm} = 2\pi k_p^2\Delta k_p\Delta\mu_m\frac{[\mu_m(k_n^2+k_p^2)-k_nk_p(1+2\mu_m^2)](1-\mu_m^2)k_nk_p}{k_n^2+k_p^2-2k_nk_p\mu_m} \qquad (2.89)$$

and

$$\mathcal{N}_{npm} = 2\pi k_p^2\Delta k_p\Delta\mu_m\frac{k_n^2k_p^2(1-\mu_m^2)}{k_n^2+k_p^2-2k_pk_n\mu_m}. \qquad (2.90)$$

$Q(k_{npm};t,s)$ is the discretised version of $Q(|\mathbf{k}-\mathbf{j}|;t,s)$ and generally has to be calculated by logarithmic interpolation between the nearest centre values $k_n \leq |\mathbf{k}-\mathbf{j}| \leq k_{n+1}$. The $\mathcal{L}_{npm}$ and $\mathcal{N}_{npm}$ coefficients can be calculated just once, at the beginning of a calculation, and then stored for use in subsequent timesteps.

Time discretisation and integration

We divide the period from $t = 0$ to the present time t into intervals Δt_i. In these computations the time step Δt_i at each time t_i is taken to be the smaller

of the characteristic times for convection ($1/(u_{rms}(t)k_{top})$) and viscous decay ($1/(\nu k_{top}^2)$). In fact, the characteristic time for scalar diffusion ($1/(\kappa k_{top}^2)$) should also be included in this comparison, especially for small Prandtl number when $1/(\kappa k_{top}^2) \ll 1/(\nu k_{top}^2)$ but the use of the exact exponential diffusive (and viscous) decay in the time difference equation (see below) allows a large time step to be used. Even at $Pr = 0.1$, the integrated error (see Section 2.5) remains very low. Dr. Shanmugasundaram has performed independent calculations using smaller timesteps for the same initial conditions and there is very little difference from our results.

The time integrals on the right hand sides of Equations (2.85), (2.86), (2.88) and (2.89) are discretised using the trapezoidal rule to give sums for $A_n(t_i, t_j)$, $B_n(t_i, t_j)$, $C_n(t_i, t_j)$ and $D_n(t_i, t_j)$.

Equation (2.88) is reduced to a difference equation as follows (the velocity equations and the scalar energy equation are reduced similarly). First approximate $C_n(t_i, t_j)$ by

$$C_n(t_i, t_j) = \frac{1}{2}\left[C_n(t_i, t_j) + C_n(t_{i-1}, t_j)\right] \tag{2.91}$$

and then integrate over the interval Δt_i to get the implicit integration scheme

$$\begin{aligned}
&\Theta(k_n; t_i, t_j) \\
&\quad = \exp(-\kappa k_n^2 \Delta t_i)\Theta(k_n; t_{i-1}, t_j) \\
&\qquad + \frac{1}{2\kappa k_n^2}\left[1 - \exp(-\kappa k_n^2 \Delta t_i)\right]\left[C_n(t_i, t_j) + C_n(t_{i-1}, t_j)\right],
\end{aligned} \tag{2.92}$$

with the initial condition

$$\begin{aligned}
\Theta(k_n; t_0, t_0) &= \Theta(k_n; 0, 0) \\
&= E^{\theta\theta}(k_n, 0)/4\pi k_n^2,
\end{aligned} \tag{2.93}$$

where $E^{\theta\theta}(k_n, 0)$ is the specified initial θ-energy spectrum. To use this implicit scheme, at the ith step we do the following for $Q(k; t, t')$, $Q(k; t, t)$, $\Theta(k; t, t')$ and $\Theta(k; t, t)$ (shown here for $\Theta(k; t, t')$ only):

predictor compute temporary values of $\Theta(k_n; t_i, t_j)$ by replacing $C_n(t_i, t_j)$ on the RHS of Equation (2.92) with $C_n(t_{i-1}, t_j)$,

corrector evaluate $C_n(t_i, t_j)$ using the temporary values $\Theta(k_n; t_i, t_j)$ and then use these C values to evaluate the corrected $\Theta(k_n; t_i, t_j)$.

Each step is carried out for each value of the indices $1 \leq n \leq N$ and $0 \leq j \leq i$. In the low and medium Reynolds number calculations the predictor-corrector scheme was iterated until the difference between the temporary and current values was less than 10% of the current value. The difference between single iteration and multiple iteration calculations in the velocity case was small—only the skewness changed, by about 7%. At high Reynolds number only one iteration was performed to increase the speed of the computation. The scalar calculations required slightly more iterations per time step than the velocity calculations.

Computational details

The code was written in FORTRAN-77 and run on the EMAS system at Edinburgh University. The CPU was a Hitachi HL-80. In summary, for Spectrum I (see below) the CPU time required to reach 1 eddy turnover time ($R_\lambda(0) = 19$) is 0.5 hours for the velocity calculation plus 1 hour for the scalar calculation. For Spectrum V, the CPU time required for 0.38 eddy turnover times ($R_\lambda(0) = 245$) is 81 hours for the velocity calculation plus 114 hours for the scalar calculation. Because of the size of the data arrays (especially the $Q(k; t, t')$ array) and duration of the calculation, the computation is split into one hour long runs, chained together. This requires housekeeping, copying permanent and temporary results into files, keeping track of the computation, etc., which is an overhead of around 1% of the computation time.

2.5 Initial conditions, choice of parameters, errors

Definitions

Before discussing the parameter selection and results, we define some quantities. The energy and scalar energy spectral densities $E(k,t)$ and $E_\theta(k,t)$ are defined by

$$E(k,t) = 4\pi k^2 Q(k;t,t) \tag{2.94}$$

and

$$E_\theta(k,t) = 4\pi k^2 \Theta(k;t,t). \tag{2.95}$$

The energy $E(t)$, scalar energy $E_\theta(t)$, rms velocity $u(t)$ and rms scalar fluctuation $\theta(t)$ are defined by

$$\int_0^\infty E(k,t)\,dk = E(t) \tag{2.96}$$

$$= \frac{3}{2}u^2 \tag{2.97}$$

and

$$\int_0^\infty E_\theta(k,t)\,dk = E_\theta(t) \tag{2.98}$$

$$= \theta^2. \tag{2.99}$$

The viscous and conductive dissipations are given by

$$\epsilon(t) = \int_0^\infty 2\nu k^2 E(k,t)\,dk \tag{2.100}$$

and

$$\epsilon_\theta(t) = \int_0^\infty 2\kappa k^2 E_\theta(k,t)\,dk\,. \tag{2.101}$$

For the case of isotropic homogeneous flow the energy and scalar energy equations can be written in the forms

$$\frac{\partial E(k,t)}{\partial t} + \epsilon(k,t) = T(k,t) \tag{2.102}$$

and

$$\frac{\partial E_\theta(k,t)}{\partial t} + \epsilon_\theta(k,t) = T_\theta(k,t), \tag{2.103}$$

where

$$\epsilon(k,t) \equiv 2\nu k^2 E(k,t) \tag{2.104}$$

$$\epsilon_\theta(k,t) \equiv 2\kappa k^2 E_\theta(k,t) \tag{2.105}$$

are the viscous and conductive dissipation spectral densities and $T(k,t)$ and $T_\theta(k,t)$ are the velocity and scalar transfer spectral densities. In the case of LET, Equations (2.102) and (2.103) are just $4\pi k^2 \times$ Equations (2.79) and (2.82).

The integral scales for the velocity and scalar field are defined by

$$L(t) = \left[\frac{3\pi}{4}\int_0^\infty k^{-1}E(k,t)\,dk\right]/E(t) \tag{2.106}$$

$$L_\theta(t) = \left[\frac{3\pi}{4}\int_0^\infty k^{-1}E_\theta(k,t)\,dk\right]/E_\theta(t). \tag{2.107}$$

The Taylor microscale is

$$\lambda(t) = \left(\frac{15\nu}{\epsilon(t)}\right)^{1/2} u(t) \tag{2.108}$$

and the Corrsin microscale is

$$\lambda_\theta(t) = \left(\frac{6\kappa}{\epsilon_\theta(t)}\right)^{1/2} \theta(t). \tag{2.109}$$

The Reynolds numbers defined by $L(t)$ and $\lambda(t)$ are

$$R_L(t) = \frac{u(t)L(t)}{\nu}, \tag{2.110}$$

$$R_\lambda(t) = \frac{u(t)\lambda(t)}{\nu}. \tag{2.111}$$

The Prandtl number is

$$Pr = \frac{\nu}{\kappa}. \tag{2.112}$$

The velocity derivative skewness $S(t)$ and the velocity-scalar derivative skewness $S_{u\theta}(t)$ give a measure of the efficiency of energy or scalar energy transfer by the non-linear terms in the Navier-Stokes equations/scalar transport equations. The velocity derivative skewness is defined as

$$S(t) = -\frac{\langle(\partial u_1(\mathbf{x},t)/\partial x_1)^3\rangle}{\langle(\partial u_1(\mathbf{x},t)/\partial x_1)^2\rangle^{3/2}} \tag{2.113}$$

$$= \frac{2}{35}\frac{\int_0^\infty k^2 T(k,t)\,dk}{(\epsilon(t)/15\nu)^{3/2}}. \tag{2.114}$$

The velocity-scalar derivative skewness is defined as

$$S_{u\theta}(t) = -\frac{\langle(\partial u_1(\mathbf{x},t)/\partial x_1)(\partial\theta(\mathbf{x},t)/\partial x_1)^2\rangle}{\langle(\partial u_1(\mathbf{x},t)/\partial x_1)^2\rangle^{1/2}\langle(\partial\theta(\mathbf{x},t)/\partial x_1)^2\rangle} \tag{2.115}$$

$$= \frac{1}{15}\frac{\int_0^\infty k^2 T_\theta(k,t)\,dk}{(\epsilon(t)/15\nu)^{1/2}(\epsilon_\theta(t)/6\kappa)}. \tag{2.116}$$

Note that the definition of $S_{u\theta}$ in terms of T_θ is 1/2 the definition in [24], which is incorrect: the results reported in [24] *do* use the correct definition [26].

An eddy turnover time is defined using the initial rms velocity and integral length scale

$$\text{1 eddy turnover time (ett)} = L(0)/u(0). \tag{2.117}$$

At low Reynolds number we expect the energy and scalar energy spectra to be self-similar under convective scaling, using the scaled quantities

$$\tilde{k}(t) = L(t)k, \tag{2.118}$$

$$\tilde{E}(\tilde{k},t) = E(k,t)/u^2(t)L(t) \tag{2.119}$$

and

$$\tilde{k}(t) = L_\theta(t)k, \tag{2.120}$$

$$\tilde{E}_\theta(\tilde{k},t) = E_\theta(k,t)/\theta^2(t)L_\theta(t), \tag{2.121}$$

or

$$\tilde{k}(t) = \lambda(t)k, \tag{2.122}$$

$$\tilde{E}(\tilde{k},t) = E(k,t)/u^2(t)\lambda(t) \tag{2.123}$$

and

$$\tilde{k}(t) = \lambda_\theta(t)k, \tag{2.124}$$

$$\tilde{E}_\theta(\tilde{k},t) = E_\theta(k,t)/\theta^2(t)\lambda_\theta(t). \tag{2.125}$$

For the dissipation and transfer spectra, and for high Reynolds number the energy and scalar energy, we expect self-similarity under Kolmogorov scaling:

$$\tilde{k}(t) = k/k_d(t), \tag{2.126}$$

$$\tilde{E}(\tilde{k},t) = E(k,t)/(v_d^2(t)/k_d(t)), \tag{2.127}$$

$$\tilde{\epsilon}(\tilde{k},t) = \epsilon(k,t)/v_d^3(t), \tag{2.128}$$

$$\tilde{T}(\tilde{k},t) = T(k,t)/v_d^3(t), \tag{2.129}$$

$$\tilde{E}_\theta(\tilde{k},t) = E_\theta(k,t)/(\theta_d^2(t)/k_d(t)), \tag{2.130}$$

$$\tilde{\epsilon}_\theta(\tilde{k},t) = \epsilon_\theta(k,t)/v_d(t)\theta_d^2(t), \tag{2.131}$$

$$\tilde{T}_\theta(\tilde{k},t) = T_\theta(k,t)/v_d(t)\theta_d^2(t), \tag{2.132}$$

where

$$k_d(t) = \left(\frac{\epsilon(t)}{\nu^3}\right)^{1/4}, \tag{2.133}$$

$$v_d(t) = (\epsilon(t)\nu)^{1/4}, \tag{2.134}$$

$$\theta_d(t) = \left(\frac{\epsilon_\theta^2(t)}{\epsilon(t)}\nu\right)^{1/4} \tag{2.135}$$

are the Kolmogorov wavenumber, velocity and temperature, respectively. For the scalar field there are two other possible scales defined by the Batchelor wavenumber

$$k_B(t) = \left(\frac{\epsilon(t)}{\nu\kappa^2}\right)^{1/4} \tag{2.136}$$

and the Obukhov-Corrsin wavenumber

$$k_{OC}(t) = \left(\frac{\epsilon(t)}{\kappa^3}\right)^{1/4}. \tag{2.137}$$

In terms of the Kolmogorov scaled quantities, the scaled wavenumbers and scalar energy spectra are

$$\tilde{k}^B(t) = Pr^{-1/2}\tilde{k}(t), \tag{2.138}$$

$$\tilde{E}_\theta^B(\tilde{k}^B,t) = Pr^{5/6}\tilde{E}_\theta(\tilde{k},t), \tag{2.139}$$

$$\tilde{\epsilon}_\theta^B(\tilde{k}^B,t) = Pr^{1/2}\tilde{\epsilon}_\theta(\tilde{k},t), \tag{2.140}$$

$$\tilde{k}^{OC}(t) = Pr^{-3/4}\tilde{k}(t), \tag{2.141}$$

$$\tilde{E}_\theta^{OC}(\tilde{k}^{OC},t) = Pr^{5/4}\tilde{E}_\theta(\tilde{k},t). \tag{2.142}$$

Initial conditions and computational parameters

The first 'parameter' choice is the initial spectrum; on this hinges the choice of discretisation, wavenumber range, etc. The initial spectra chosen for low and medium Reynolds numbers are shown in Figure 2.1. Each may be written in the form

$$E(k,0) = c_1 k^{c_2}\exp(-c_3 k^{c_4}), \tag{2.143}$$

$$E_\theta(k,0) = c_1 k^{c_2}\exp(-c_3 k^{c_4}). \tag{2.144}$$

The values of the constants are given in Table 2.1. In most of the computations the initial scalar spectrum has the same form as the initial velocity spectrum. For the velocity spectra, $u(0) = 1$ and for the scalar spectra $\theta(0) = 1$.

At high Reynolds number an initial spectrum with the Kolmogorov form $k^{-5/3}$ was chosen with $u(0) = 5.18$ and $\theta(0) = 3.45$, see Table 2.2.

These spectra were used for the velocity field in [45] and their numerical parameters and behaviour are well characterised. They give a good range of R_λ at 1 eddy turnover time: spectra I, II, III have $R_\lambda \sim 20$, IV $R_\lambda \sim 40$ and V $R_\lambda \sim 550$. At $R_\lambda \sim 20$ convective scaling of the energy and scalar energy spectra and two-time correlations appears most appropriate, at $R_\lambda \sim 550$ Kolmogorov scaling is appropriate and at $R_\lambda \sim 40$ both scalings appear to be appropriate.

Spectra I, II and III are a family of curves with a peak at $k \sim 5$; spectrum IV peaks at much lower wavenumber; spectrum V is used to look for the Kolmogorov spectrum (we do start with the initial spectrum proportional to the Kolmogorov spectrum but using other initial spectra results in the Kolmogorov form [44]).

Almost all the calculations use the same initial spectral form for the velocity and scalar fields. Two further sets of calculations were performed with velocity/scalar initial spectra I/IV and IV/I to check that there were no special effects due to similar initial spectra and also to look at the effect of the ratio of k^u_{peak} to k^θ_{peak} on the decay of scalar energy, which has been studied in [57, 58, 61].

For most of the results reported the choice of the kinematic viscosity ν was the same as in the calculations in [45] (see Table 2.3).

In addition to the spectra I,II,III,IV and V, with the viscosities shown in Table 2.3, further computations were performed with increased viscosities and, in some cases, reduced spectral magnitudes to produce more data to clarify the relation between the velocity-scalar derivative skewness $S_{u\theta}$, the Reynolds number R_λ and the Prandtl number Pr. These computations are not reported in detail here.

Having chosen our velocity field (via the velocity initial spectrum, kinematic viscosity and the LET velocity equations) and the scalar initial spectrum, the last major parameter is the Prandtl number. The values chosen were $Pr = 0.1, 0.5, 1.0$ mainly to allow direct comparison with Kerr's direct numerical simulation [24]. Experimental results are for air ($Pr = 0.725$) and water ($Pr \sim 9.0$) and further calculations were done at $Pr = 0.725$ for spectra IV and V to compare with the

results of Yeh and van Atta [61] and Champagne *et al.* [8].

The rest of the parameters to be chosen are computational (see Table 2.3).

1. **Range of wavenumber.** The behaviour at small wavenumber is not investigated—this may mean that the results for energy and scalar energy decay are not valid at long times since the low wavenumber modes are then dominant. The value of the lowest wavenumber k_{bot} is not critical to the dynamics of the velocity or scalar fields and the values chosen in [45] are generally used. (For computations with decreased ν and/or decreased energy/scalar energy magnitude k_{bot} may be decreased). The calculations are run to 1 or 2 eddy turnover times at which point the peaks of the energy and scalar energy spectra are still well within the chosen wavenumber range. At the other end of the range, k_{top} must be greater than the larger of the Kolmogorov wavenumber k_d and the Obukhov-Corrsin wavenumber k_{OC} to ensure that the dissipation of energy/scalar energy is fully captured. Too low a value of k_{top} will cause a build-up of energy/scalar energy at the top of the wavenumber range. k_{top} must also be large enough for the integrals in the calculation of S and $S_{u\theta}$ to converge to the asymptotic values. Unfortunately this is not the case and the skewnesses reported are perhaps 5% too low. There is a problem with increasing k_{top}, apart from the increase in computation time. At wavenumbers greater than k_d, Q and Θ are very small, too small for the floating-point range of the computer used. This leads to zero-divide errors when the propagator $H(k;t,t') = Q(k;t,t')/Q(k;t',t')$ is calculated. It is possible to get $k_{top} \sim 1.5k_d$ before getting zero-divide errors but the values of k_{top} chosen in [45] are used. Increasing k_{top} has little effect on the results except for S and $S_{u\theta}$ which increase by 5%.

2. **Wavenumber resolution.** The discretisation of wavenumber space is logarithmic to get the greatest range without sacrificing detail at low to medium wavenumber where the interaction term dominates viscous and diffusive effects. At high Reynolds number the known power-law behaviour of the energy/scalar energy spectrum indicates the use of logarithmic discretisation. The logarithmic step is 1/4 octave for the low Reynolds number

computations and 1/3 octave for the medium and high Reynolds number computations. These are the values used in [45]. Increasing the wavenumber resolution has very little effect, except on the skewnesses which decrease by 5%.

3. μ **resolution.** $\Delta\mu$ is 0.08, i.e. 25 steps in $(-1,1)$ and decreasing $\Delta\mu$ to 0.04 has very little effect, even on the skewnesses, which decrease by 2%.

4. **Time step.** The time step was variable and was determined by the velocity parameters. It was the smaller of the convective characteristic time for the largest wavenumber $(1/u(t)k_{top})$ and the viscous decay characteristic time $(1/\nu k_{top}^2)$. To speed up the high Reynolds number computations the time step $(= 1/u(t)k_{top})$ was multiplied by 2 and thus lay between the two characteristic times. Using the time step from the velocity calculation does speed up the calculations slightly, since the time step increases as the rms velocity decreases in time (all the flows are dominated by convective terms). However, in the case of small Prandtl number the diffusive characteristic time $(1/\kappa k_{top}^2)$ can be much less than the time step chosen. The effects of this are mitigated by the use in the numerical algorithm of the exact time evolution for diffusive decay ($\sim \exp(-\kappa k^2 \Delta t)$). The integrated error in the scalar energy, $\Delta_\theta \equiv (1/\epsilon_\theta)\partial E_\theta/\partial t - 1$ (see below), is much larger for $Pr = 0.1$ than for $Pr = 0.5$ or $Pr = 1.0$ up to about 0.25 eddy turnover times but drops to a value similar to that for $Pr = 0.5$ or $Pr = 1.0$ by 1 eddy turnover time: the effect is most marked with spectra II and III. So the results at $Pr = 0.1$ need to be viewed with some care, although they are consistent with results at $Pr = 0.5$ and $Pr = 1.0$.

5. **Iterations** All the computations except at high Reynolds number iterated the predictor-corrector scheme until the difference in values of Q, Θ, H and $H^{\theta\theta}$ between the nth and $(n-1)$th iteration was less than 10%. To speed up the high Reynolds number computation a single predictor-corrector iteration was used (this gave very little difference in the velocity field in previous work [45]). At low Reynolds number the difference between multiple and

single iteration was seen only in change of 5% in the skewnesses. Decreasing the tolerance to 1% made no perceptible difference to the results and required 6–7 iterations per time step, compared to 4–5 with the tolerance set to 10%.

6. All the calculations except at the highest Reynolds number were run to at least 1 eddy turnover time. The highest Reynolds number computation was run to 0.38 eddy turnover times. (Note: the computational time goes as $t^3_{evolved}$).

The effects of the choice of computational parameters have been checked extensively for a calculation with velocity initial spectrum I, scalar initial spectrum I, $\nu = 0.1189$ and $Pr = 0.5$. In Figure 2.2 the evolution of the scalar energy, dissipation and skewness is plotted, along with the evolution of the Reynolds numbers. The multiple lines correspond to choices of the computational parameters:

1. original parameters (used in the rest of the results), variable timestep, multiple iterations,
2. $2\times$ wavenumber resolution,
3. $2\times$ μ resolution,
4. $2\times$ wavenumber and μ resolution,
5. k_{bot} decreased one logarithmic step,
6. k_{top} increased one logarithmic step,
7. k_{bot} decreased and k_{top} increased,
8. fixed time step,
9. fixed time step, decreased 15%,
10. fixed time step, increased 15%,
11. single iteration.

The most sensitive parameter is the velocity-scalar derivative skewness which varies by 10%, tending to increase when the wavenumber range is increased and decrease when the wavenumber resolution is increased or the time step decreased. The integrated error (see below) remains small for all the choices. In Figure 2.3 the effect of the computational parameters on the evolved scalar energy spectrum is shown. There are slight differences in the magnitude of the spectra but some of this is due to differences in the evolved times at which the spectra were calculated.

Dr. V. Shanmugasundaram has run further computations with the same initial conditions but using smaller time steps and increased wavenumber and μ resolution. The major difference between his results and those presented here is in the velocity-scalar derivative skewness values , which are up to 12% lower in his computations.

Errors

It is difficult to find an analytical estimate of the errors in the predictor-corrector scheme and wavenumber integration and discretisation errors in k, μ, t (see [28] for a similar problem). To check the accuracy (within the LET approximation) of the computer calculations we look at the conservation of energy and scalar energy. The energy and scalar energy balance equations (Equations (2.102) and (2.103)) can be integrated over k to yield the integrated energy balance equations

$$\frac{dE(t)}{dt} + \epsilon(t) = 0, \tag{2.145}$$

$$\frac{d_\theta E(t)}{dt} + \epsilon_\theta(t) = 0. \tag{2.146}$$

The overall error can be measured by

$$\Delta = \frac{1}{\epsilon(t)}\frac{dE(t)}{dt} + 1, \tag{2.147}$$

$$\Delta_\theta = \frac{1}{\epsilon_\theta(t)}\frac{dE_\theta(t)}{dt} + 1. \tag{2.148}$$

More detailed measures are

$$\Delta(k,t) = \frac{\partial E(k,t)}{\partial t} + \epsilon(k,t) - T(k,t), \tag{2.149}$$

$$\Delta_\theta(k,t) = \frac{\partial E_\theta(k,t)}{\partial t} + \epsilon_\theta(k,t) - T_\theta(k,t). \tag{2.150}$$

Note that $\Delta(t)$ is a relative error and $\Delta(k,t)$ is an absolute error. $\Delta(t)$ and $\Delta_\theta(t)$ are used throughout the computations to check the accuracy. $\Delta(t) \sim 10^{-4}$ to 10^{-3} at 1 eddy turnover time for all the velocity initial spectra used [45]. $\Delta(t)$ is much larger than this in the initial stages of a computation but settles down very quickly. For low and medium Reynolds numbers $\Delta_\theta(t) \sim 10^{-3}$ at 1 eddy turnover time. It is larger in the initial stages (≤ 5 time steps) of a computation, especially for $Pr = 0.1$ and initial spectra II and III but in all cases $\Delta_\theta(t) \lesssim 10^{-2}$ by 0.5 eddy turnover times. For high Reynolds number $\Delta_\theta(t) \sim 10^{-2}$ at 0.38 eddy turnover times (the end of the computation).

$\Delta_\theta(k,t)$ was used to check the effects of computational parameters (see above) and the detailed scalar energy balance at 1 eddy turnover time is shown in Figure 2.4. Again, some of the variation is due to slightly different evolution times for the various computations. $\Delta_\theta(k,t)$ cannot be distinguished from zero except for the single iteration case, where it has a maximum value of about 0.02.

Original formulation and errors

The computations were first done using the formulation given by Equation (2.75). These calculations did not conserve scalar energy. At high Reynolds number ($R_\lambda(0) = 245$) the computations failed after the 3rd time step, when the scalar energy became negative. At low Reynolds number $\Delta_\theta(t)$ was very large, around 15%. $\Delta_\theta(t)$ was improved by increasing the wavenumber and μ resolution; decreasing the time step had no effect. At $6\times$ the wavenumber resolution and $4\times$ the μ resolution $\Delta_\theta(t)$ drops to $5\times$ the $\Delta_\theta(t)$ in the same calculation using the present formulation (Equation (2.73)) with $1\times$ the wavenumber and μ resolution. Decreasing the time step had no effect on the $\Delta_\theta(t)$. Using $\Delta_\theta(k,t)$, it was found that most of the error occurred at large k.

The main difference between the two formulations lies in the geometrical factors, although there will be some difference in the $H^{\theta\theta}Q\Theta$ terms due to interpolation and boundary effects. The geometrical factor in the original formulation is

$$\begin{aligned} N(\mathbf{k},\mathbf{j}) &= k^2(1-\mu_{\mathbf{kj}}^2) \\ &= k^2(1-\mu^2), \end{aligned} \tag{2.151}$$

where we write μ for $\mu_{\mathbf{kj}}$. The geometrical factor in the present formulation is

$$\begin{aligned} N(\mathbf{k},\mathbf{k}-\mathbf{j}) &= k^2(1-\mu_{\mathbf{k},\mathbf{k}-\mathbf{j}}^2) \\ &= k^2\frac{j^2(1-\mu^2),}{(\mathbf{k}-\mathbf{j})^2}. \end{aligned} \tag{2.152}$$

Note that $N(\mathbf{k},\mathbf{k}-\mathbf{j})$ is symmetric under $\mathbf{k} \leftrightarrow \mathbf{j}$.

One of the basic assumptions of LET is that the interactions are predominantly local in wavenumber. If we take the limit $\mathbf{j} \to \mathbf{k}$, i.e. local in wavenumber, then $N(\mathbf{k},\mathbf{k}-\mathbf{j}) \to -1$ and $N(\mathbf{k},\mathbf{j}) \to 0$. This indicates that the present formulation is more suitable for representing local in wavenumber effects than the original formulation, so that the wavenumber and μ discretisation can be coarser.

The effect of the geometrical factor was checked for the velocity case as well. Using $L(\mathbf{k},\mathbf{k}-\mathbf{j})$ instead of $L(\mathbf{k},\mathbf{j})$ (and swapping $\mathbf{k}$ and $\mathbf{k}-\mathbf{j}$ in the HQQ terms) increased $\Delta(t)$ in a low Reynolds number computation.

It thus appears that the choice of wavenumber argument in the transfer term integral is crucial for the numerical computation of LET.

2.6 Results

The results of the LET calculations can be divided into the following areas

1. At low Reynolds numbers we look at varying Prandtl numbers and varying initial spectra to investigate the behaviour of LET.

2. The effect of different peak wavenumbers in the velocity field and the scalar field is considered.

3. At medium Reynolds number we compare our results with the grid turbulence experiments of Yeh and van Atta [61].

4. At high Reynolds number we show that LET gives a $k^{-5/3}$ inertial-convective range and find a value for the Obukhov-Corrsin constant β.

5. We show the effect of Reynolds number on the scaling of the time separation in the two-time correlation $\Theta(k;t,t_{ref})/[\Theta(k;t,t)\Theta(k;t_{ref},t_{ref})]^{1/2}$.

6. The change in the detailed scalar energy balance with increasing Reynolds number is discussed.

7. The dependence of the velocity-scalar derivative skewness $S_{u\theta}$ on R_λ and Pr is compared with direct numerical simulation and experiment.

Table 2.3 lists the computational parameters of the principal calculations. In order to fill out the $S_{u\theta}$ *vs.* R_λ graphs, many more computations were performed with different ν (and κ) and initial spectral magnitudes. Tables 2.4 and 2.5 give the initial integral parameters (energy, dissipation, rms values, etc.) for the velocity and scalar fields. Tables 2.6 and 2.7 give the integral parameters at 1 eddy turnover time (ett), where 1 eddy turnover time = $L(0)/u(0)$, the initial velocity integral scale divided by the initial rms velocity.

Low Reynolds number

At low Reynolds number we concentrate on run I/I with $Pr = 0.5$ to look at the behaviour of LET. The evolution of the integral parameters for this computation is shown in Figure 2.5. The following points can be noted:

1. The scalar energy E_θ decreases uniformly, but the scalar dissipation ϵ_θ and the velocity-scalar derivative skewness $S_{u\theta}$ have large transients. These are due to the initial transfer of scalar energy to higher wavenumbers from the very peaked initial spectrum. At smaller Pr (i.e. κ larger) the overshoots

are much smaller or disappear (see Figure 2.13). There are similar transients in the LET velocity field [45], and also in EDQNM [38]. All spectra, correlations, etc. are measured at times beyond the transient behaviour (in this case beyond 0.5 eddy turnover times).

2. The skewness settles down but shows a slow increase with time.

3. The integrated error Δ_θ is always less than 2% and is negligible at 1 eddy turnover time.

In Figures 2.6, 2.7 and 2.8 the evolution of the scalar energy, scalar dissipation and scalar transfer is shown from $t = 0$ to $t = 1$ eddy turnover time. The scalar energy spectrum decays, with k^θ_{peak} decreasing in time. The scalar dissipation is initially peaked at the peak of the initial spectrum but soon spreads out to higher wavenumbers.

With a suitable choice of scaling of the scalar energy and the wavenumber, the scalar energy spectrum will become self-similar. There are several choices for the wavenumber and scalar energy scales: integral: $1/L_u$ and $\theta^2 L_u$, or $1/L_\theta$ and $\theta^2 L_\theta$; microscale: $1/\lambda_u$ and $\theta^2\lambda_u$, or $1/\lambda_\theta$ and $\theta^2\lambda_\theta$; Kolmogorov: k_d and Θ_d^2/k_d. All of these scalings were tested on the scalar energy spectra for all of the computations shown in Table 2.3. The best overall for low and medium Reynolds number was scalar integral scaling, with scaled wavenumber $kL_\theta(t)$ and scaled scalar energy $E_\theta(k,t)/\theta^2(t)L_\theta(t)$. This gave good collapse of data, both at the scalar energy peak and at higher wavenumbers, whereas λ_θ and k_d scaling were generally poor at the peak but very good at higher wavenumbers. However, at high Reynolds number Kolmogorov scaling is best. Spectra II and III and $Pr = 0.1$ do not scale well at the scalar energy peak for any scaling. Figure 2.9 shows the self-similarity of the scalar energy spectrum under scalar integral scaling for spectra I/I, $Pr = 0.5$.

The the scalar dissipation and transfer spectra also become self-similar, using Kolmogorov scaling (which is dependent on the total dissipation). Batchelor and Obukhov-Corrsin scaling are variations on Kolmogorov scaling and only affect comparisons across Prandtl number. Figures 2.10 and 2.11 show the excellent

self-similarity of ϵ_θ and T_θ under Kolmogorov scaling.

We now consider the effect of Prandtl number in the I/I computations. Figures 2.12, 2.13 and 2.14 show the evolution of scalar energy, dissipation and skewness. For fixed ν, decreased Pr means increased κ, so we expect to see stronger decay of E_θ as Pr decreases, as shown in Figure 2.12. At large Pr the scalar dissipation peaks in the initial period due to the transfer of energy to larger wavenumbers, where dissipation is more effective, then decays in time. At low Pr dissipation is effective over a larger range of wavenumber so there is no transient redistribution of scalar energy. The strong decay of the scalar energy leads to a strong decay of the dissipation (note that Figure 2.13 is scaled by $\epsilon_\theta(0)$ which is much larger for $Pr = 0.1$). The skewness $S_{u\theta}$ increases with decreasing Pr, see Figure 2.14 (this is discussed at the end of this Chapter).

The main effect of Pr on the scaled spectra (Figures 2.15, 2.16 and 2.17) is in the ratio of the energy peak to the energy at higher wavenumbers. For κ large the scalar energy at large wavenumbers has been strongly dissipated, compared with E_θ at lower wavenumbers. This leads to a shift downwards in wavenumber of the peaks in E_θ, ϵ_θ and T_θ, and a relative increase in the peak values, as the Prandtl number is decreased.

The choice of initial spectra I/I, II/II or III/III has little effect on the evolved spectra away from the scalar energy peak (see Figures 2.18, 2.19 and 2.20).

The two-time correlations of the scalar field $\Theta(k;t,t_{ref})/[\Theta(k;t,t)\Theta(k;t_{ref},t_{ref})]^{1/2}$ can be plotted against the time separation $t_{ref} - t$ as shown in Figure 2.21. The wavenumbers range from k_{bot} to k_{top}. With a suitable choice of scaling, the curves in Figure 2.21 should coincide and the effects of convective, Kolmogorov and dissipative decay scaling are shown in Figures 2.22, 2.23 and 2.24. Convective scaling seems to be best for this relatively low Reynolds number computation. The Prandtl number has very little effect on the scaled curves and an example at middling wavenumber is shown in Figure 2.25. The propagator $H^{\theta\theta}(k;t_{ref},t) = \Theta(k;t_{ref},t)/\Theta(k;t,t)$ is shown in Figure 2.26, scaled by convective time scales. The non-zero slope at $t_{ref} - t = 0$ is due to the time decay of $\Theta(t,t)$.

Different velocity and scalar initial spectra

Calculations I/I, I/IV, IV/I and IV/IV were made in order to look at the effect of changing the relative length scales of the velocity and scalar fields.

Figures 2.27, 2.28 and 2.29 show the effect on the integral parameters. After an initial period, the scalar energy decay appears to depend on the velocity field: $\epsilon_\theta (= -\partial E_\theta/\partial t)$ separates into the groups I/I, I/IV and IV/I, IV/IV. However, the scalar energy and the velocity-scalar derivative skewness appear to depend on the ratio of the velocity and scalar length scales ($k_{peak}(IV) < k_{peak}(I)$).

At 1 eddy turnover time, the energy spectrum (Figure 2.30) show a clear grouping by scalar initial spectrum: IV/IV and I/IV, IV/I and I/I. This grouping is less clear, or not present, in the scalar dissipation and transfer spectra (Figures 2.31 and 2.32).

The effect of the ratio of k^θ_{peak} to k^u_{peak} on the scalar energy decay rate has been investigated by Warhaft and Lumley [58]. In grid turbulence experiments previous to Warhaft and Lumley's work the decay rate of θ^2 showed large variation between experiments (the decay of u^2 did not). Warhaft and Lumley suggested that the effect may be due to differing length scales for the scalar field and found a linear relation between the thermal to mechanical decay timescale ratio (in our notation $= (\epsilon_\theta/E_\theta)/(\epsilon/E)$) and the ratio $k^\theta_{peak}/k^u_{peak}$, where k^θ_{peak}, k^u_{peak} is the peak of the E_θ, E spectrum respectively. However, further experiments by Sreenivasan *et al.* [57] found no dependence of the thermal to mechanical ratio and the peak wavenumber ratio (strictly the ratio of the turbulence generating grid size to the heating grid size).

The present results are not directly comparable since the evolution time is about 1 eddy turnover time compared with 3–4 ett in Warhaft and Lumley's work, which means that we do not see universal decay laws $E \sim t^{-a}$ and $E_\theta \sim t^{-b}$ typical at long times. However, we can still look at $(\epsilon_\theta/E_\theta)/(\epsilon/E)$ and the LET results are in fair agreement with the results of Warhaft and Lumley (see Figure 2.33).

Comparison with grid turbulence

Computation IV/IV with $Pr = 0.725$ is quite close to the experimental conditions of Yeh and van Atta [61], with whom we can compare scalar energy, dissipation and transfer spectra.

In our units, values of the relevant parameters for run IV/IV, $Pr = 0.725$ and Yeh and van Atta's experimental conditions (their Table 1) are compared in Table 2.8. The unit conversion is based on the Kolmogorov scales $1/k_d$, τ_d and θ_d.

The scalar energy, dissipation and transfer spectra are compared in Figures 2.34, 2.35 and 2.36. The results are in fair agreement, considering that the conditions are not identical and also that the unit conversion based on the Kolmogorov scales may not be the most appropriate: at this R_λ, L_θ scaling seems as good as Kolmogorov scaling for the scalar energy spectrum, as shown in Figures 2.37 and 2.38. The two-time correlations (Figures 2.39 and 2.40) also show little to choose between convective and Kolmogorov scaling.

High Reynolds number

The high Reynolds number calculations are based on spectrum V. The computations have been evolved to 0.38 eddy turnover times only ($R_\lambda(0.38 \text{ ett}) = 558$) but the integral parameters (see Figures 2.41, 2.42 and 2.43) and spectra (se Figures 2.44, 2.45 and 2.46 for $Pr = 0.5$) appear to be fully evolved. The scalar energy decay is small because of the small κ, even for $Pr = 0.1$. The spectra are self-similar under Kolmogorov scaling and show good collapse of the curves at different times. For $Pr = 0.5$ the scalar energy spectrum has a well defined inertial-convective range proportional to $k^{-5/3}$ (see Figures 2.44 and 2.52). As the Prandtl number is decreased from 1, the Obukhov-Corrsin, Batchelor and Kolmogorov wavenumbers separate. At $Pr = 0.1$ we still (just) see an inertial-convective range proportional to $k^{-5/3}$ (see Figure 2.52). However, no k^{-3} [12] or $k^{-17/3}$ [6] ranges are seen, because the separation of wavenumbers is not large enough ($k_{O-C} = 0.18 k_d$, $k_{O-C} < k_B < k_d$). At $Pr = 0.725$ and $Pr = 1.0$ we start to see a 'bump' near 0.1 k_d (see Figure 2.52) which is the precursor of a k^{-1} range

(seen in sea water, $Pr = 9.5$, in [15]).

Figures 2.47, 2.48 and 2.49 show the effect of different scaling on the collapse of the scalar energy curves for different Prandtl number. Figure 2.47 is 'plain' Kolmogorov scaling, with no Prandtl number dependence. Of the two, Obukhov-Corrsin scaling gives a better collapse than Batchelor scaling (but note that this is a log-log plot).

The scalar dissipation spectrum for different Prandtl number is plotted in Figure 2.50 on a log-linear plot to highlight the exponential tail in the spectrum. This is apparent for $Pr = 0.1$ only. Gibson [12] has postulated that Batchelor scaling will hold in the dissipation range and the curves of Figure 2.50 do collapse under this scaling (see Figure 2.51).

The value of the Kolmogorov constant α in the expression

$$E(k) = \alpha \epsilon^{2/3} k^{-5/3} \tag{2.153}$$

for the energy spectrum in the inertial range is predicted by LET to be $\alpha = 2.53$ using the spectrum V calculation ($R_\lambda = 550$). The experimental range is 1.5–1.6. The Obukhov-Corrsin constant β in the corresponding equation for the scalar energy spectrum in the inertial-convective range,

$$E_\theta(k) = \beta \epsilon_\theta \epsilon^{-1/3} k^{-5/3}, \tag{2.154}$$

can be estimated from Figure 2.52 which is a plot of the Kolmogorov normalised scalar energy spectrum multiplied by $(k/k_d)^{-5/3}$. β appears to depend on Prandtl number, but this is probably due to the 'bump' affecting the short inertial range for $Pr = 0.725$ and $Pr = 1.0$; at $Pr = 0.1$ there is almost no inertial range. If we choose the $Pr = 0.5$ curve we get $\beta = 1.13$ compared with the experimental range 0.7–0.8. So both the Kolmogorov and Obukhov-Corrsin constants are over-estimated by the LET theory. However the ratio $\beta/\alpha = 0.45$, which is the eddy Prandtl number at sufficiently high Reynolds number [47], is very close to the accepted experimental value 0.44.

In Figure 2.53 we compare the results for computation V/V and $Pr = 0.725$

with the atmospheric boundary layer experiments of Champagne *et al.* [8]. The 'bump' is almost non-existent in the one-dimensional spectrum for the LET calculation. This and the large value of β are consistent with LET underestimating the transfer of scalar energy. However, the velocity-scalar derivative skewness, which is a measure of the transfer efficiency, is equal to the experimental value for this Reynolds number (see below) which would imply that LET correctly estimates the transfer of scalar energy.

Scaling of two-time correlations

Figures 2.22 and 2.23 for $R_\lambda = 19$, Figures 2.39 and 2.40 for $R_\lambda = 41$ and Figures 2.54 and 2.55 for $R_\lambda = 558$ compare the effects of convective and Kolmogorov scaling for the two-time correlations. $R_\lambda = 19$ may not be low enough to clearly show the superiority of convective scaling but it does appear better than Kolmogorov scaling. At $R_\lambda = 41$ convective scaling seems to be marginally better, but Kolmogorov scaling is better at higher wavenumbers. At $R_\lambda = 558$ Kolmogorov scaling is superior. Figure 2.56 shows the propagator at $R_\lambda = 558$ using Kolmogorov scaling. At all these Reynolds numbers the Prandtl number has very little effect on the correlation (see Figures 2.25, 2.57 and 2.58).

Detailed scalar energy balance

As the Reynolds number increases, we expect the range of wavenumbers where dissipation occurs to become distinct from the range where scalar energy production occurs (in the case of decaying turbulence, where the rate of change of scalar energy is the largest), as is the case for the LET calculations of the velocity field [44]. This can be seen by comparing Figures 2.59, 2.60 and 2.61, where R_λ increases from 19 to 41 to 558. At low Reynolds number, the ϵ_θ range and $\partial E_\theta/\partial t$ range are overlapping but by $R_\lambda = 558$ the ranges are distinct, linked by the transfer term T_θ.

Dependence of $S_{u\theta}$ on R_λ and Pr

In addition to the principal computations listed in Table 2.3, many more computations at a variety of R_λ(1 ett) were performed to find the dependence of the velocity-scalar derivative skewness $S_{u\theta}$ on the Reynolds number and Prandtl number, shown in Figure 2.62. (The values for computation V/V at $R_\lambda = 558$ are listed in Table 2.9). The general trend is for the skewness to increase up to $R_\lambda \sim 10$, then slowly decrease with Reynolds number.

Experimental values for $S_{u\theta}$ are scarce. Larcheveque *et al.* [35] summarise experiments in a skewness *vs.* Prandtl number graph, but for $Pr = 0.7$ (air) $S_{u\theta}$ ranges from -0.4 to -0.62. Antonia and Chambers [2] plot skewness *vs.* Reynolds number, mainly for $Pr = 0.7$ but for R_λ much larger than the range in Figure 2.62; their results can be compared with Table 2.9; at $R_\lambda = 558$ and $Pr \sim 0.725$, they find $S_{u\theta} = -0.33$ which compares favourably with LET's value.

In the range of R_λ shown in Figure 2.62, we compare LET's results with those from the direct numerical simulation of Kerr [24]. These results are for low wavenumber forced velocity and scalar fields and so are for stationary turbulence. For $Pr = 0.5$ and $0 < R_\lambda < 10$ the results agree very well. However, above $R_\lambda = 10$ the simulation values increase with increasing Pr, while the LET $-S_{u\theta}$ values decrease with increasing Pr which is what we might expect if the velocity field is driving the scalar transfer (higher Pr implies higher κ for the same ν thus a stronger 'sink' of scalar energy at high wavenumbers and thus larger scalar energy transfer from low k to high k). Also, the LET $-S_{u\theta}$ values for $Pr = 0.5$ and $Pr = 1.0$ show a slow decrease with Reynolds number, while the simulation values become constant above $R_\lambda \sim 30$. Kerr suggests that at high Reynolds number the velocity-scalar derivative skewness becomes independent of Reynolds number and Prandtl number, with a value of -0.5. This is at variance with Antonia and Chambers [2] who suggest a $S_{u\theta} \sim -R_\lambda^{0.15}$ dependence.

Table 2.1: Values of the constants c in Equations (2.143) and (2.144). For the scalar spectrum c_1 is $2/3\times$ the value shown.

Spectrum number	c_1	c_2	c_3	c_4
I	0.00524	4	0.0884	2
II	0.0663	1	0.0221	2
III	0.0663	1	0.210	1
IV	0.4	1	0.5	1

Table 2.2: Initial spectrum for high Reynolds number calculations.

Spectrum number	
V	$E(k,0) = 2\pi k^{-5/3}$
V	$E_\theta(k,0) = (4/3)\pi k^{-5/3}$

Table 2.3: Computational parameters

Initial spectra velocity/scalar	k_{bot}	k_{top}	$\Delta(oct)$	ν	Pr	$\Delta t(0)$	Δt(1 ett)
I/I	1.83	29.3	0.25	0.0119	0.1,0.5,1.0	0.034	0.045
I/IV	0.281	35.9	0.333	0.0119	0.5,1.0	0.028	0.037
II/II	1.09	29.3	0.25	0.0119	0.1,0.5,1.0	0.034	0.048
III/III	1.09	49.3	0.25	0.01	0.1,0.5,1.0	0.02	0.03
IV/I	0.281	35.9	0.333	0.008	0.5,0.725,1.0	0.027	0.034
IV/IV	0.281	35.9	0.333	0.008	0.1,0.5,0.725,1.0	0.027	0.034
V/V	0.111	71.8	0.333	0.008	0.1,0.5,0.725,1.0	0.0054	0.0056

Table 2.4: Integral parameters at $t = 0$, velocity field

Initial spectrum	E	ϵ	R_L	R_λ
I	1.48	1.01	43.0	35.0
II	1.46	1.62	43.3	27.3
III	1.47	4.05	39.9	18.8
IV	1.59	0.616	133	58.5
V	40.2	22.5	5521	245

Table 2.5: Integral parameters at $t = 0$, scalar field

Initial spectrum	Pr	E_θ	ϵ_θ	L_θ	λ_θ
I/I	0.1	0.990	6.73	0.514	0.418
I/I	0.5	0.990	1.35	0.514	0.418
I/I	1.0	0.990	0.673	0.514	0.418
I/IV	0.5	1.06	1.22	1.03	0.454
I/IV	1.0	1.06	0.610	1.03	0.454
II/II	0.1	0.975	10.8	0.522	0.328
II/II	0.5	0.975	2.15	0.522	0.328
II/II	1.0	0.975	1.08	0.522	0.328
III/III	0.1	0.978	27.0	0.413	0.190
III/III	0.5	0.978	5.40	0.413	0.190
III/III	1.0	0.978	2.70	0.413	0.190
IV/I	0.5	1.00	0.907	0.527	0.420
IV/I	0.7	1.00	0.625	0.527	0.420
IV/I	1.0	1.00	0.454	0.527	0.420
IV/IV	0.1	1.06	4.11	1.03	0.454
IV/IV	0.5	1.06	0.821	1.03	0.454
IV/IV	0.7	1.06	0.566	1.03	0.454
IV/IV	1.0	1.06	0.410	1.03	0.454
V/V	0.1	26.8	150	8.53	0.378
V/V	0.5	26.8	30.0	8.53	0.378
V/V	0.7	26.8	20.6	8.53	0.378
V/V	1.0	26.8	15.0	8.53	0.378

Table 2.6: Integral parameters at $t = 1$ ett, velocity field

Initial spectrum	E	ϵ	R_L	R_λ	$-S$
I/I	0.846	1.11	30.9	19.0	0.466
I/IV	0.869	1.13	32.9	19.4	0.484
II	0.769	0.933	36.4	18.8	0.442
III	0.681	0.983	37.2	17.7	0.460
IV	1.02	0.515	122	41.0	0.416
V	36.9	3.65	5424	558	0.349

Table 2.7: Integral parameters at $t = 1$ ett, scalar field

Initial spectrum	Pr	E_θ	ϵ_θ	L_θ	λ_θ	$-S_{u\theta}$
I/I	0.1	0.0555	0.221	0.754	0.546	0.533
I/I	0.5	0.286	0.759	0.508	0.299	0.392
I/I	1.0	0.440	0.917	0.435	0.239	0.316
I/IV	0.5	0.529	0.706	1.35	0.422	0.441
I/IV	1.0	0.653	0.753	1.16	0.321	0.373
II/II	0.1	0.0940	0.230	1.08	0.697	0.529
II/II	0.5	0.290	0.584	0.697	0.344	0.401
II/II	1.0	0.415	0.724	0.582	0.157	0.319
III/III	0.1	0.133	0.407	0.928	0.572	0.508
III/III	0.5	0.336	0.828	0.614	0.285	0.423
III/III	1.0	0.451	0.970	0.520	0.216	0.366
IV/I	0.5	0.198	0.339	0.584	0.306	0.366
IV/I	0.725	0.258	0.406	0.526	0.265	0.327
IV/I	1.0	0.353	0.517	0.474	0.233	0.303
IV/IV	0.1	0.215	0.209	2.13	0.907	0.518
IV/IV	0.5	0.422	0.378	1.40	0.423	0.388
IV/IV	0.725	0.492	0.428	1.27	0.356	0.346
IV/IV	1.0	0.533	0.435	1.19	0.313	0.322
V/V	0.1	21.2	5.85	9.30	1.70	0.455
V/V	0.5	22.9	5.09	8.70	0.848	0.357
V/V	0.725	23.2	4.90	8.59	0.723	0.332
V/V	1.0	23.5	4.74	8.49	0.629	0.310

Table 2.8: Comparison of the parameters for computation IV/IV, $Pr = 0.725$ with the experimental conditions of Yeh and van Atta [61]

	u	ϵ	λ	R_λ	θ	ϵ_θ	λ_θ
IV/IV	0.83	0.52	0.4	41	0.99	0.43	0.39
Yeh and van Atta	0.77	0.53	0.37	35	1.2	0.43	0.47

Table 2.9: Velocity-scalar derivative skewness at various Pr for velocity initial spectrum V, scalar initial spectrum V, at 0.38 eddy turnover times, $R_\lambda = 558$.

Pr	$-S_{u\theta}$
0.1	0.46
0.5	0.36
0.725	0.33
1.0	0.31

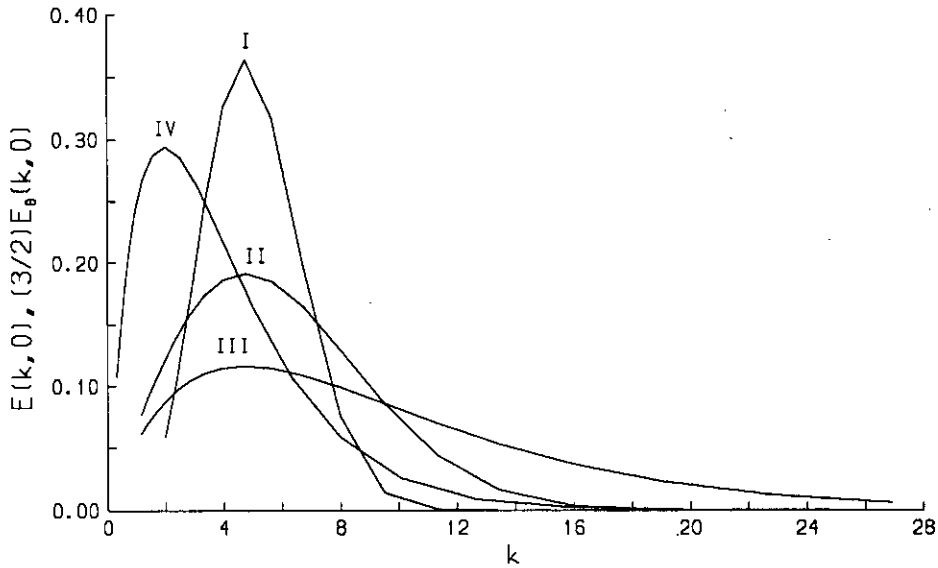

Figure 2.1: Initial spectra.

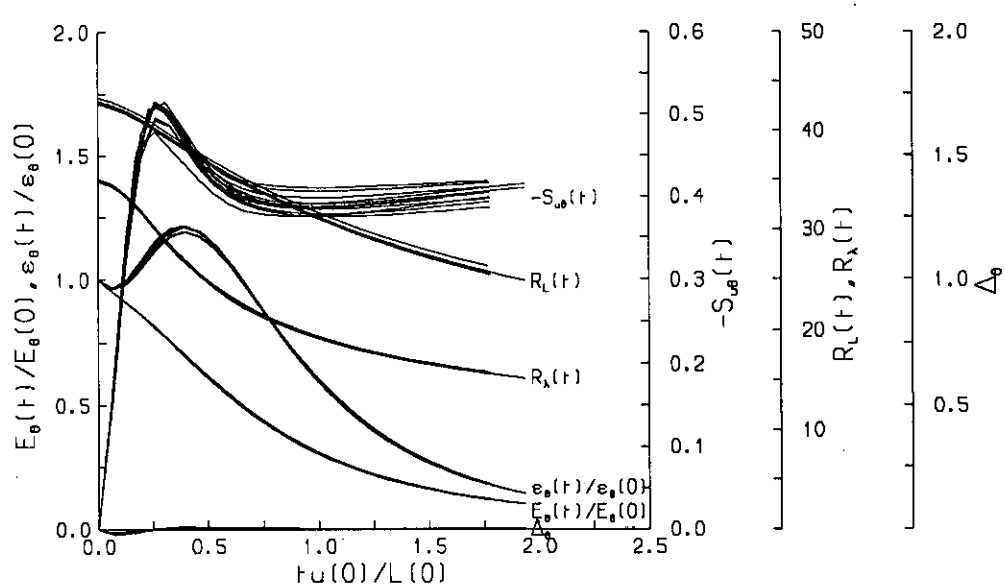

Figure 2.2: Evolution of the integral parameters for $Pr = 0.5$, velocity initial spectrum I, scalar initial spectrum I. Effect of varying the computational parameters.

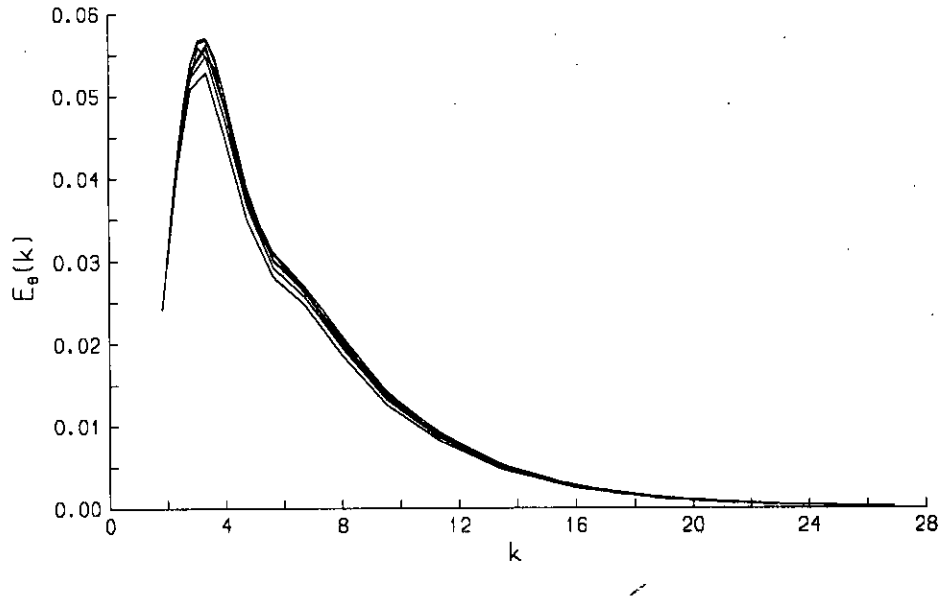

Figure 2.3: Scalar energy spectrum at 1 eddy turnover time, $R_\lambda = 19$, for $Pr = 0.5$, velocity initial spectrum I, scalar initial spectrum I. Effect of varying the computational parameters.

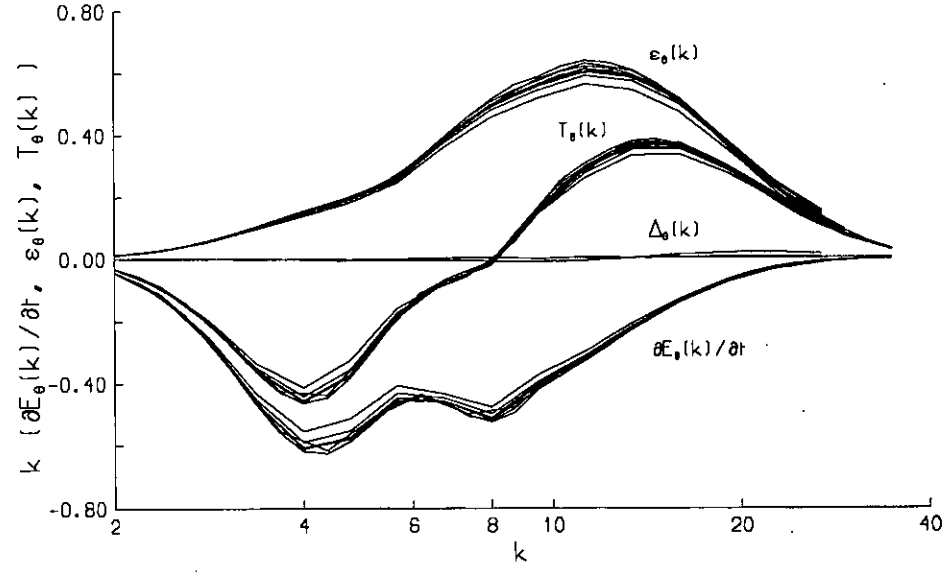

Figure 2.4: Detailed scalar energy balance at 1 eddy turnover time, $R_\lambda = 19$, for $Pr = 0.5$, velocity initial spectrum I, scalar initial spectrum I. Effect of varying the computational parameters.

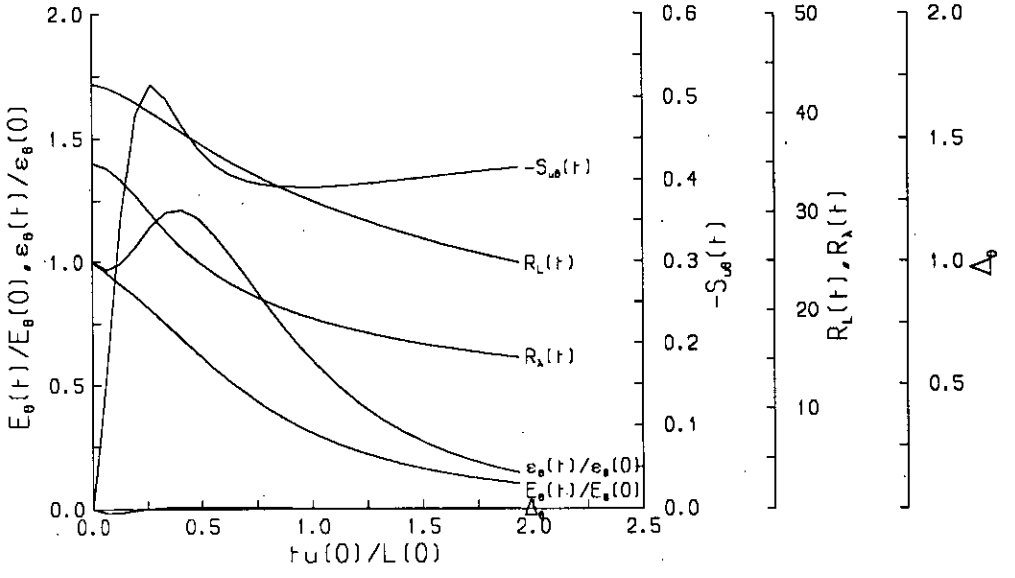

Figure 2.5: Evolution of the integral parameters for $Pr = 0.5$, velocity initial spectrum I, scalar initial spectrum I.

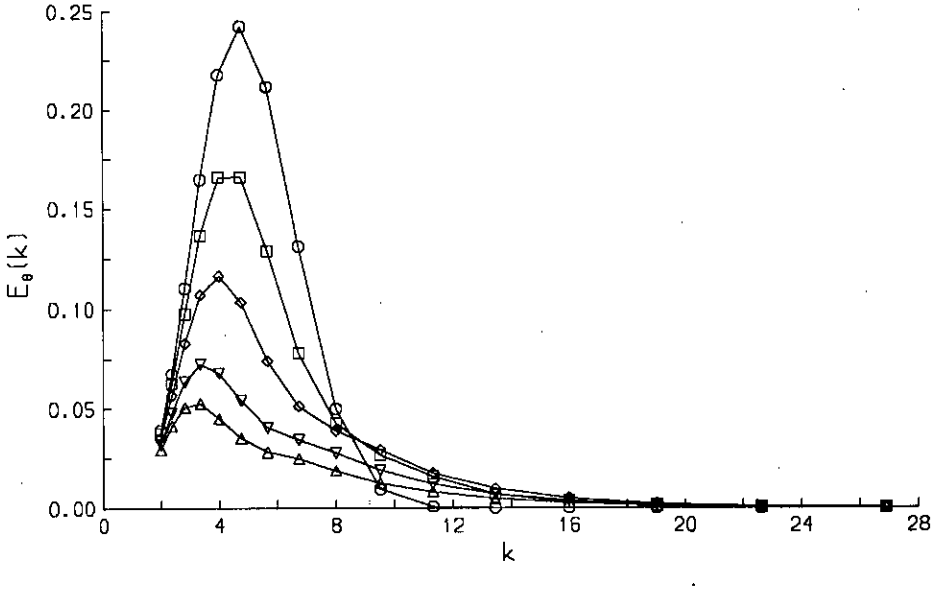

Figure 2.6: Evolution of the scalar energy spectrum for $Pr = 0.5$, velocity initial spectrum I, scalar initial spectrum I. ○, $t = 0.0$ ett(eddy turnover time); □, $t = 0.25$ ett; ◇, $t = 0.5$ ett; ▽, $t = 0.75$ ett; △, $t = 1.0$ ett.

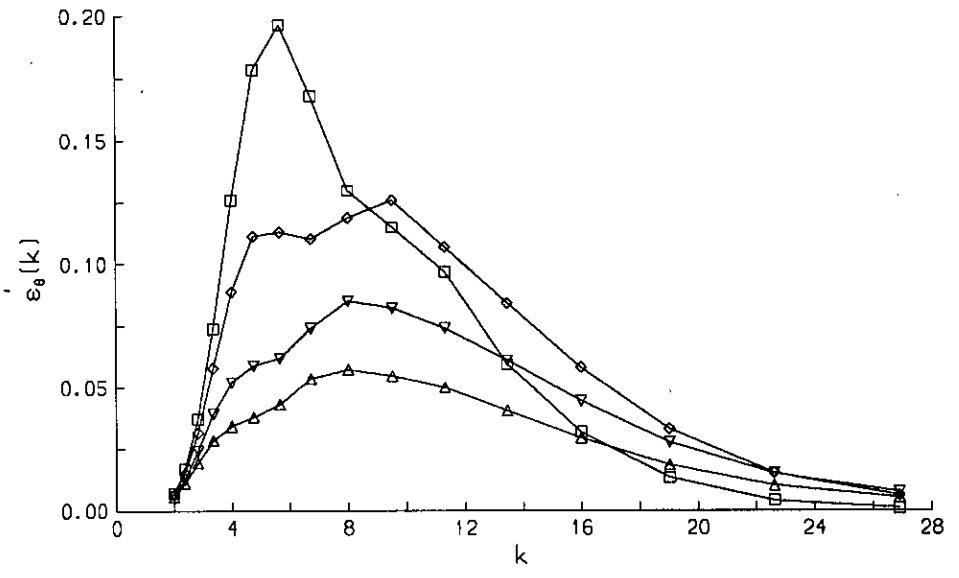

Figure 2.7: Evolution of the scalar dissipation spectrum for $Pr = 0.5$, velocity initial spectrum I, scalar initial spectrum I. □, $t = 0.25$ ett(eddy turnover time); ◇, $t = 0.5$ ett; ▽, $t = 0.75$ ett; △, $t = 1.0$ ett.

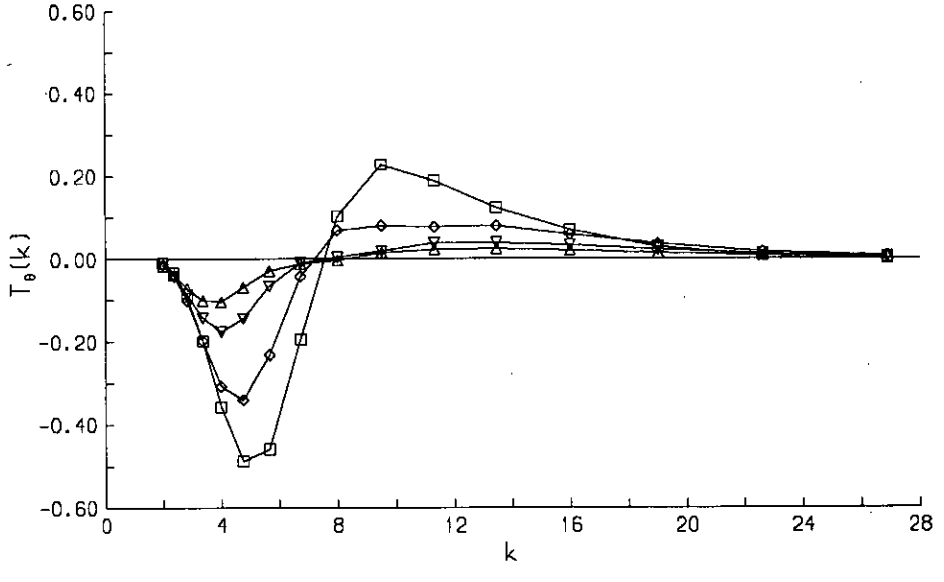

Figure 2.8: Evolution of the scalar transfer spectrum for $Pr = 0.5$, velocity initial spectrum I, scalar initial spectrum I. □, $t = 0.25$ ett(eddy turnover time); ◇, $t = 0.5$ ett; ▽, $t = 0.75$ ett; △, $t = 1.0$ ett.

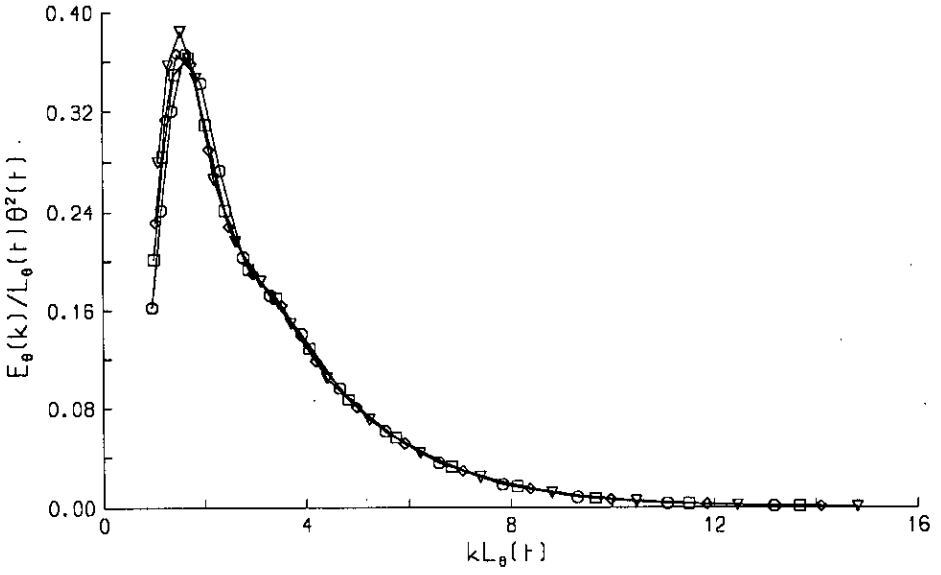

Figure 2.9: Self-similarity of the scalar energy spectrum for $Pr = 0.5$, velocity initial spectrum I, scalar initial spectrum I. Scalar integral scaling used. ○, $t = 0.75$ ett(eddy turnover time); □, $t = 1.0$ ett; ◇, $t = 1.25$ ett; ▽, $t = 1.5$ ett.

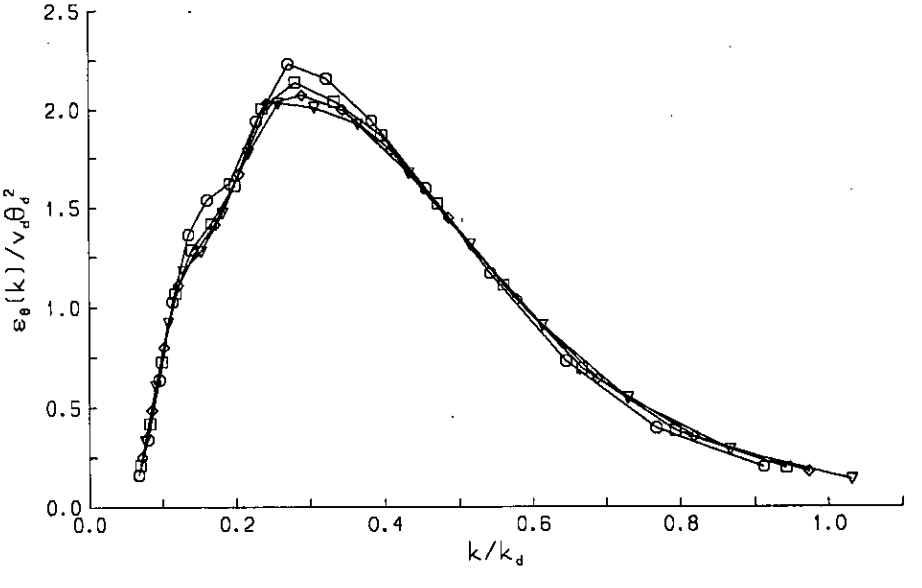

Figure 2.10: Self-similarity of the scalar dissipation spectrum for $Pr = 0.5$, velocity initial spectrum I, scalar initial spectrum I. Kolmogorov scaling used. ○, $t = 0.75$ ett(eddy turnover time); □, $t = 1.0$ ett; ◇, $t = 1.25$ ett; ▽, $t = 1.5$ ett.

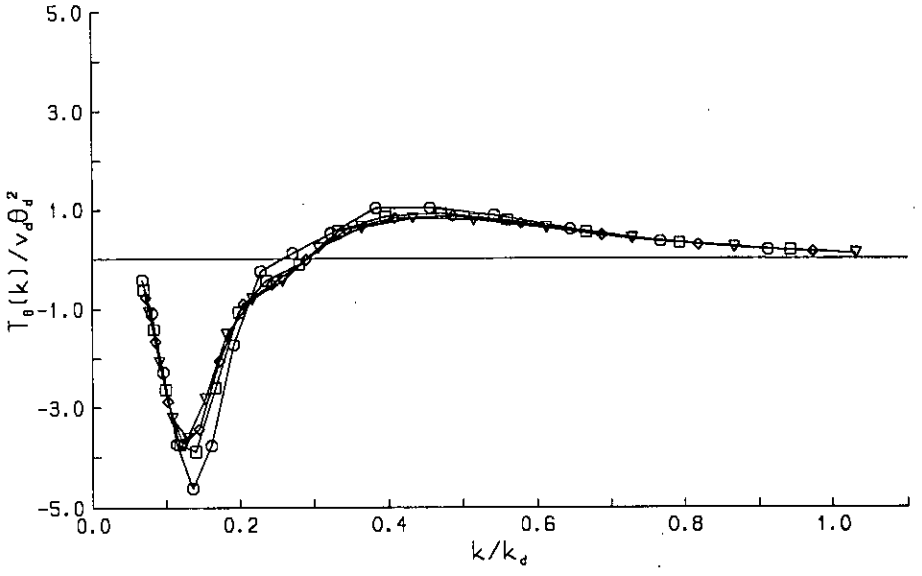

Figure 2.11: Self-similarity of the scalar transfer spectrum for $Pr = 0.5$, velocity initial spectrum I, scalar initial spectrum I. Kolmogorov scaling used. ○, $t = 0.75$ ett(eddy turnover time); □, $t = 1.0$ ett; ◇, $t = 1.25$ ett; ▽, $t = 1.5$ ett.

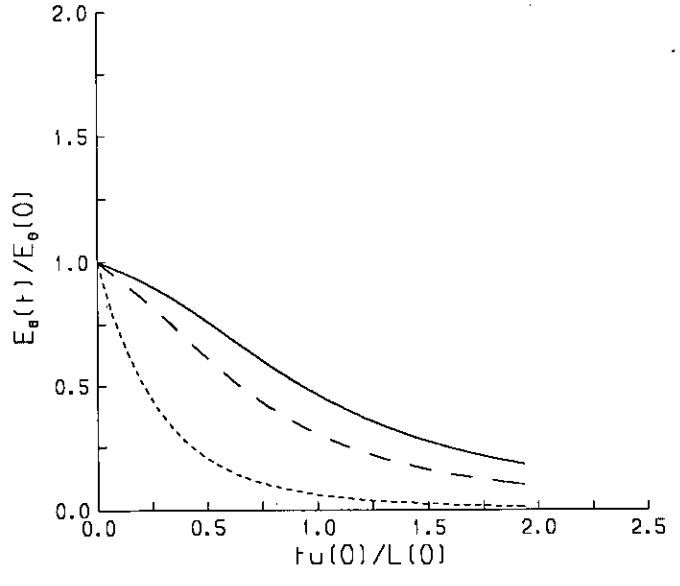

Figure 2.12: Evolution of the scalar energy for various Pr, velocity initial spectrum I, scalar initial spectrum I. ·····, $Pr = 0.1$; — — —, $Pr = 0.5$; ————, $Pr = 1.0$.

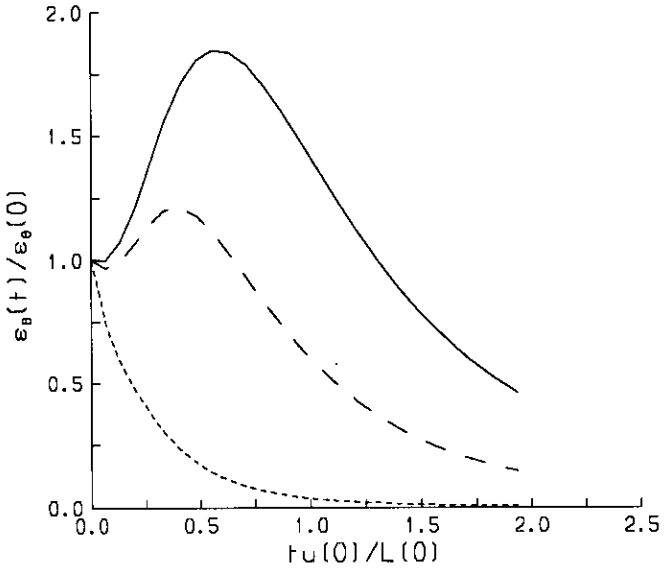

Figure 2.13: Evolution of the scalar dissipation for various Pr, velocity initial spectrum I, scalar initial spectrum I. ----------, $Pr = 0.1$; — — —, $Pr = 0.5$; ————, $Pr = 1.0$.

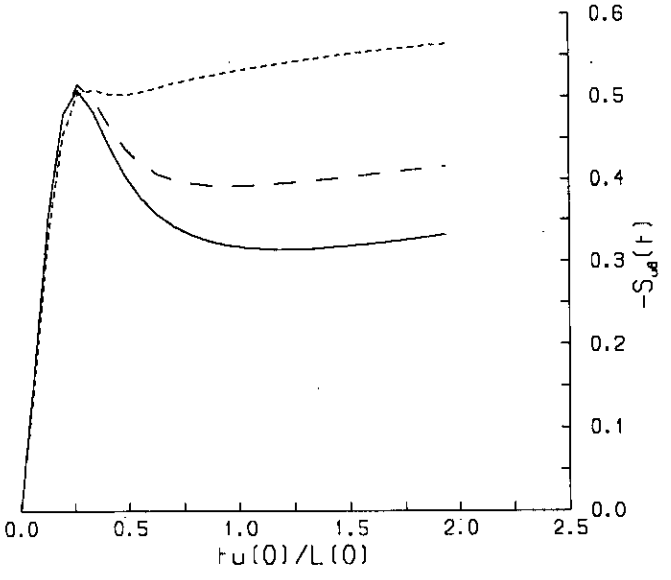

Figure 2.14: Evolution of the velocity-scalar derivative skewness for various Pr, velocity initial spectrum I, scalar initial spectrum I. ----------, $Pr = 0.1$; — — —, $Pr = 0.5$; ————, $Pr = 1.0$.

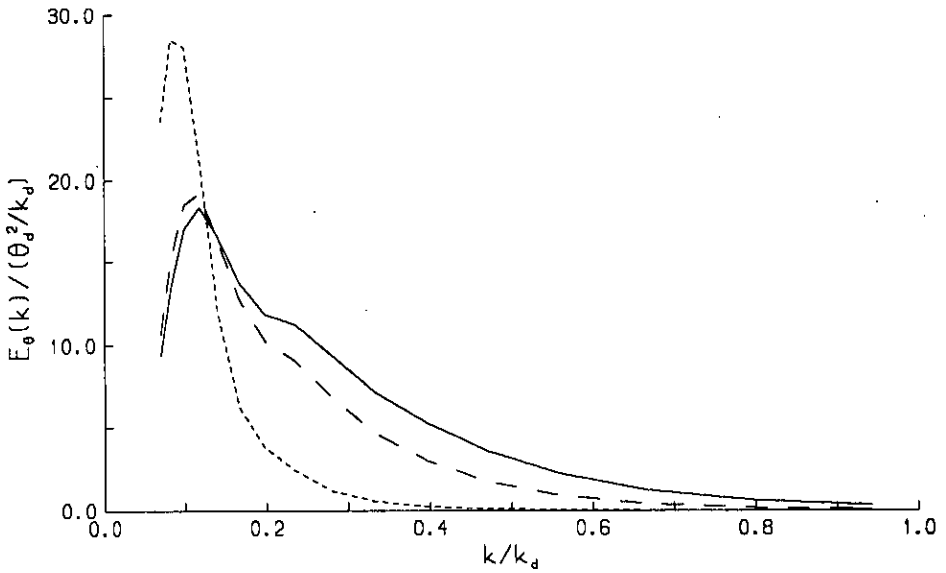

Figure 2.15: Scalar energy spectrum at 1 eddy turnover time, $R_\lambda = 19$, for various Pr, velocity initial spectrum I, scalar initial spectrum I. Kolmogorov scaling used. ----------, $Pr = 0.1$; — — —, $Pr = 0.5$; ————, $Pr = 1.0$.

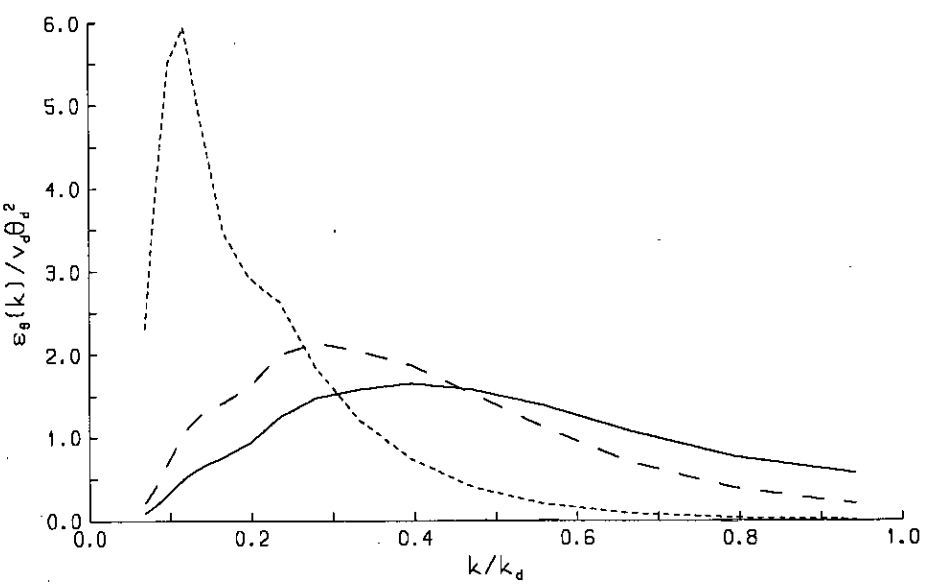

Figure 2.16: Scalar dissipation spectrum at 1 eddy turnover time, $R_\lambda = 19$, for various Pr, velocity initial spectrum I, scalar initial spectrum I. Kolmogorov scaling used. ----------, $Pr = 0.1$; — — —, $Pr = 0.5$; ————, $Pr = 1.0$.

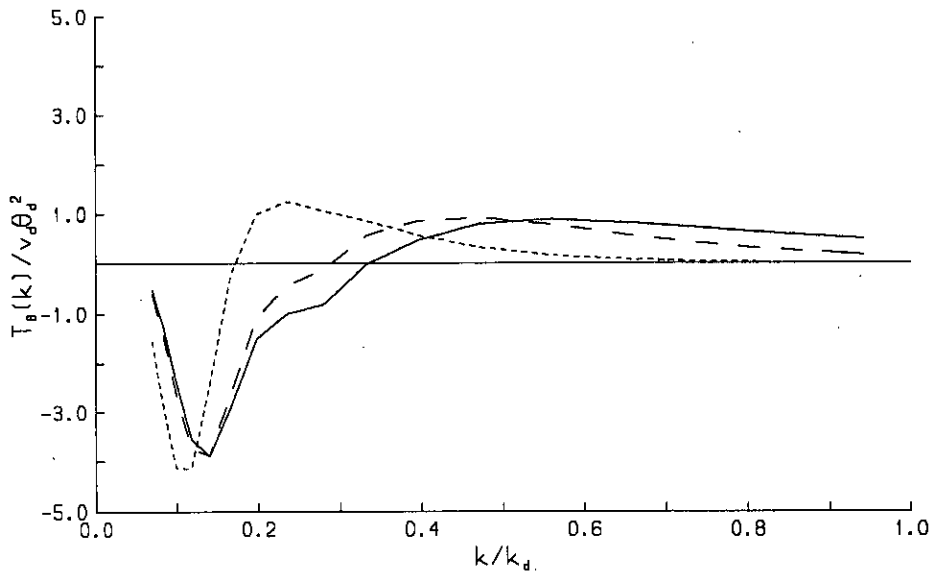

Figure 2.17: Scalar transfer spectrum at 1 eddy turnover time, $R_\lambda = 19$, for various Pr, velocity initial spectrum I, scalar initial spectrum I. Kolmogorov scaling used. ----------, $Pr = 0.1$; — — —, $Pr = 0.5$; ————, $Pr = 1.0$.

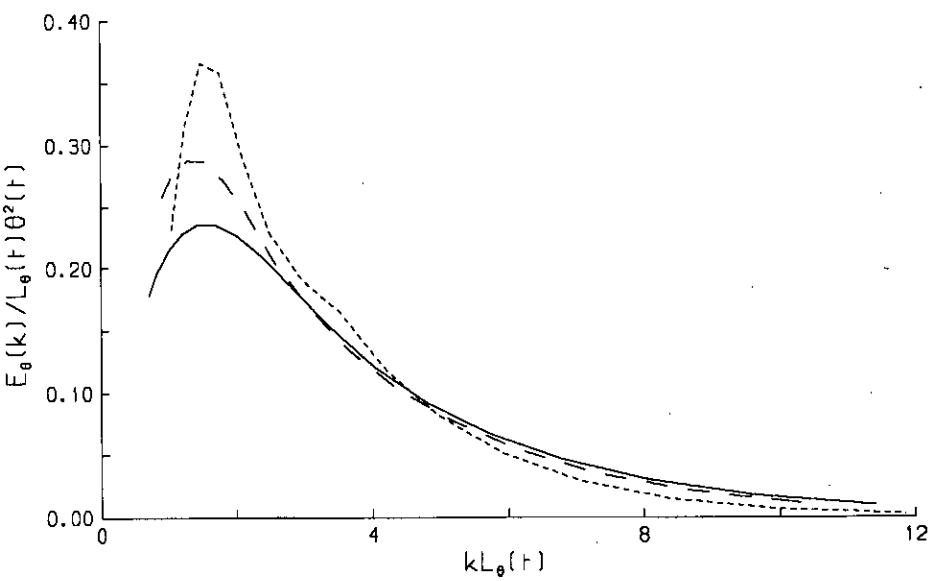

Figure 2.18: Scalar energy spectrum at R_λ=18 for $Pr = 0.5$, various initial spectra. Scalar integral scaling used. ----------, velocity initial spectrum I, scalar initial spectrum I; — — —, velocity i.s. II, scalar i.s. II; ————, velocity i.s. III, scalar i.s. III.

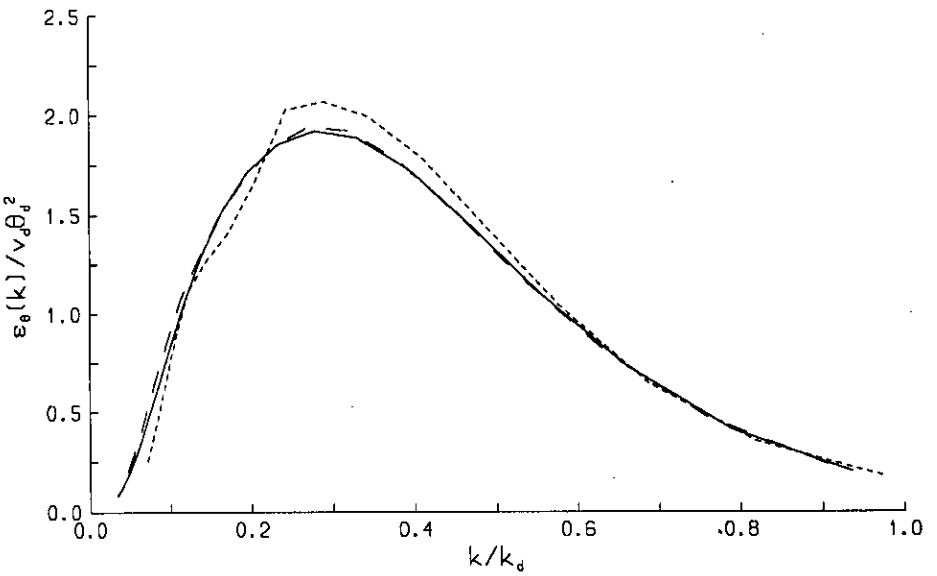

Figure 2.19: Scalar dissipation spectrum at R_λ=18 for Pr = 0.5, various initial spectra. Kolmogorov scaling used. ----------, velocity initial spectrum I, scalar initial spectrum I; — — —, velocity i.s. II, scalar i.s. II; ————, velocity i.s. III, scalar i.s. III.

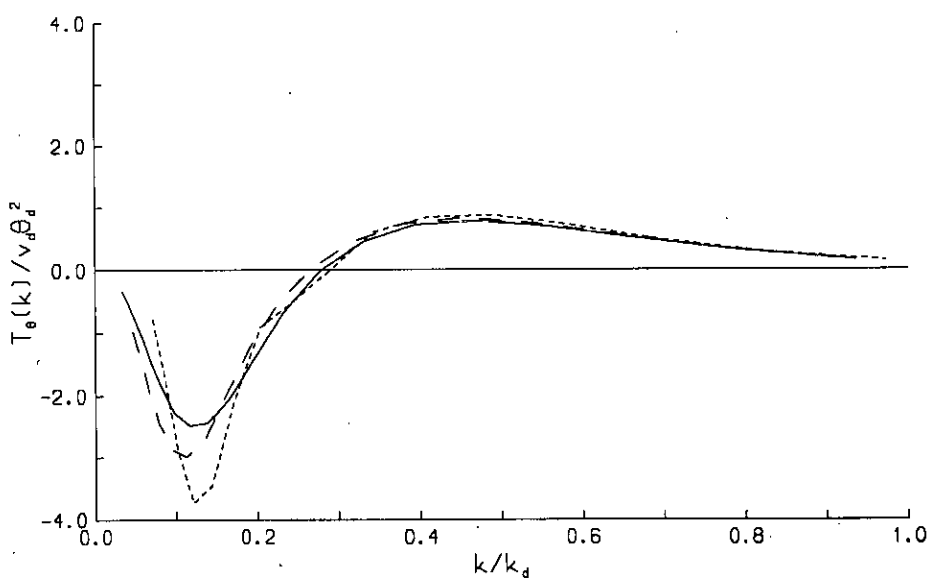

Figure 2.20: Scalar transfer spectrum at R_λ=18 for Pr = 0.5, various initial spectra. Kolmogorov scaling used. ----------, velocity initial spectrum I, scalar initial spectrum I; — — —, velocity i.s. II, scalar i.s. II; ————, velocity i.s. III, scalar i.s. III.

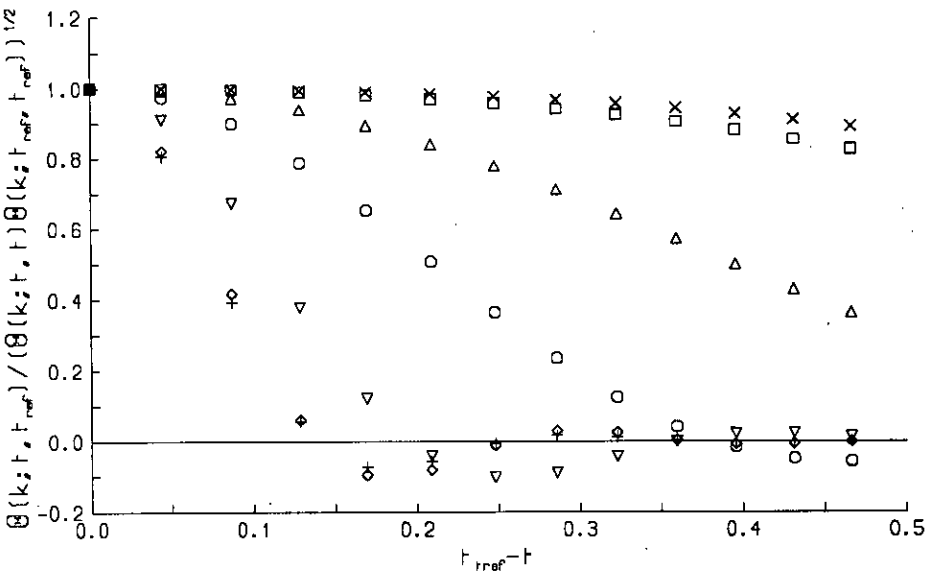

Figure 2.21: Two-time correlation functions for the scalar at $t_{ref} = 1$ eddy turnover time, $R_\lambda = 19$, for $Pr = 0.5$, velocity initial spectrum I, scalar initial spectrum I. Time separation unscalled. $\times$, $k/k_d = 0.07$; $\square$, $k/k_d = 0.1$; $\triangle$, $k/k_d = 0.17$; $\bigcirc$, $k/k_d = 0.28$; $\triangledown$, $k/k_d = 0.47$; $\diamond$, $k/k_d = 0.79$; $+$, $k/k_d = 0.94$.

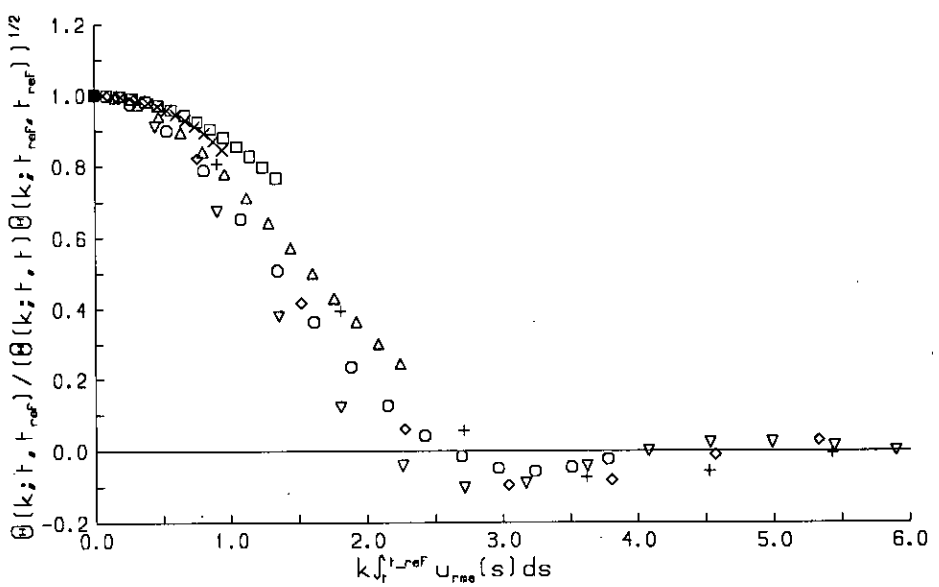

Figure 2.22: Two-time correlation functions for the scalar at $t_{ref} = 1$ eddy turnover time, $R_\lambda = 19$, for $Pr = 0.5$, velocity initial spectrum I, scalar initial spectrum I. Time separation scaled by the convective time scale. $\times$, $k/k_d = 0.07$; $\square$, $k/k_d = 0.1$; $\triangle$, $k/k_d = 0.17$; $\bigcirc$, $k/k_d = 0.28$; $\triangledown$, $k/k_d = 0.47$; $\diamond$, $k/k_d = 0.79$; $+$, $k/k_d = 0.94$.

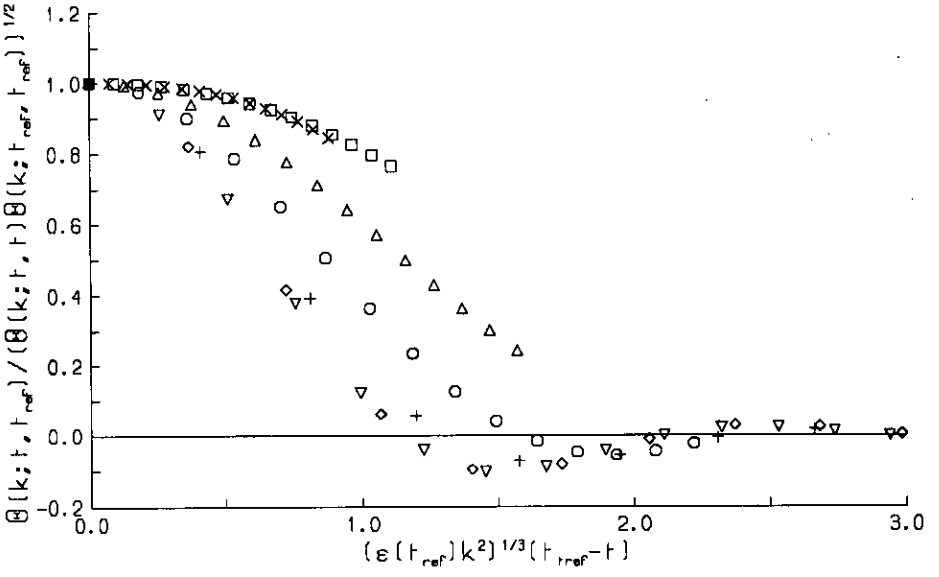

Figure 2.23: Two-time correlation functions for the scalar at $t_{ref} = 1$ eddy turnover time, $R_\lambda = 19$, for $Pr = 0.5$, velocity initial spectrum I, scalar initial spectrum I. Time separation scaled by the Kolmogorov time scale. $\times$, $k/k_d = 0.07$; $\square$, $k/k_d = 0.1$; $\triangle$, $k/k_d = 0.17$; $\bigcirc$, $k/k_d = 0.28$; $\triangledown$, $k/k_d = 0.47$; $\diamond$, $k/k_d = 0.79$; $+$, $k/k_d = 0.94$.

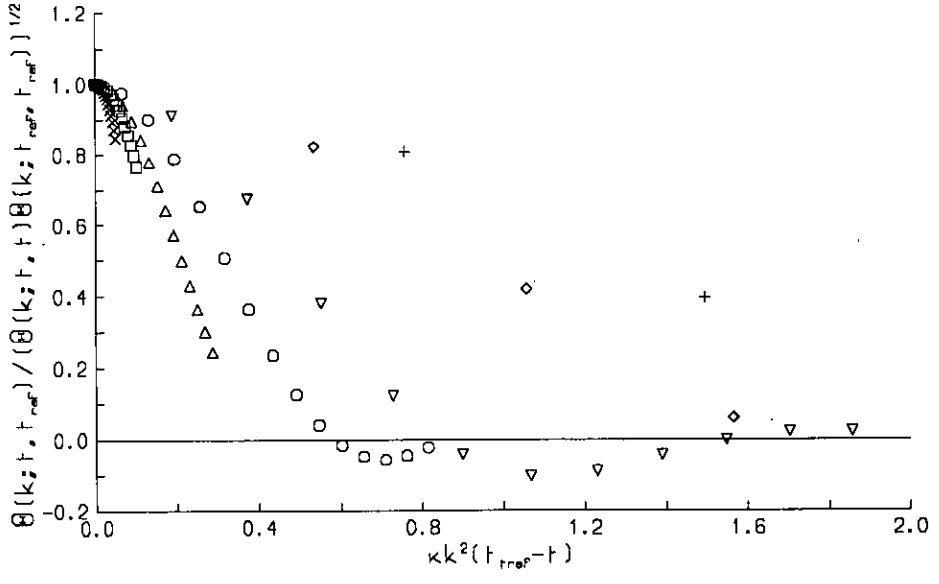

Figure 2.24: Two-time correlation functions for the scalar at $t_{ref} = 1$ eddy turnover time, $R_\lambda = 19$, for $Pr = 0.5$, velocity initial spectrum I, scalar initial spectrum I. Time separation scaled by the dissipative decay time scale. $\times$, $k/k_d = 0.07$; $\square$, $k/k_d = 0.1$; $\triangle$, $k/k_d = 0.17$; $\bigcirc$, $k/k_d = 0.28$; $\triangledown$, $k/k_d = 0.47$; $\diamond$, $k/k_d = 0.79$; $+$, $k/k_d = 0.94$.

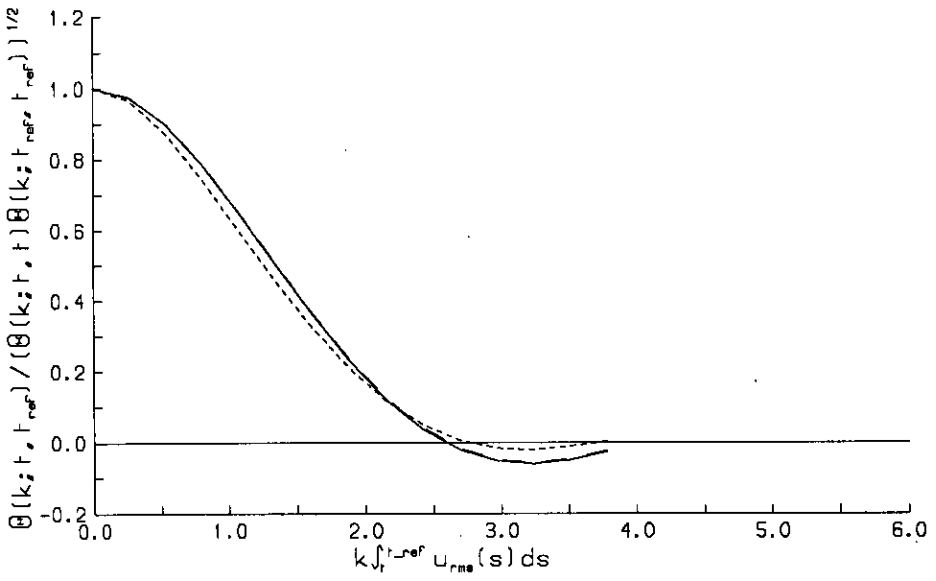

Figure 2.25: Two-time correlation functions for the scalar at $t_{ref} = 1$ eddy turnover time, $R_\lambda = 19$, for $k/k_d = 0.28$, for various Pr, velocity initial spectrum I, scalar initial spectrum I. Time separation scaled by the convective time scale. ----------, $Pr = 0.1$; — — —, $Pr = 0.5$; ————, $Pr = 1.0$.

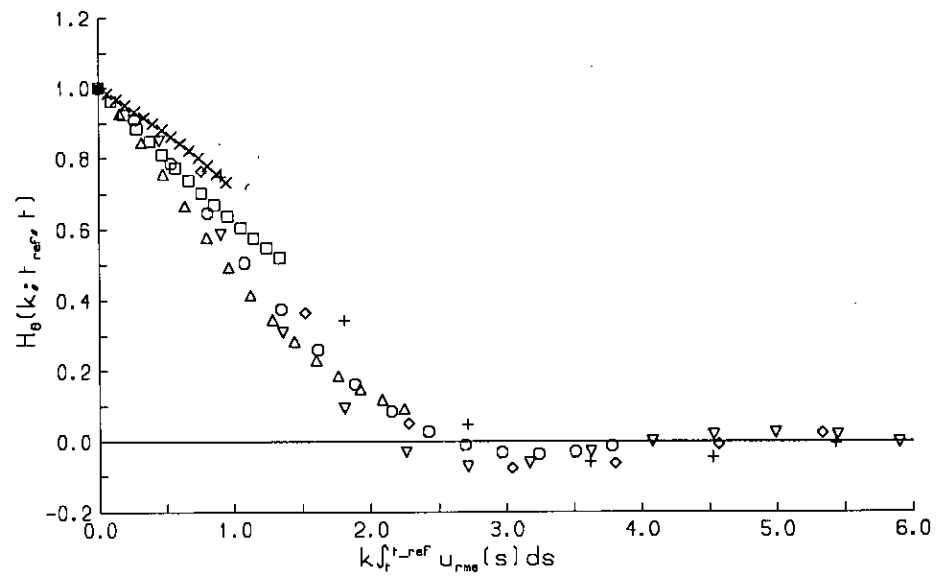

Figure 2.26: Propagator functions for the scalar at $t_{ref} = 1$ eddy turnover time, $R_\lambda = 19$, for $Pr = 0.5$, velocity initial spectrum I, scalar initial spectrum I. Time separation scaled by the convective time scale. $\times$, $k/k_d = 0.07$; $\square$, $k/k_d = 0.1$; $\triangle$, $k/k_d = 0.17$; $\bigcirc$, $k/k_d = 0.28$; $\triangledown$, $k/k_d = 0.47$; $\diamond$, $k/k_d = 0.79$; $+$, $k/k_d = 0.94$.

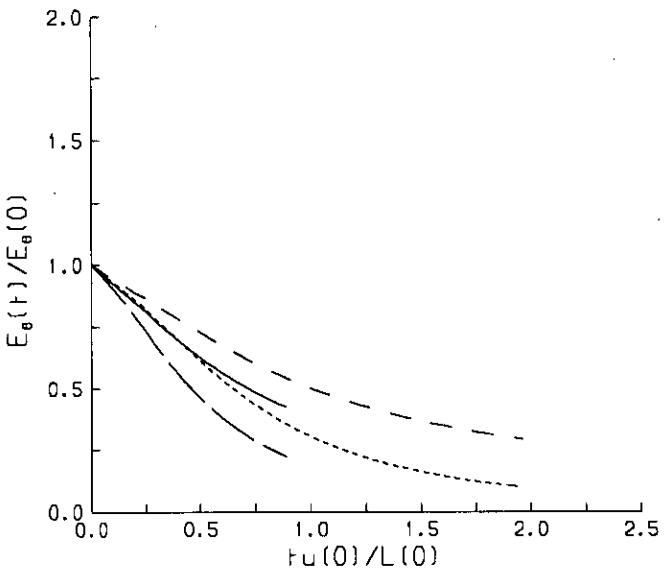

Figure 2.27: Evolution of the scalar energy for $Pr = 0.5$, various initial spectra. ----------, velocity initial spectrum I, scalar initial spectrum I; — — —, velocity i.s. I, scalar i.s. IV; —— ——, velocity i.s. IV, scalar i.s. I; ————, velocity i.s. IV, scalar i.s. IV.

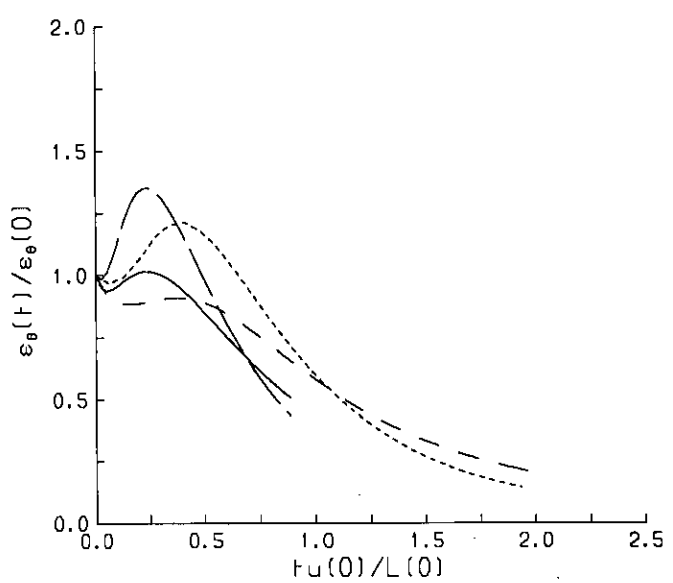

Figure 2.28: Evolution of the scalar dissipation for $Pr = 0.5$, various initial spectra. ----------, velocity initial spectrum I, scalar initial spectrum I; — — —, velocity i.s. I, scalar i.s. IV; —— ——, velocity i.s. IV, scalar i.s. I; ————, velocity i.s. IV, scalar i.s. IV.

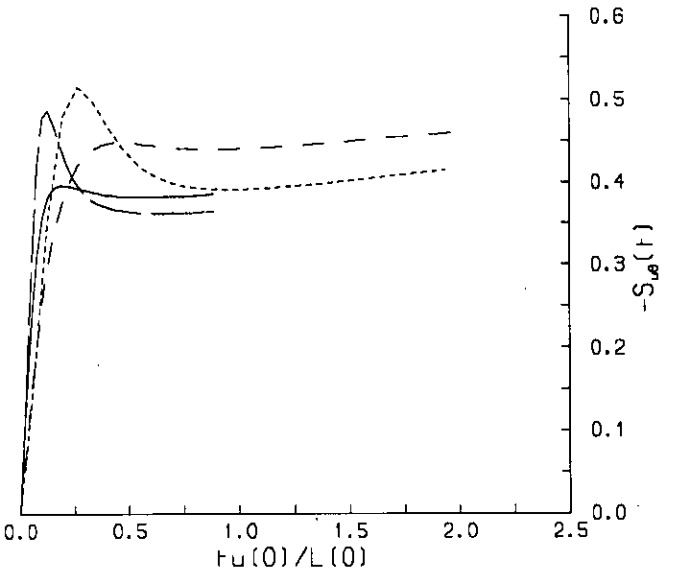

Figure 2.29: Evolution of the velocity scalar derivative skewness for $Pr = 0.5$, various initial spectra. ----------, velocity initial spectrum I, scalar initial spectrum I; — — —, velocity i.s. I, scalar i.s. IV; —— ——, velocity i.s. IV, scalar i.s. I; ————, velocity i.s. IV, scalar i.s. IV.

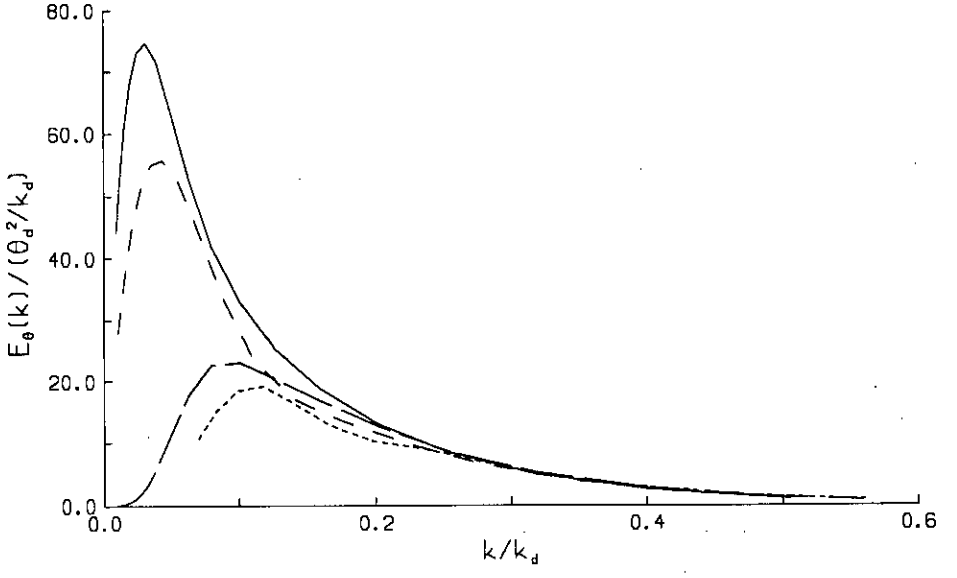

Figure 2.30: Scalar energy spectrum at 1 eddy turnover time for $Pr = 0.5$, various initial spectra. ----------, velocity initial spectrum I, scalar initial spectrum I; — — —, velocity i.s. I, scalar i.s. IV; —— ——, velocity i.s. IV, scalar i.s. I; ————, velocity i.s. IV, scalar i.s. IV.

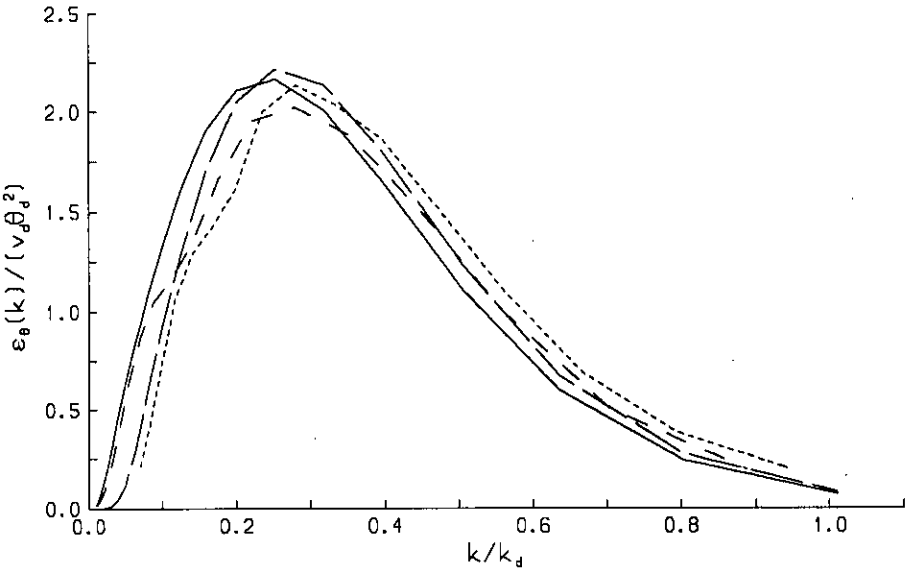

Figure 2.31: Scalar dissipation spectrum at 1 eddy turnover time for $Pr = 0.5$, various initial spectra. ----------, velocity initial spectrum I, scalar initial spectrum I; — — —, velocity i.s. I, scalar i.s. IV; —— ——, velocity i.s. IV, scalar i.s. I; ————, velocity i.s. IV, scalar i.s. IV.

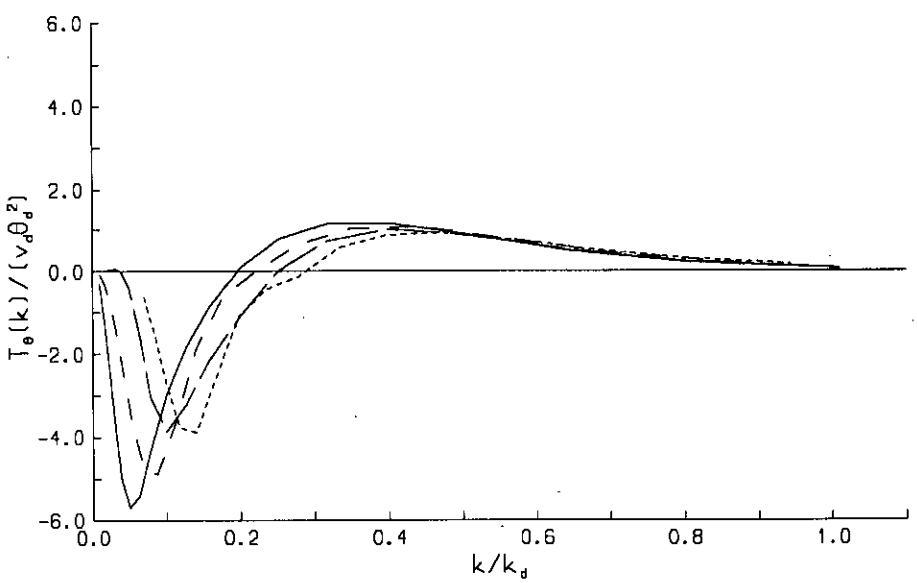

Figure 2.32: Scalar transfer spectrum at 1 eddy turnover time for $Pr = 0.5$, various initial spectra. ----------, velocity initial spectrum I, scalar initial spectrum I; — — —, velocity i.s. I, scalar i.s. IV; —— ——, velocity i.s. IV, scalar i.s. I; ————, velocity i.s. IV, scalar i.s. IV.

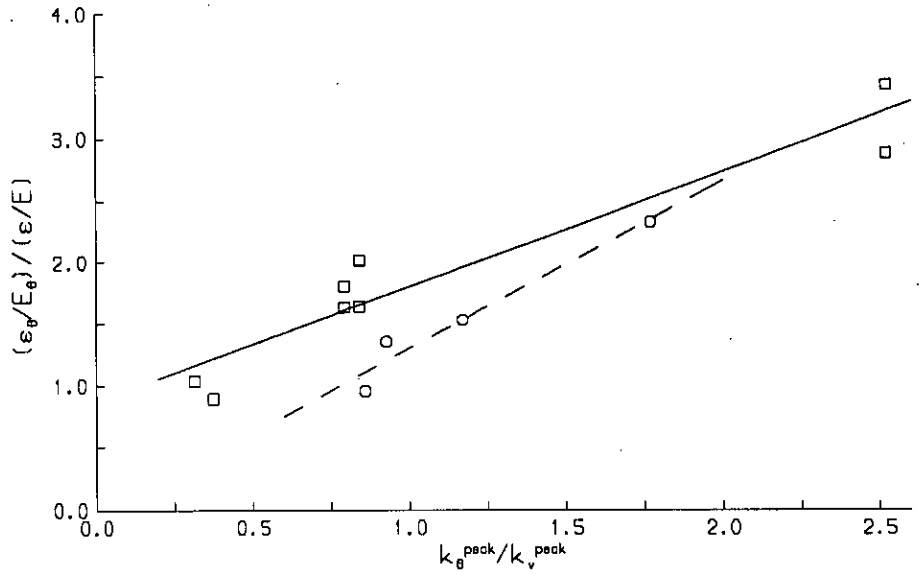

Figure 2.33: Ratio of thermal to mechanical timescales. □————, present work; ○— — —, experimental results of Warhaft and Lumley[58].

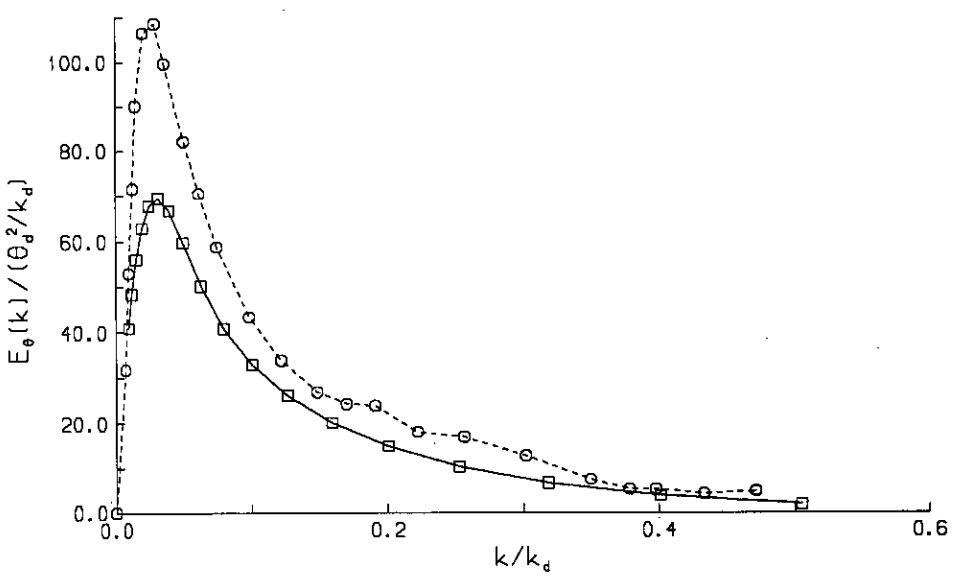

Figure 2.34: □, scalar energy spectrum at 1 eddy turnover time for $Pr = 0.725$, velocity initial spectrum IV, scalar initial spectrum IV; ○, scalar energy spectrum from Yeh and van Atta[61].

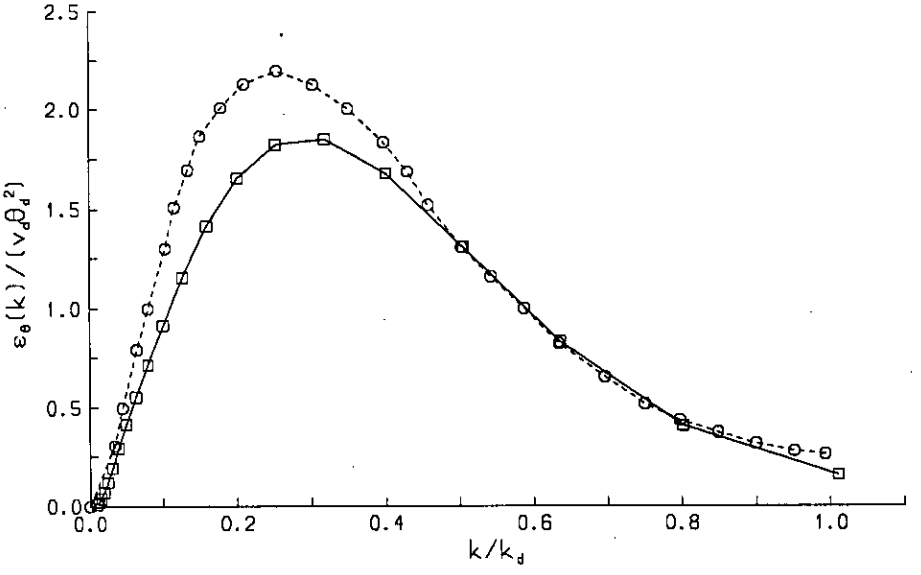

Figure 2.35: □, scalar dissipation spectrum at 1 eddy turnover time for $Pr = 0.725$, velocity initial spectrum IV, scalar initial spectrum IV; ○, scalar dissipation spectrum from Yeh and van Atta[61].

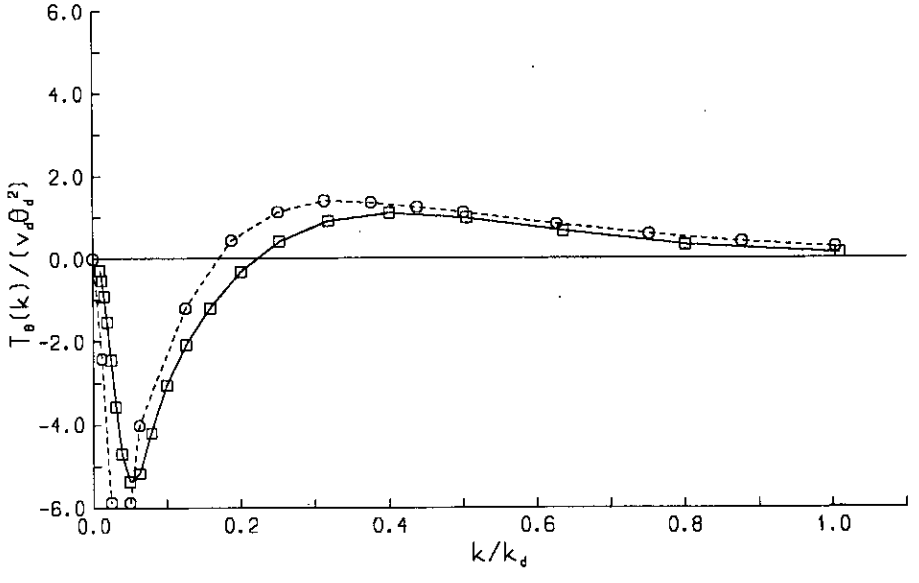

Figure 2.36: □, scalar transfer spectrum at 1 eddy turnover time for $Pr = 0.725$, velocity initial spectrum IV, scalar initial spectrum IV; ○, scalar transfer spectrum from Yeh and van Atta[61].

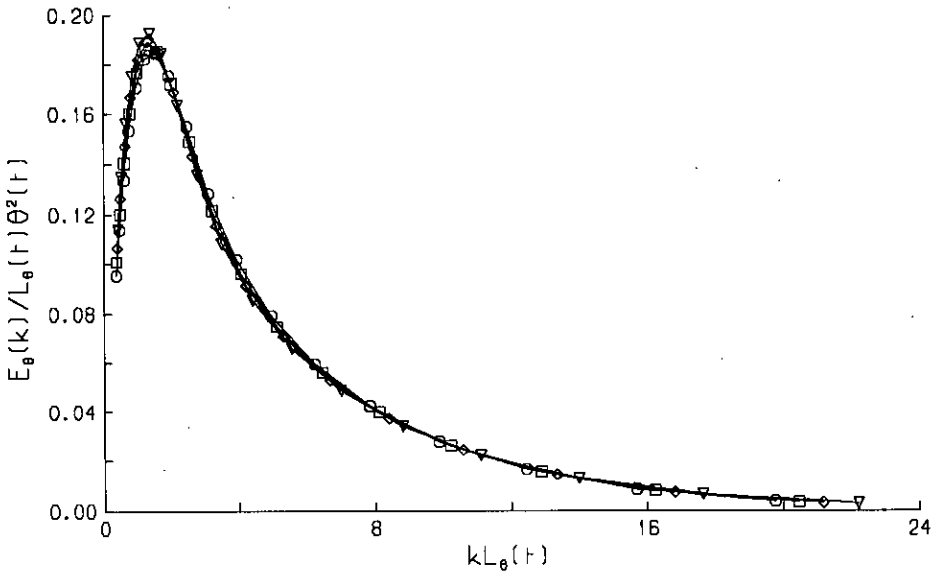

Figure 2.37: Self-similarity of the scalar energy spectrum for $Pr = 0.5$, velocity initial spectrum IV, scalar initial spectrum IV. Scalar integral scaling used. ○, $t = 0.6$ ett(eddy turnover time); □, $t = 0.7$ ett; ◇, $t = 0.8$ ett; ▽, $t = 0.9$ ett.

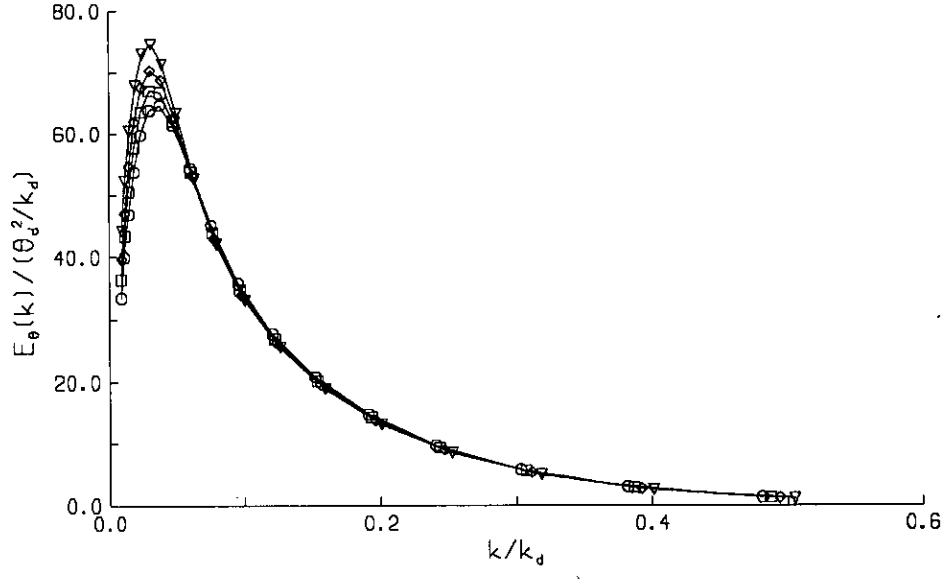

Figure 2.38: Self-similarity of the scalar energy spectrum for $Pr = 0.5$, velocity initial spectrum IV, scalar initial spectrum IV. Kolmogorov scaling used. ○, $t = 0.6$ ett(eddy turnover time); □, $t = 0.7$ ett; ◇, $t = 0.8$ ett; ▽, $t = 0.9$ ett.

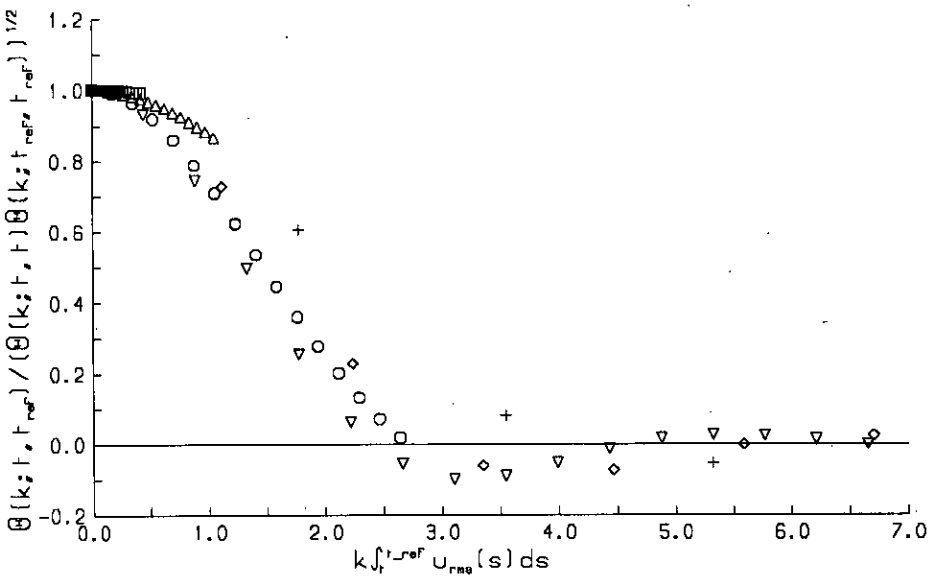

Figure 2.39: Two-time correlation functions for the scalar at $t_{ref} = 1$ eddy turnover time, $R_\lambda = 41$, for $Pr = 0.5$, velocity initial spectrum IV, scalar initial spectrum IV. Time separation scaled by the convective time scale. $\times$, $k/k_d = 0.01$; $\square$, $k/k_d = 0.016$; $\triangle$, $k/k_d = 0.04$; $\bigcirc$, $k/k_d = 0.1$; $\triangledown$, $k/k_d = 0.25$; $\diamond$, $k/k_d = 0.63$; $+$, $k/k_d = 1.0$.

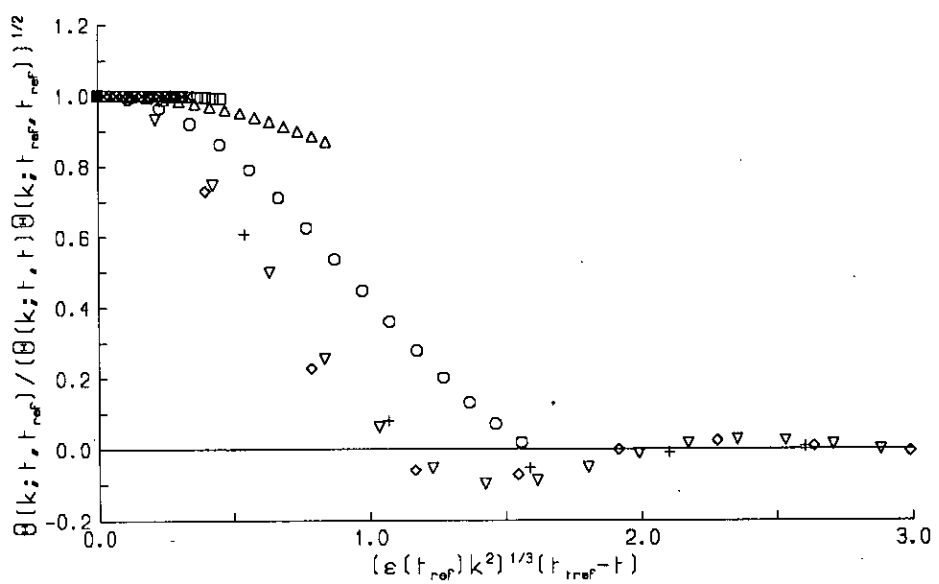

Figure 2.40: Two-time correlation functions for the scalar at $t_{ref} = 1$ eddy turnover time, $R_\lambda = 41$, for $Pr = 0.5$, velocity initial spectrum IV, scalar initial spectrum IV. Time separation scaled by the Kolmogorov time scale. $\times$, $k/k_d = 0.01$; $\square$, $k/k_d = 0.016$; $\triangle$, $k/k_d = 0.04$; $\bigcirc$, $k/k_d = 0.1$; $\triangledown$, $k/k_d = 0.25$; $\diamond$, $k/k_d = 0.63$; $+$, $k/k_d = 1.0$.

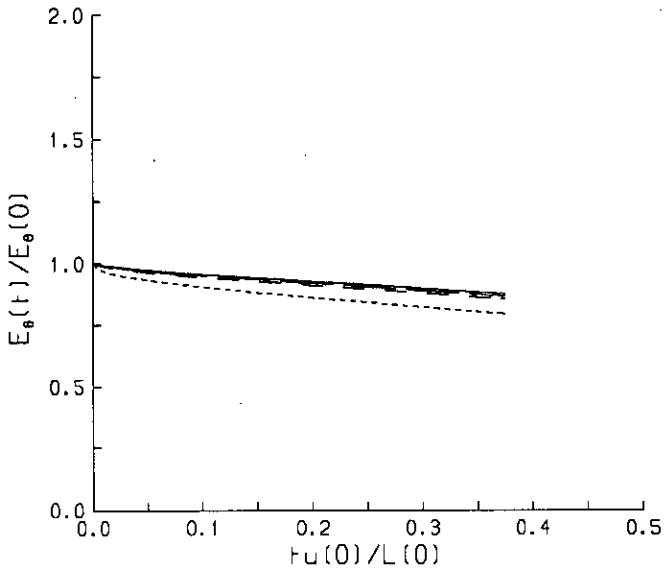

Figure 2.41: Evolution of the scalar energy for various Pr, velocity initial spectrum V, scalar initial spectrum V. ----------, $Pr = 0.1$; — — —, $Pr = 0.5$; —— ——, $Pr = 0.725$; ————, $Pr = 1.0$.

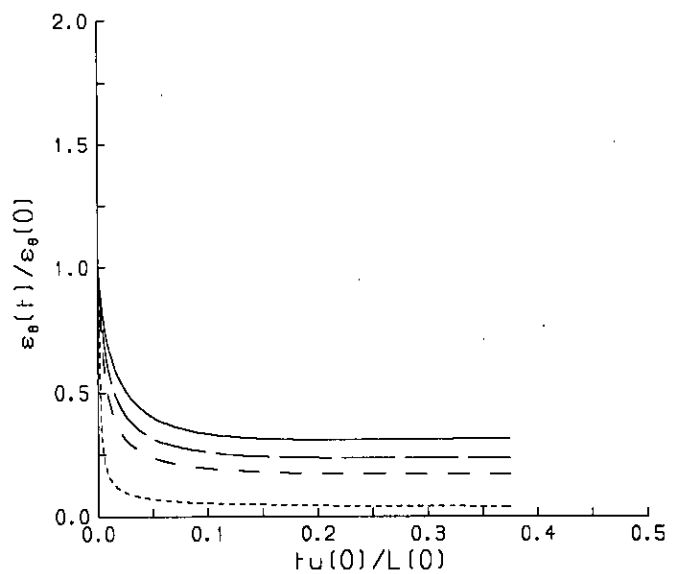

Figure 2.42: Evolution of the scalar disspation for various Pr, velocity initial spectrum V, scalar initial spectrum V. ----------, $Pr = 0.1$; — — —, $Pr = 0.5$; —— ——, $Pr = 0.725$; ————, $Pr = 1.0$.

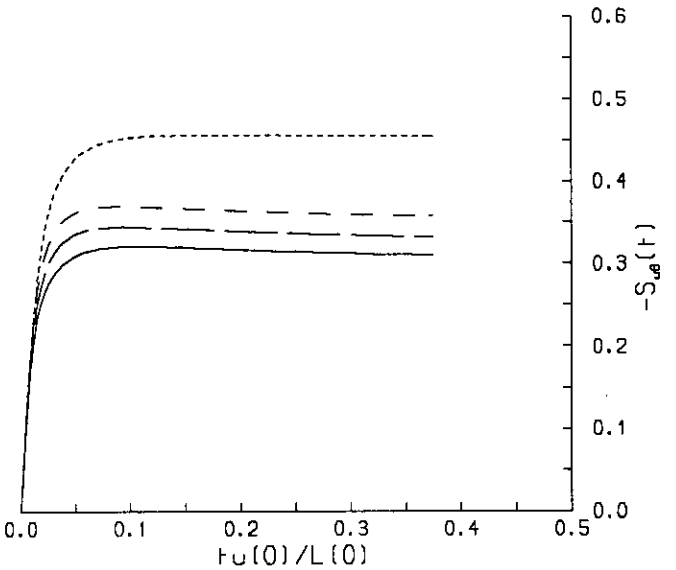

Figure 2.43: Evolution of the velocity-scalar derivative skewness for various Pr, velocity initial spectrum V, scalar initial spectrum V. ----------, $Pr = 0.1$; — — —, $Pr = 0.5$; —— ——, $Pr = 0.725$; ————, $Pr = 1.0$.

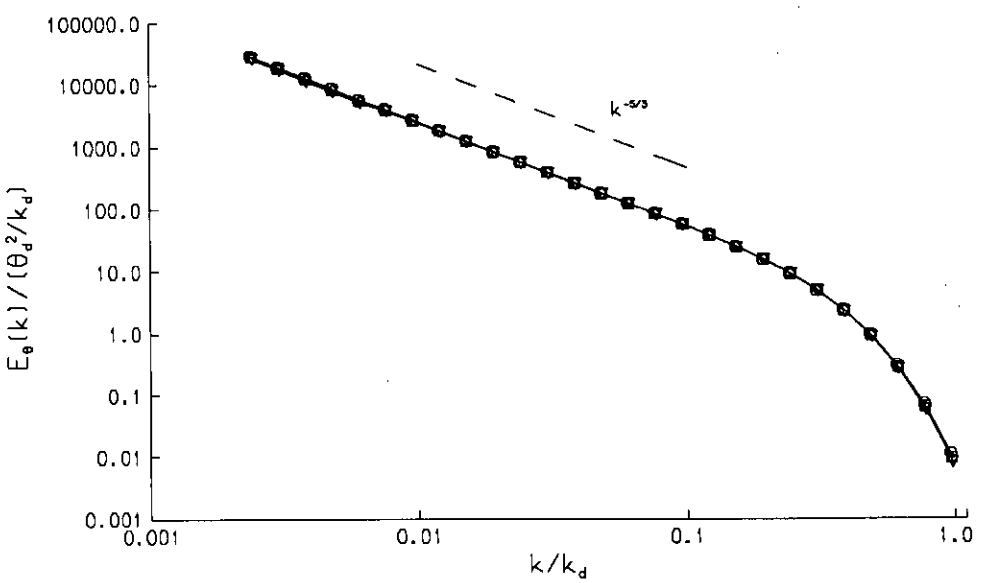

Figure 2.44: Self-similarity of the scalar energy spectrum for $Pr = 0.5$, velocity initial spectrum V, scalar initial spectrum V. Kolmogorov scaling used. ○, $t = 0.23$ ett(eddy turnover time); □, $t = 0.28$ ett; ◇, $t = 0.33$ ett; ▽, $t = 0.38$ ett.

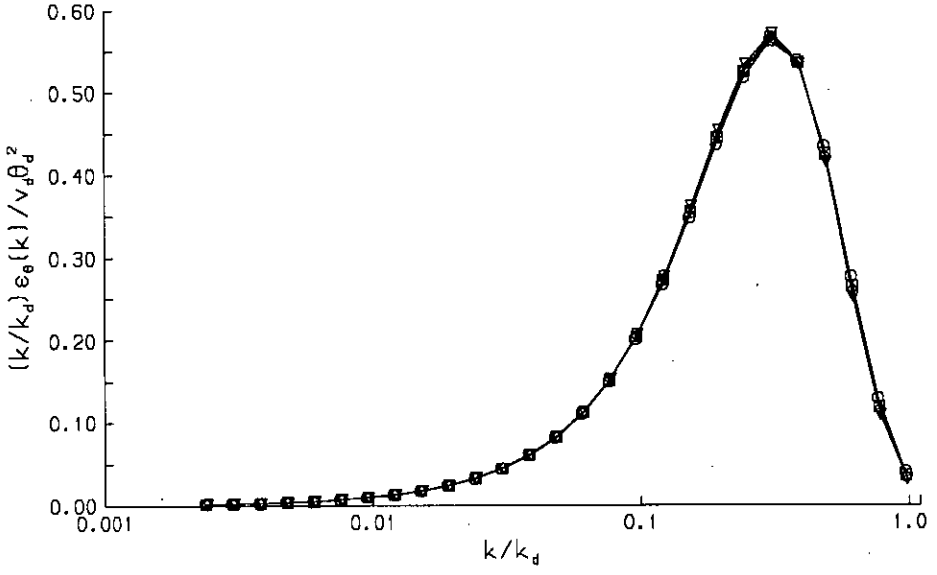

Figure 2.45: Self-similarity of the scalar dissipation spectrum for $Pr = 0.5$, velocity initial spectrum V, scalar initial spectrum V. Kolmogorov scaling used. ○, $t = 0.23$ ett(eddy turnover time); □, $t = 0.28$ ett; ◇, $t = 0.33$ ett; ▽, $t = 0.38$ ett.

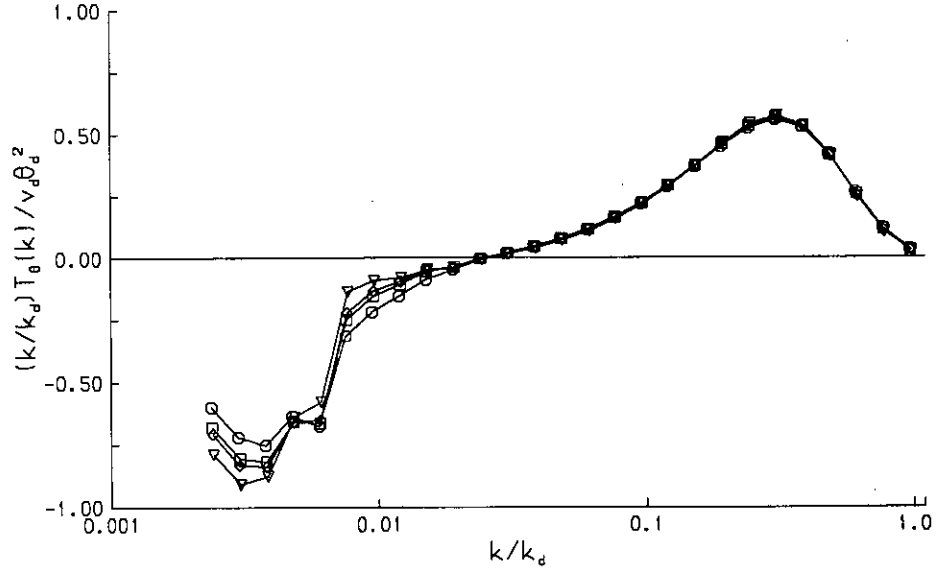

Figure 2.46: Self-similarity of the scalar transfer spectrum for $Pr = 0.5$, velocity initial spectrum V, scalar initial spectrum V. Kolmogorov scaling used. ○, $t = 0.23$ ett(eddy turnover time); □, $t = 0.28$ ett; ◇, $t = 0.33$ ett; ▽, $t = 0.38$ ett.

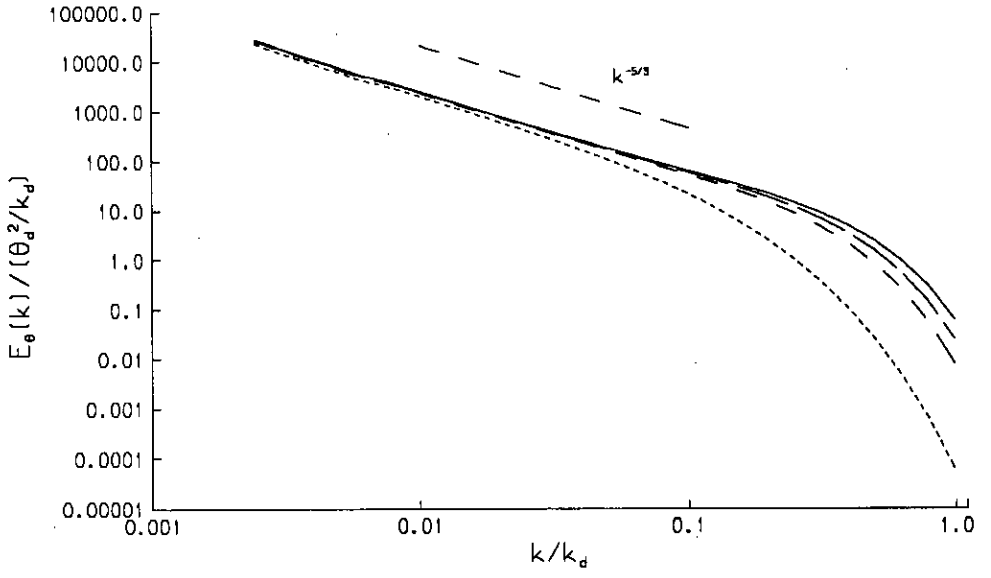

Figure 2.47: Scalar energy spectrum at 0.38 eddy turnover time, $R_\lambda = 558$, for various Pr, velocity initial spectrum V, scalar initial spectrum V. Kolmogorov scaling used. ----------, $Pr = 0.1$; — — —, $Pr = 0.5$; —— ——, $Pr = 0.725$; ————, $Pr = 1.0$.

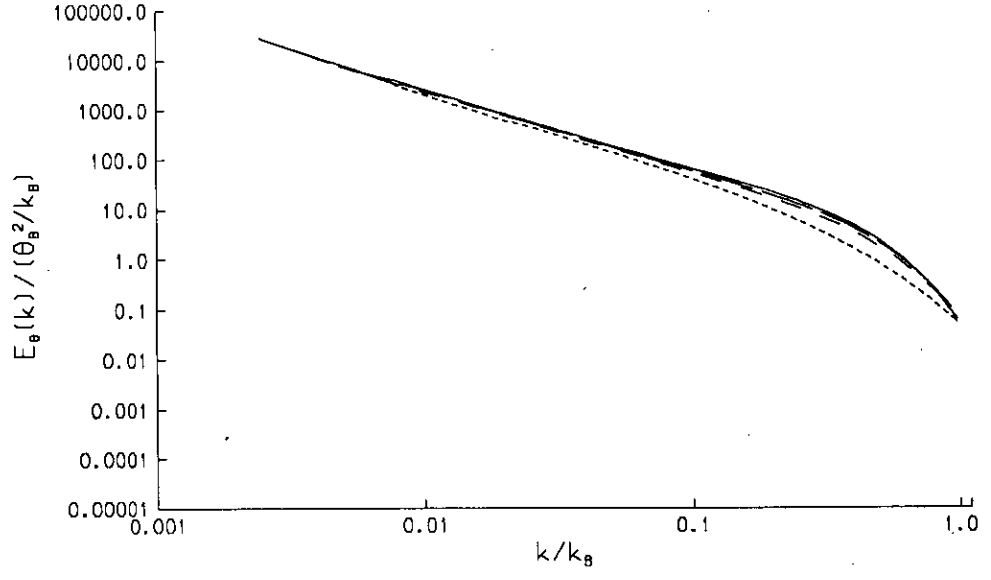

Figure 2.48: Scalar energy spectrum at 0.38 eddy turnover time, $R_\lambda = 558$, for various Pr, velocity initial spectrum V, scalar initial spectrum V. Batchelor scaling used. ----------, $Pr = 0.1$; — — —, $Pr = 0.5$; —— ——, $Pr = 0.725$; ————, $Pr = 1.0$.

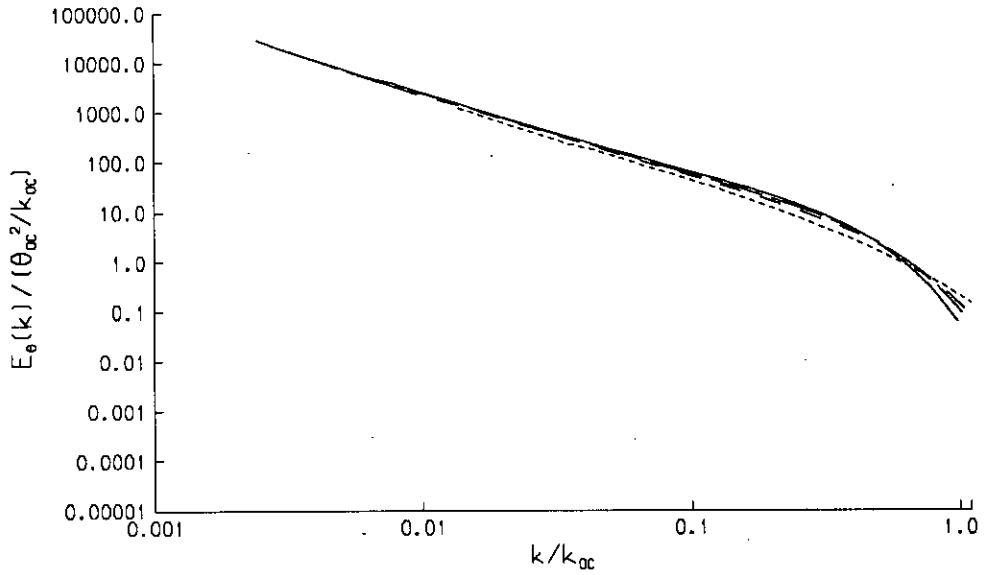

Figure 2.49: Scalar energy spectrum at 0.38 eddy turnover time, $R_\lambda = 558$, for various Pr, velocity initial spectrum V, scalar initial spectrum V. Obukhov-Corrsin scaling used. ----------, $Pr = 0.1$; — — —, $Pr = 0.5$; —— ——, $Pr = 0.725$; ————, $Pr = 1.0$.

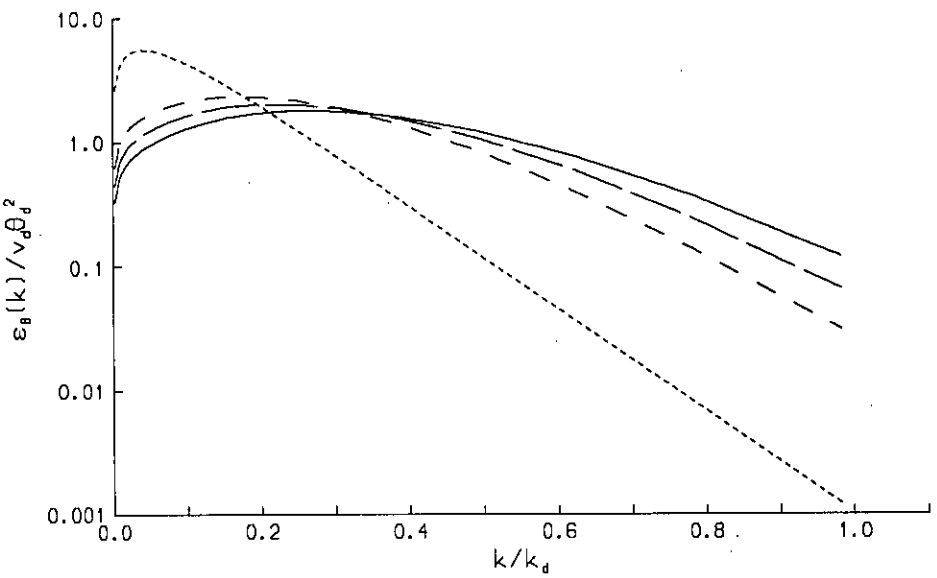

Figure 2.50: Scalar dissipation spectrum at 0.38 eddy turnover time, $R_\lambda = 558$, for various Pr, velocity initial spectrum V, scalar initial spectrum V. Kolmogorov scaling used, with linear-log scale to show $\exp(-ak)$ behaviour. ----------, $Pr = 0.1$; — — —, $Pr = 0.5$; —— ——, $Pr = 0.725$; ————, $Pr = 1.0$.

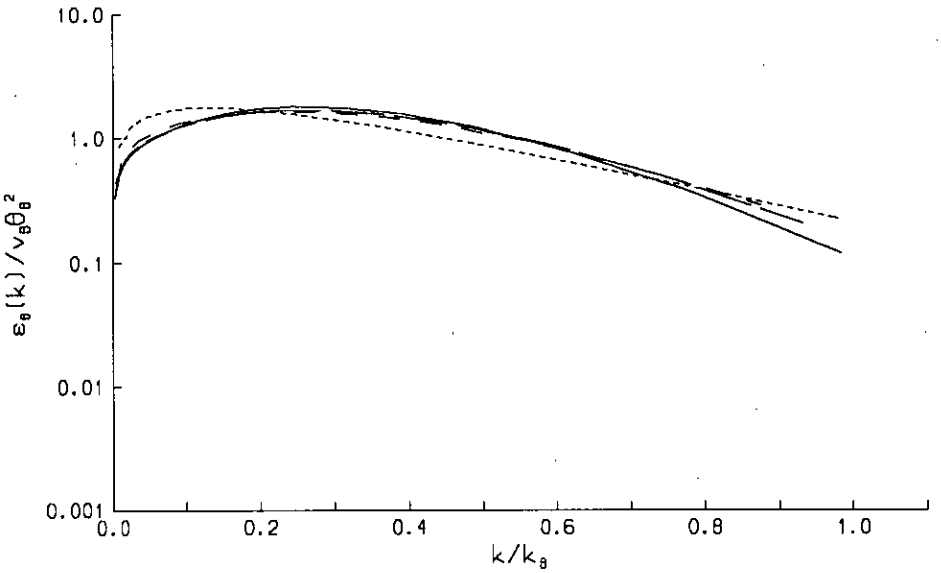

Figure 2.51: Scalar dissipation spectrum at 0.38 eddy turnover time, $R_\lambda = 558$, for various Pr, velocity initial spectrum V, scalar initial spectrum V. Batchelor scaling used, with linear-log scale to show $\exp(-ak)$ behaviour. ----------, $Pr = 0.1$; — — —, $Pr = 0.5$; —— ——, $Pr = 0.725$; ————, $Pr = 1.0$.

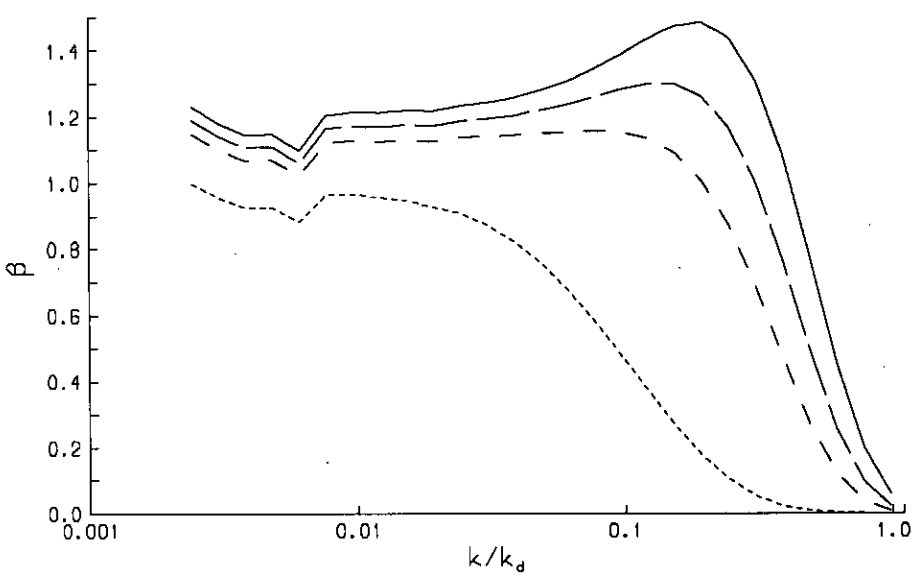

Figure 2.52: Kolmogorov scaled scalar energy spectrum, multiplied by $(k/k_d)^{5/3}$ to find β, the three-dimensional Obukhov-Corrsin constant, at 0.38 eddy turnover time, $R_\lambda = 558$, for various Pr, velocity initial spectrum V, scalar initial spectrum V. ----------, $Pr = 0.1$; — — —, $Pr = 0.5$; —— ——, $Pr = 0.725$; ————, $Pr = 1.0$.

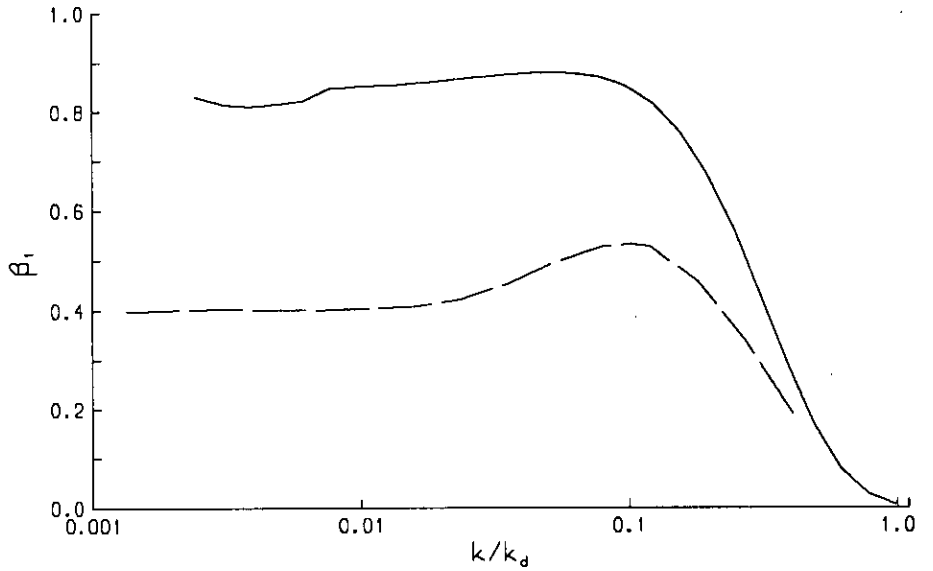

Figure 2.53: ————, Kolmogorov scaled one-dimensional scalar energy spectrum, multiplied by $(k/k_d)^{5/3}$ to find β_1, the one-dimensional Obukhov-Corrsin constant, at 0.38 eddy turnover time, $R_\lambda = 558$, , velocity initial spectrum V, scalar initial spectrum V; —— ——, experimental results of Champagne *et al.*[8].

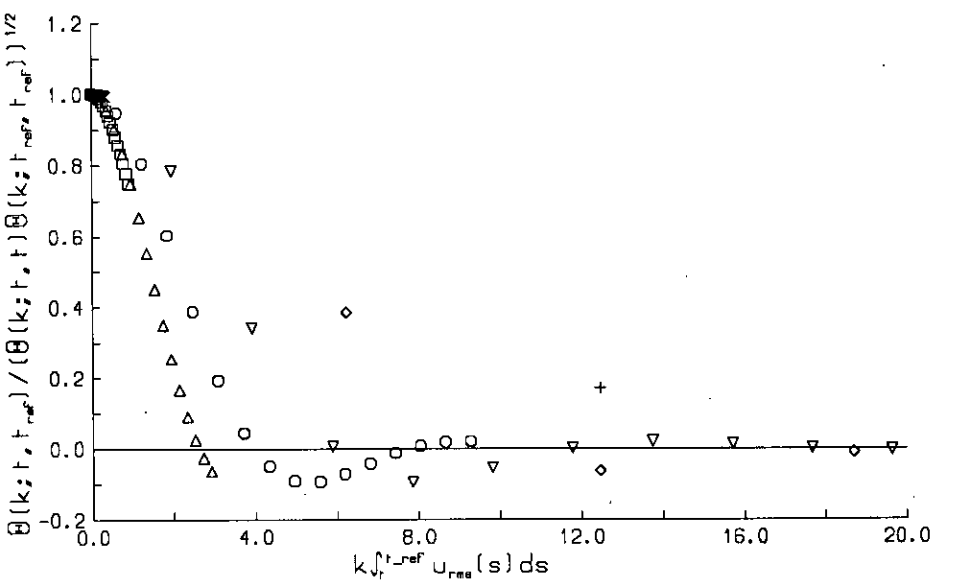

Figure 2.54: Two-time correlation functions for the scalar at $t_{ref} = 0.38$ eddy turnover time, $R_\lambda = 558$, for $Pr = 0.5$, velocity initial spectrum V, scalar initial spectrum V. Time separation scaled by the convective time scale. $\times$, $k/k_d = 0.002$; $\square$, $k/k_d = 0.006$; $\triangle$, $k/k_d = 0.02$; $\bigcirc$, $k/k_d = 0.06$; $\triangledown$, $k/k_d = 0.2$; $\diamond$, $k/k_d = 0.6$; $+$, $k/k_d = 1.2$.

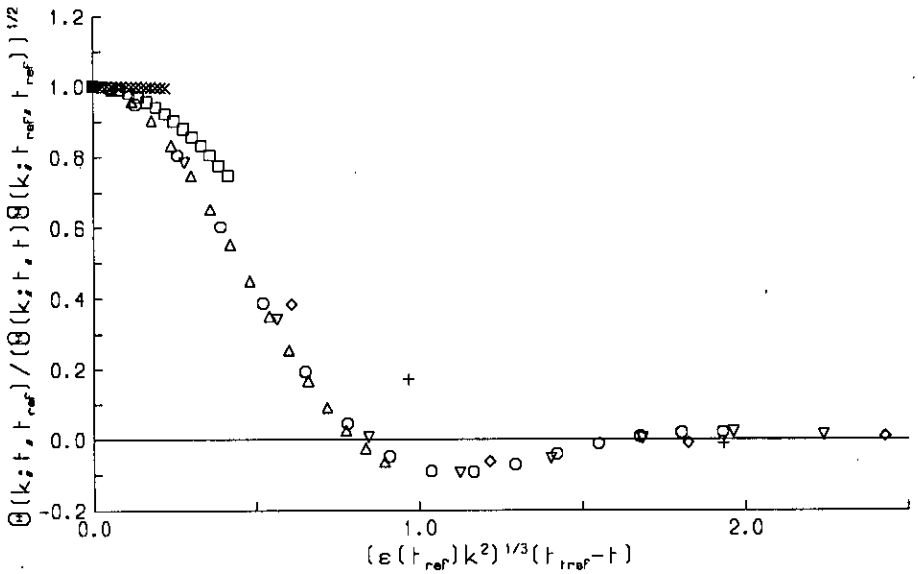

Figure 2.55: Two-time correlation functions for the scalar at $t_{ref} = 0.38$ eddy turnover time, $R_\lambda = 558$, for $Pr = 0.5$, velocity initial spectrum V, scalar initial spectrum V. Time separation scaled by the Kolmogorov time scale. $\times$, $k/k_d = 0.002$; $\square$, $k/k_d = 0.006$; $\triangle$, $k/k_d = 0.02$; $\bigcirc$, $k/k_d = 0.06$; $\triangledown$, $k/k_d = 0.2$; $\diamond$, $k/k_d = 0.6$; $+$, $k/k_d = 1.2$.

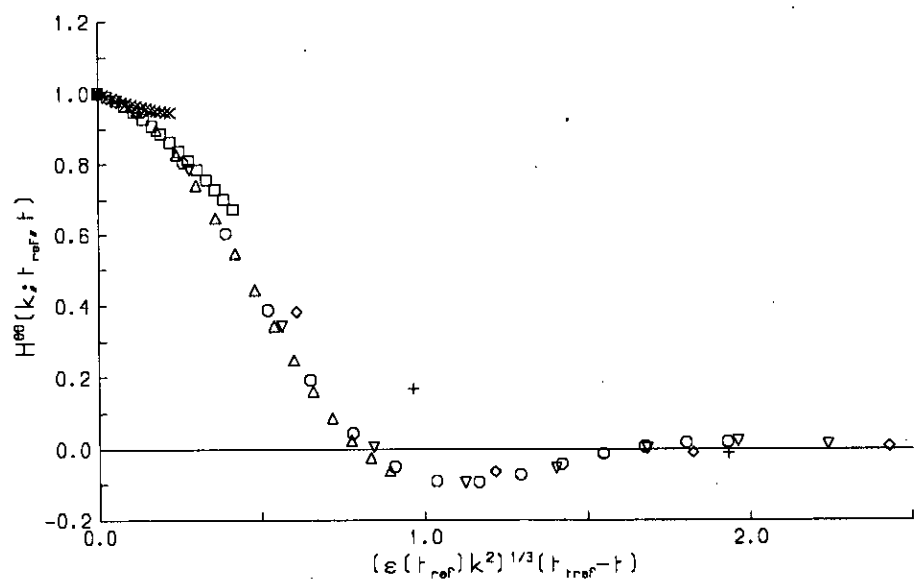

Figure 2.56: Propagator functions for the scalar at $t_{ref} = 0.38$ eddy turnover time, $R_\lambda = 558$, for $Pr = 0.5$, velocity initial spectrum V, scalar initial spectrum V. Time separation scaled by the Kolmogorov time scale. $\times$, $k/k_d = 0.002$; $\square$, $k/k_d = 0.006$; $\triangle$, $k/k_d = 0.02$; $\bigcirc$, $k/k_d = 0.06$; $\triangledown$, $k/k_d = 0.2$; $\diamond$, $k/k_d = 0.6$; $+$, $k/k_d = 1.2$.

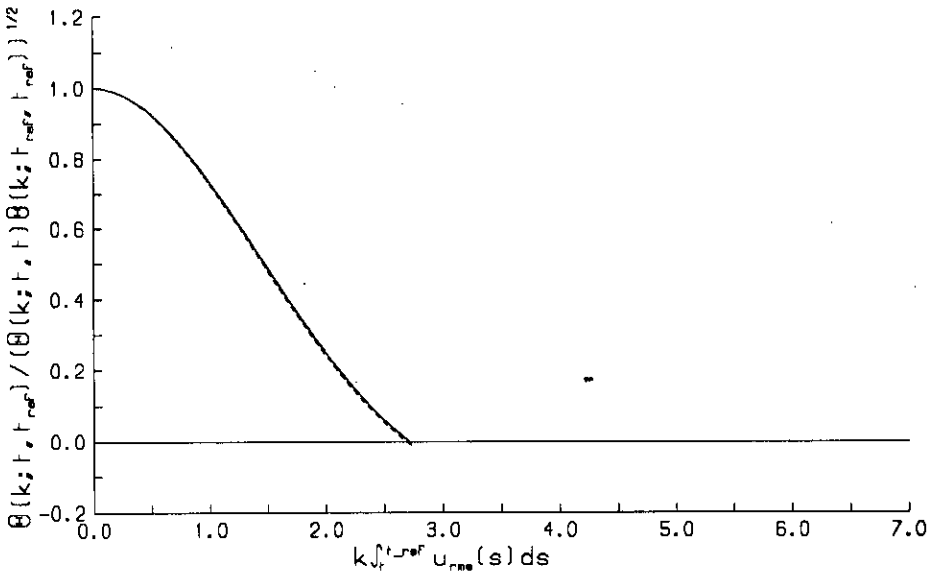

Figure 2.57: Two-time correlation functions for the scalar at $t_{ref} = 1$ eddy turnover time, $R_\lambda = 41$, for $k/k_d = 0.1$, for various Pr, velocity initial spectrum IV, scalar initial spectrum IV. Time separation scaled by the convective time scale. ----------, $Pr = 0.1$; — — —, $Pr = 0.5$; —— ——, $Pr = 0.725$; ————, $Pr = 1.0$.

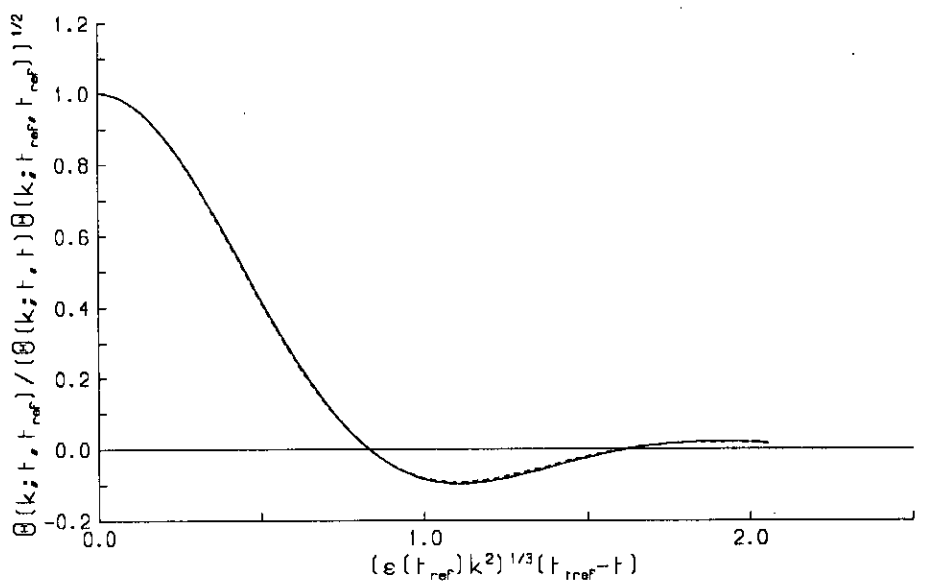

Figure 2.58: Two-time correlation functions for the scalar at $t_{ref} = 0.38$ eddy turnover time, $R_\lambda = 558$, for $k/k_d = 0.06$, for various Pr, velocity initial spectrum V, scalar initial spectrum V. Time separation scaled by the Kolmogorov time scale. ----------, $Pr = 0.1$; — — —, $Pr = 0.5$; —— ——, $Pr = 0.725$; ————, $Pr = 1.0$.

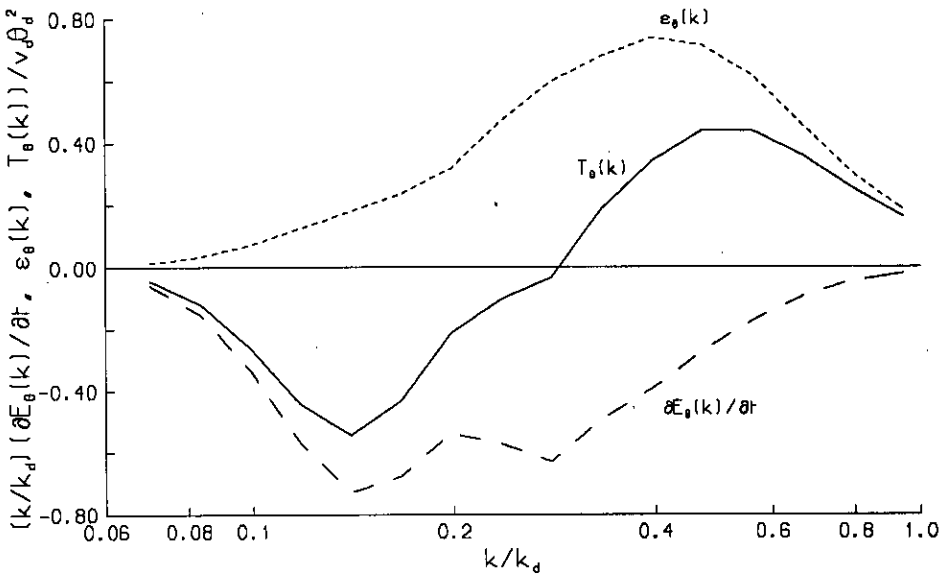

Figure 2.59: Detailed scalar energy balance at 1 eddy turnover time, $R_\lambda = 19$, for $Pr = 0.5$, velocity initial spectrum I, scalar initial spectrum I. Kolmogorov scaling used.

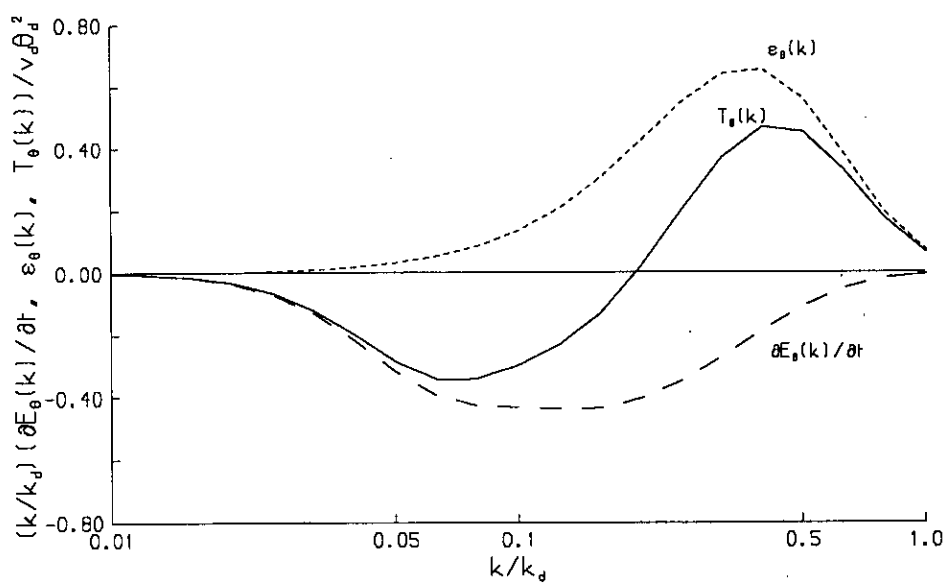

Figure 2.60: Detailed scalar energy balance at 1 eddy turnover time, $R_\lambda = 41$, for $Pr = 0.5$, velocity initial spectrum IV, scalar initial spectrum IV. Kolmogorov scaling used.

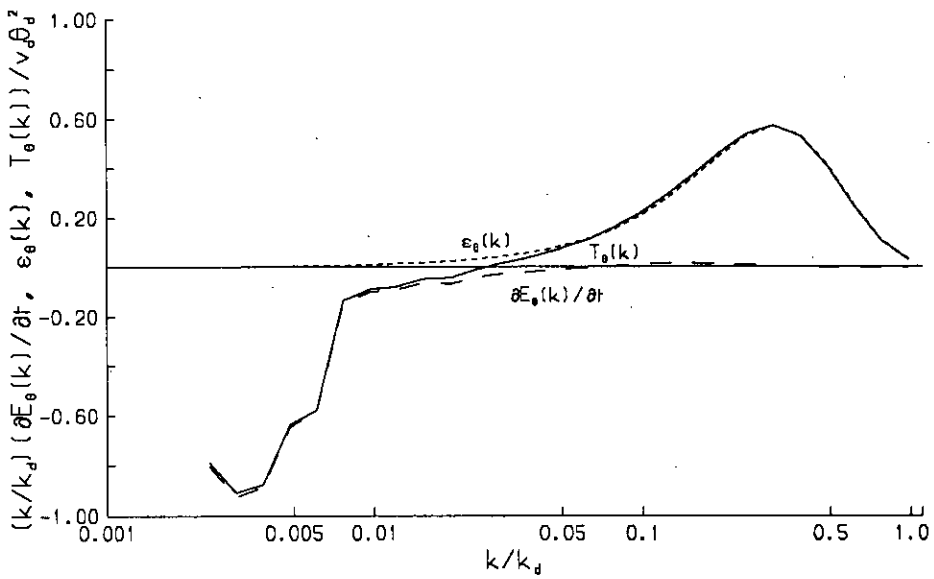

Figure 2.61: Detailed scalar energy balance at 0.38 eddy turnover time, $R_\lambda = 558$, for $Pr = 0.5$, velocity initial spectrum V, scalar initial spectrum V. Kolmogorov scaling used.

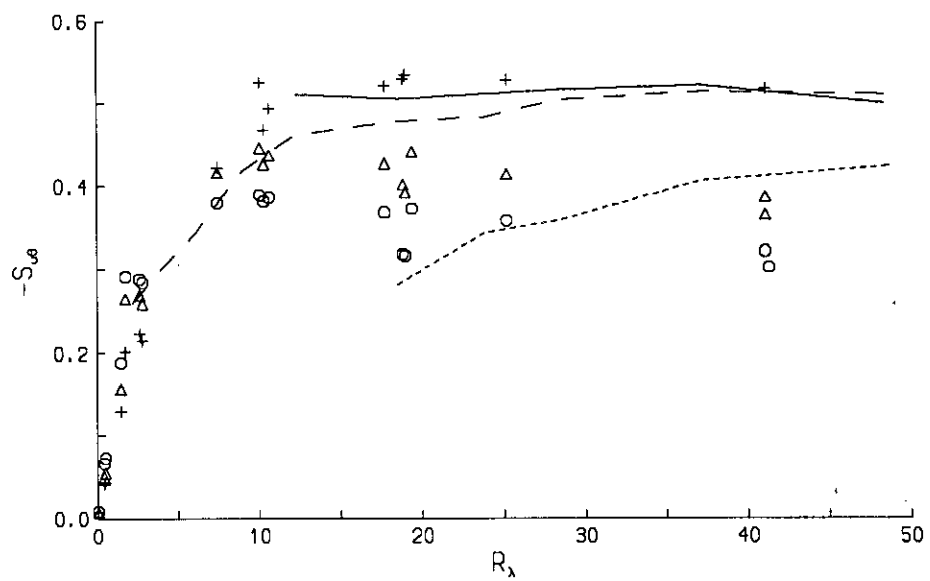

Figure 2.62: Dependence of the velocity scalar derivative skewness on R_λ and Pr. LET: +, $Pr = 0.1$; △, $Pr = 0.5$; ○, $Pr = 1.0$. Direct numerical simulation (Kerr[24]): ----------, $Pr = 0.1$; — — —, $Pr = 0.5$; ————, $Pr = 1.0$.

Chapter 3

Random Galilean Transformations

3.1 Introduction

Kraichnan postulated that all approximations for turbulence have to be invariant under a Random Galilean Transformation (RGT), defined by him. In this chapter, first LET is shown to be invariant under an ordinary 'deterministic' Galilean transformation, and then the concept of RGT is analysed. It is shown that the RGT invalidates the assumptions required to develop any LET-like theory from the Navier-Stokes equations, so it is not surprising that LET, DIA, etc. are not Random Galilean Invariant.

3.2 Background

In his 1959 paper [27] developing the Direct Interaction Approximation (DIA), a renormalised perturbation theory developed in an Eulerian frame, Kraichnan considered the very high Reynolds number limit of DIA and found that the time correlation $\langle \mathbf{u}(\mathbf{k},t)\mathbf{u}(\mathbf{k},t-\tau)\rangle$ and the response function $G(k,t,t-\tau)$ (this is H in Chapters 1 and 2) for stationary turbulence were given by $J_1(2v_0k\tau)/v_0k\tau$, where v_0 is the rms velocity, k is the wavenumber of interest and τ is the time separation. These functions enter into the calculation of the inertial range energy

spectrum to give

$$E(k) \;=\; A(\epsilon\nu_0)^{1/2}k^{-3/2}, \tag{3.1}$$

where ϵ is the total dissipation. At the time of publication there was no clear experimental evidence that the exponent of k should be $-5/3$ (Kolmogorov's theory, see [43]) or $-3/2$ (Kraichnan). Soon afterwards the very high Reynolds number results of Grant, Stewart and Moilliet [16] showed an inertial range over several decades with exponent $-5/3$. Subsequent experiments have confirmed the value of $-5/3$ but none has such a large inertial range as Grant, Stewart and Moilliet (see [43], Figure 2.4).

Given this strong experimental evidence against $k^{-3/2}$, and recognising that the appearance of ν_0 in the correlation, response and spectrum expressions would not be consistent with the local-in-wavenumber cascade of energy (implied by Kolmogorov's theory and supported by DIA), Kraichnan [30] analysed the failure of DIA as the general failure of Eulerian renormalised perturbation theories to differentiate between the dynamics at moderately high wavenumber and the convection by low wavenumber velocities. Consider a high Reynolds number turbulent flow, with a wide range of modes excited and the bulk of the kinetic energy at low wavenumbers. In an Eulerian view, the τ dependence of the two time velocity correlation $\langle \mathbf{u}(\mathbf{k},t)\mathbf{u}(\mathbf{k},t-\tau)\rangle$ will be dominated by the convection effects of the low wavenumber velocities — to see the local, 'real', distortions, the low wavenumber velocities must be subtracted out. Obviously this convection will affect measurements of two time correlations done in a laboratory frame but will not affect measurements of kinetic energy $\langle \mathbf{u}(\mathbf{k},t)\mathbf{u}(\mathbf{k},t)\rangle$ where the time separation is zero.

DIA replaces a triple moment by a product of two double moments, for instance in the equation for the kinetic energy, which is approximated by

$$\left(\frac{\partial}{\partial t} + 2\nu_0 k^2\right) Q(k;t,t)$$
$$= \; -\int d^3j\, L(\mathbf{k},\mathbf{j}) \times$$

$$\times \left\{ \int_{-\infty}^{t} ds\, G(k;t,s)Q(j;t,s)Q(|\mathbf{k}-\mathbf{j}|;t,s) \right.$$
$$\left. - \int_{-\infty}^{t} ds\, G(j;t,s)Q(|\mathbf{k}-\mathbf{j}|;t,s)Q(k;t,s) \right\}. \qquad (3.2)$$

Q is the velocity double-correlation in homogeneous isotropic turbulence and L ia a geometric factor; these quantities are defined in Section 2.3. G is the renormalised response function (similar to H for LET). It can be seen that the triple moment is a simultaneous moment and that it has been approximated by a product of two-time moments; this, according to Kraichnan, is where the trouble lies. In [30] Kraichnan uses a very simple model to illustrate the problems with DIA, and all other Eulerian renormalised perturbation theories. The model consists of an ensemble, each realisation of which is a non-self-interacting 'velocity' field being convected by a constant (in space) velocity field. This model is then developed into the Random Galilean Transformation in [31] and Kraichnan postulates that renormalised perturbation theories should be invariant under a Random Galilean Transformation. The Eulerian renormalised perturbation theories such as DIA and LET are not invariant and thus must be discarded, according to Kraichnan.

Although Kraichnan's asymptotic arguments (in [27]) are persuasive, the numerical results are inconsistent. We can discount [28] which gives a $k^{-3/2}$ energy spectrum behaviour for DIA at $R_\lambda \approx 800$ because in this simulation the response function and the velocity correlation characteristic time are explicitly set proportional to $1/v_0 k$, so the result will be $k^{-3/2}$, of course. A full simulation (i.e. solving the renormalised perturbation theory equations with no further assumptions) was done by Herring and Kraichnan [17] for several closures but unfortunately DIA was not tested at high Reynolds number. In a referee's report on [46], Herring writes that he tried out DIA at high R_λ and found convective scaling (i.e. with a characteristic time proportional to $1/v_0 k$) of response and correlation, and suggested that McComb, Shanmugasundaram and Hutchinson's result (Kolmogorov scaling for DIA) [46] arises because the lowest wavenumbers were neglected. This is untenable since the energy containing range in their calculations was above the minimum wavenumber. McComb, Shanmugasundaram and Hutchinson found that the response and correlation function characteristic times scaled as $(\epsilon k^2)^{1/3}$

at $R_\lambda \approx 1000$ for both LET and DIA, i.e. Kolmogorov scaling rather than convective scaling. They also found a $k^{-5/3}$ range in the energy spectrum even when starting from an initial spectrum proportional to $k^{-3/2}$. The reason for the differences between these numerical results may lie in the treatment of the geometrical factors and the integration over wavenumber. This is discussed more fully in Chapter 2, where it was seen that an unsuitable choice of the formulation for the geometric factor has disastrous consequences in the numerical calculation of the LET approximation for passive scalar transport.

3.3 Random Galilean Transformations defined as a model for low wavenumber convection

Kraichnan [31] defines a Random Galilean Transformation formally as follows, with $\mathbf{u}(\mathbf{x},t)$ the velocity field in $\mathbf{x}$ space and $\mathbf{c}$ ($\mathbf{v}$ in [31]) a velocity,

> Suppose that $\mathbf{u}(\mathbf{x},t)$ is augmented by an addition $\mathbf{c}$ which is constant in space and time, statistically independent of $\mathbf{u}(\mathbf{x},t)$ at any instant, and Gaussianly distributed. This means that the systems in the ensemble are subjected to uniform translations that differ randomly from system to system. At any instant t, the uniform translation is equivalent to a relabeling of space points $\mathbf{x} \rightarrow \mathbf{x} + (t - t_0)\mathbf{c}$.

For an isotropic, homogeneous flow (at least) this transformation is meant to model the turbulent energy containing modes of the flow, which are at low but non-zero wavenumber. The modelled modes must include most of the energy since the rms velocity v_0 enters into the various asymptotic results for DIA (e.g. $E(k) \sim v_0 k^{-3/2}$). Under such a transformation, the Navier-Stokes equations are invariant, but the DIA *equations* are not [31]; the reasons for this are discussed at length in subsequent sections. In the remainder of this section we will discuss the differences between a Random Galilean Transformation and convection due to low wavenumber modes in order to question the validity of the Random Galilean Transformation model.

If we consider an ensemble of isotropic, homogeneous velocity fields, without any random, constant in space additional velocities, we generally specify the

ensemble either by initial conditions (for decaying turbulence) or by the forcing term. When the initial conditions are specified (i.e. we are treating decaying turbulence) the energy spectrum is specified at some initial time t_0, with requirement that $\mathbf{u}(\mathbf{k}, t_0)$ is Gaussian, leading to a well defined ensemble. For stationary turbulence—here t_0 is $-\infty$ and any initial velocity field has no influence—the forcing is specified by the force autocorrelation spectrum, with the requirement that $\mathbf{f}(\mathbf{k}, t)$ is Gaussian, again leading to a well defined ensemble. Taking stationary forced turbulence specified by the force autocorrelation as our example, we can model convection by large scales by a RGT or by extra forcing $\mathbf{f}'$ at low wavenumber. The RGT, as in [31], is specified by $\langle c_\alpha c_\alpha \rangle$ and the requirement that $\mathbf{c}$ is Gaussian. The extra forcing $\mathbf{f}'$ is specified by the $\mathbf{f}'$ force autocorrelation and the requirement that $\mathbf{f}'$ is Gaussian. The differences between these two types of changes are as follows:

1. **RGT** The ensemble needs to be specified by the force autocorrelation and by $\langle c_\alpha c_\alpha \rangle$. An RGT is more a change in the type of ensemble than a kinematical symmetry operation.

   force The ensemble will in general change but will still be specified by a (new) force autocorrelation.

2. **RGT** The energy $\langle u_\alpha(\mathbf{k}, t) u_\alpha(\mathbf{k}, t) \rangle$ remains unchanged for $k \neq 0$

   force The energies will in general change as the Reynolds number will have changed (increased).

3. **RGT** The constant in space velocity $\mathbf{c}$ gives a δ-function at $k = 0$, i.e. a finite amount of kinetic energy as $k \to 0$.

   force The energy is proportional to k-space volume as $k \to 0$.

4. **RGT** The operators (e.g. $\partial/\partial t$) as well as the fields are random variables (see Section 3.5 below).

   force The operators are unchanged.

5. **RGT** The solution of the Navier-Stokes equations with the non-linear term removed (the zero order solution) is no longer Gaussian (see Section 3.5

below).

force The zero order solution remains Gaussian.

Thus it seems that an RGT does not capture the essence of the low wavenumber/large scale motion. (Note that the analysis in [30], which has a non-self-interacting velocity field being convected by a constant in space velocity is not a valid approximation — it breaks down at long times $\sim 1/v_0 k$ and arbitrarily splits the velocity field in two).

3.4 Properties of the Navier-Stokes equations, exact moment equations, perturbation expansions and LET under a (deterministic) Galilean transformation

As a preamble to the treatment of RGTs we look at ordinary Galilean transformations. This sets the notation and the background for RGTs, although there are significant differences. In addition this clears up some doubts about the invariance of LET under deterministic Galilean transformations. In this section, and the section on RGTs, we will consider LET rather than DIA; the arguments for LET go through for DIA since they are both in the same class of Eulerian renormalised perturbation theories and are both non-invariant under RGTs. The derivation of LET is detailed in Section 2.3

We need to take some care over the transformations, especially with regard to the operators. Consider two vector spaces U,V where U is the space of forces and velocity differences, including the fluctuation about a mean velocity, and V is the space of total velocities, including the mean velocity. Then we can see that in the solenoidal Navier-Stokes equation

$$\left(\frac{\partial}{\partial t} + \nu k^2\right) v_\alpha(\mathbf{k},t) - M_{\alpha\beta\gamma}(\mathbf{k}) \int v_\beta(\mathbf{k}-\mathbf{j},t) v_\gamma(\mathbf{j},t)\, d^3j \;\; = \;\; f_\alpha(\mathbf{k},t) \quad (3.3)$$

$v \in V$, since this is the total velocity, and $f \in U$. Thus the operators act between

the following spaces:

$$\frac{\partial}{\partial t} \;:\; V \to U \tag{3.4}$$

$$\nu k^2 \;:\; V \to U \tag{3.5}$$

$$M_{\alpha\beta\gamma}(\mathbf{k}) \int d^3j \;:\; V \to U \tag{3.6}$$

Once we know the nature of the operators and the fields the transformations are trivial.

Setting

There are two frames S and $S^\dagger$, with $S^\dagger$ moving with velocity $\mathbf{c}$ with respect to S.

$(\mathbf{x}, t)$ space

The coordinates transform as follows:

$$\mathbf{x}^\dagger = \mathbf{x} - \mathbf{c}t \tag{3.7}$$

$$t^\dagger = t \tag{3.8}$$

$$\mathbf{x} = \mathbf{x}^\dagger + \mathbf{c}t \tag{3.9}$$

$$t = t^\dagger, \tag{3.10}$$

differential operators as:

$$\left.\frac{\partial}{\partial t^\dagger}\right|_{\mathbf{x}^\dagger} = \mathbf{c}.\nabla|_t + \left.\frac{\partial}{\partial t}\right|_{\mathbf{x}} \tag{3.11}$$

$$\nabla^\dagger|_{t^\dagger} = \nabla|_t, \tag{3.12}$$

and the total velocity and pressure as:

$$\mathbf{v}^\dagger(\mathbf{x}^\dagger, t^\dagger) = \mathbf{v}(\mathbf{x}, t) - \mathbf{c} \tag{3.13}$$

$$\mathbf{p}^\dagger(\mathbf{x}^\dagger, t^\dagger) = \mathbf{p}(\mathbf{x}, t) \tag{3.14}$$

For an ensemble of velocity fields, define the mean and fluctuating components of the field as:

$$\mathbf{V}(\mathbf{x}, t) = \langle \mathbf{v}(\mathbf{x}, t) \rangle \tag{3.15}$$

$$\mathbf{v}(\mathbf{x}, t) = \mathbf{V}(\mathbf{x}, t) + \mathbf{u}(\mathbf{x}, t) \tag{3.16}$$

$$\langle \mathbf{u}(\mathbf{x}, t) \rangle = \mathbf{0}. \tag{3.17}$$

Then (for a deterministic Galilean transformation) $\mathbf{V}(\mathbf{x}, t)$ and $\mathbf{u}(\mathbf{x}, t)$ transform as follows ($\mathbf{V}$ is a mean velocity and $\mathbf{c}$ is also a mean (constant) velocity; $\mathbf{u}$ is a fluctuating velocity):

$$\mathbf{V}^\dagger(\mathbf{x}^\dagger, t^\dagger) = \mathbf{V}(\mathbf{x}, t) - \mathbf{c} \tag{3.18}$$

$$\mathbf{u}^\dagger(\mathbf{x}^\dagger, t^\dagger) = \mathbf{u}(\mathbf{x}, t) \tag{3.19}$$

$(\mathbf{k}, t)$ space

These coordinates transform as follows:

$$\mathbf{k}^\dagger = \mathbf{k} \tag{3.20}$$

$$t^\dagger = t \tag{3.21}$$

so we will just use $\mathbf{k}$ and t in both the transformed and untransformed frames. This is one great advantage of using these coordinates. The Galilean transformation of the $(\mathbf{x} \rightarrow \mathbf{k})$ Fourier transform of a function is given by:

$$\begin{aligned} f^\dagger(\mathbf{k}, t) &= \frac{1}{2\pi} \int e^{-i\mathbf{k}.\mathbf{x}^\dagger} f^\dagger(\mathbf{x}^\dagger, t^\dagger)\, d^3x^\dagger \\ &= \frac{1}{2\pi} \int e^{-i\mathbf{k}.(\mathbf{x}-\mathbf{c}t)} f^\dagger(\mathbf{x}^\dagger, t^\dagger)\, d^3x \\ &= \frac{1}{2\pi} e^{i\mathbf{k}.\mathbf{c}t)} \int e^{-i\mathbf{k}.\mathbf{x}} f^\dagger(\mathbf{x}^\dagger, t^\dagger)\, d^3x\,, \end{aligned} \tag{3.22}$$

using the transformation rule for $\mathbf{x}$ and the fact that the Jacobian of the transformation is 1. Thus the velocity, pressure and body force transform as follows:

$$\mathbf{v}^{\dagger}(\mathbf{k},t) = e^{i\mathbf{k}.\mathbf{c}t}\mathbf{v}(\mathbf{k},t) - \mathbf{c}\delta^3(\mathbf{k}) \tag{3.23}$$

$$p^{\dagger}(\mathbf{k},t) = e^{i\mathbf{k}.\mathbf{c}t}\mathbf{p}(\mathbf{k},t) \tag{3.24}$$

$$\mathbf{f}^{\dagger}(\mathbf{k},t) = e^{i\mathbf{k}.\mathbf{c}t}\mathbf{f}(\mathbf{k},t) \tag{3.25}$$

with the reverse transformation:

$$\mathbf{v}(\mathbf{k},t) = e^{-i\mathbf{k}.\mathbf{c}t}\{\mathbf{v}^{\dagger}(\mathbf{k},t) - \mathbf{c}\delta^3(\mathbf{k})\} \tag{3.26}$$

$$\mathbf{p}(\mathbf{k},t) = e^{-i\mathbf{k}.\mathbf{c}t}\mathbf{p}^{\dagger}(\mathbf{k},t) \tag{3.27}$$

$$\mathbf{f}(\mathbf{k},t) = e^{-i\mathbf{k}.\mathbf{c}t}\mathbf{f}^{\dagger}(\mathbf{k},t) \tag{3.28}$$

For an ensemble of velocity fields, define the mean and fluctuating components of the field as:

$$\mathbf{V}(\mathbf{k},t) = \langle \mathbf{v}(\mathbf{k},t) \rangle \tag{3.29}$$

$$\mathbf{v}(\mathbf{k},t) = \mathbf{V}(\mathbf{k},t) + \mathbf{u}(\mathbf{k},t) \tag{3.30}$$

$$\langle \mathbf{u}(\mathbf{k},t) \rangle = \mathbf{0}. \tag{3.31}$$

Then, under a deterministic Galilean transformation $\mathbf{V}(\mathbf{k},t)$ and $\mathbf{u}(\mathbf{k},t)$ transform as follows:

$$\mathbf{V}^{\dagger}(\mathbf{k},t) = e^{i\mathbf{k}.\mathbf{c}t}\mathbf{V}(\mathbf{k},t) - \mathbf{c}\delta^3(\mathbf{k}) \tag{3.32}$$

$$\mathbf{u}^{\dagger}(\mathbf{k},t) = e^{i\mathbf{k}.\mathbf{c}t}\mathbf{u}(\mathbf{k},t) \tag{3.33}$$

It is important to stress that, *since* $\mathbf{c}$ *is not random, we can commute the transformation and the averaging.* (Compare this with RGTs later, where $\mathbf{c}$ is a random variable and cannot be simply pulled out of averages in order to re-arrange equations).

Treating $\partial/\partial t + \nu k^2$ as a single operator, it transforms as follows:

$$\left(\frac{\partial}{\partial t} + \nu k^2\right)^{\dagger} v_\alpha^\dagger(\mathbf{k},t)$$
$$= e^{i\mathbf{k}.\mathbf{c}t}\left(\frac{\partial}{\partial t} + \nu k^2\right) e^{-i\mathbf{k}.\mathbf{c}t}\left[v_\alpha^\dagger(\mathbf{k},t) + c_\alpha \delta^3(\mathbf{k})\right]. \qquad (3.34)$$

Similarly, the non-linear term transforms as follows:

$$\left(M_{\alpha\beta\gamma}(\mathbf{k})\int d^3j\right)^{\dagger} v_\beta^\dagger(\mathbf{k}-\mathbf{j},t)v_\gamma^\dagger(\mathbf{j},t)$$
$$= e^{i\mathbf{k}.\mathbf{c}t} M_{\alpha\beta\gamma}(\mathbf{k})\int d^3j \times$$
$$e^{-i(\mathbf{k}-\mathbf{j}).\mathbf{c}t}\left[v_\beta^\dagger(\mathbf{k}-\mathbf{j},t) + c_\beta\delta^3(\mathbf{k}-\mathbf{j})\right]$$
$$\times e^{-i\mathbf{j}.\mathbf{c}t}\left[v_\gamma^\dagger(\mathbf{j},t) + c_\gamma\delta^3(\mathbf{j})\right] \qquad (3.35)$$

It is important to recognise that:

1. The operators must be transformed. $\partial/\partial t$ and M are not separately invariant; together they form the total time derivative, which is Galilean invariant, of course. Since we want to separate these operators to develop a perturbation expansion in powers of M (effectively), we must transform them individually.

2. The domains and ranges of the operators have to be taken into account.

3. $\mathbf{c}$ is part of the mean velocity $\mathbf{V}$

Galilean Invariance of the Navier-Stokes Equations

With these transformation rules, the Navier Stokes equation can be shown to be Galilean invariant. This is demonstrated here for fluid filling all of space. The solenoidal Navier-Stokes momentum equation in $(\mathbf{k},t)$ space is:

$$\left(\frac{\partial}{\partial t} + \nu k^2\right) v_\alpha(\mathbf{k},t) - M_{\alpha\beta\gamma}(\mathbf{k})\int v_\beta(\mathbf{k}-\mathbf{j},t)v_\gamma(\mathbf{j},t)\,d^3j = f_\alpha(\mathbf{k},t). \qquad (3.36)$$

Multiplying Equation (3.36) by $e^{i\mathbf{k}.\mathbf{c}t}$, with v written as the inverse GT of $v^\dagger$, we get:

$$\begin{aligned}
& e^{i\mathbf{k}.\mathbf{c}t}\left(\frac{\partial}{\partial t}+\nu k^2\right)e^{-i\mathbf{k}.\mathbf{c}t}\left[v_\alpha^\dagger(\mathbf{k},t)+c_\alpha\delta^3(\mathbf{k})\right] \\
& -e^{i\mathbf{k}.\mathbf{c}t}M_{\alpha\beta\gamma}(\mathbf{k})\int d^3j \\
& e^{-i(\mathbf{k}-\mathbf{j}).\mathbf{c}t}\left[v_\beta^\dagger(\mathbf{k}-\mathbf{j},t)+c_\beta\delta^3(\mathbf{k}-\mathbf{j})\right] \\
& \times e^{-i\mathbf{j}.\mathbf{c}t}\left[v_\gamma^\dagger(\mathbf{j},t)+c_\gamma\delta^3(\mathbf{j})\right] \\
& \quad = \; e^{i\mathbf{k}.\mathbf{c}t}f_\alpha(\mathbf{k},t). \qquad (3.37)
\end{aligned}$$

Comparing this with Equations (3.25), (3.34) and (3.35), we see that Equation (3.37) is just the transformed Navier Stokes equation

$$\begin{aligned}
& \left(\frac{\partial}{\partial t}+\nu k^2\right)^\dagger v_\alpha^\dagger(\mathbf{k},t)-\left(M_{\alpha\beta\gamma}(\mathbf{k})\int d^3j\right)^\dagger v_\beta^\dagger(\mathbf{k}-\mathbf{j},t)v_\gamma^\dagger(\mathbf{j},t) \\
& \quad = \; f_\alpha^\dagger(\mathbf{k},t). \qquad (3.38)
\end{aligned}$$

Symbolically we can write, using the definitions

$$\begin{aligned}
L &\equiv \frac{\partial}{\partial t}+\nu k^2, \\
M &\equiv M_{\alpha\beta\gamma}(\mathbf{k})\int d^3j\,, \qquad (3.39)
\end{aligned}$$

$$Lv - Mvv \;=\; f \qquad (3.40)$$

implies

$$L^\dagger v^\dagger - M^\dagger v^\dagger v^\dagger \;=\; f^\dagger \qquad (3.41)$$

So the Navier Stokes equation is invariant under Galilean transformations, as expected since it is just an expression of Newton's Second Law.

The equations for the fluctuating velocity $\mathbf{u}(\mathbf{k},t)$

Now consider an ensemble of flows so we can define averages, etc. The averaged Navier Stokes momentum equation is then

$$\begin{aligned}
&\left(\frac{\partial}{\partial t}+\nu k^2\right) V_\alpha(\mathbf{k},t) \\
&-M_{\alpha\beta\gamma}(\mathbf{k})\int V_\beta(\mathbf{k}-\mathbf{j},t)V_\gamma(\mathbf{j},t)\,d^3j \\
&-M_{\alpha\beta\gamma}(\mathbf{k})\int \langle u_\beta(\mathbf{k}-\mathbf{j},t)u_\gamma(\mathbf{j},t)\rangle\,d^3j \\
&\quad = \langle f_\alpha(\mathbf{k},t)\rangle\,.
\end{aligned} \tag{3.42}$$

and the equation for the fluctuation u is obtained by subtracting Equation (3.42) from the Navier-Stokes equation

$$\begin{aligned}
&\left(\frac{\partial}{\partial t}+\nu k^2\right) u_\alpha(\mathbf{k},t) \\
&-2M_{\alpha\beta\gamma}(\mathbf{k})\int d^3j\, V_\beta(\mathbf{k}-\mathbf{j},t)u_\gamma(\mathbf{j},t) \\
&-M_{\alpha\beta\gamma}(\mathbf{k})\int d^3j\, u_\beta(\mathbf{k}-\mathbf{j},t)u_\gamma(\mathbf{j},t) \\
&+M_{\alpha\beta\gamma}(\mathbf{k})\int d^3j\, \langle u_\beta(\mathbf{k}-\mathbf{j},t)u_\gamma(\mathbf{j},t)\rangle \\
&\quad = f_\alpha(\mathbf{k},t)-\langle f_\alpha(\mathbf{k},t)\rangle
\end{aligned} \tag{3.43}$$

The operators in the fluctuation equation, Equation (3.43), now transform slightly differently. This is because we have subtracted out the mean velocity $\mathbf{V}$ to get $\mathbf{u}$ and so there will be no additive terms in the transformation rules for operators acting on $\mathbf{u}$. $\partial/\partial t+\nu k^2$ transforms as follows (cf. Equation (3.34)):

$$\left(\frac{\partial}{\partial t}+\nu k^2\right)^\dagger u_\alpha^\dagger(\mathbf{k},t) \;=\; e^{i\mathbf{k}.\mathbf{c}t}\left(\frac{\partial}{\partial t}+\nu k^2\right)e^{-i\mathbf{k}.\mathbf{c}t}u_\alpha^\dagger(\mathbf{k},t), \tag{3.44}$$

the Vu operator transforms as follows (cf. Equation (3.35)):

$$\begin{aligned}
&\left(M_{\alpha\beta\gamma}(\mathbf{k})\int d^3j\right)^\dagger V_\beta^\dagger(\mathbf{k}-\mathbf{j},t)u_\gamma^\dagger(\mathbf{j},t) \\
&\quad = e^{i\mathbf{k}.\mathbf{c}t}M_{\alpha\beta\gamma}(\mathbf{k})\int d^3j\, e^{-i(\mathbf{k}-\mathbf{j}).\mathbf{c}t}\left[V_\beta^\dagger(\mathbf{k}-\mathbf{j},t)+c_\beta\delta^3(\mathbf{k}-\mathbf{j})\right]\times \\
&\qquad e^{-i\mathbf{j}.\mathbf{c}t}u_\gamma^\dagger(\mathbf{j},t)
\end{aligned} \tag{3.45}$$

and the uu operator transforms as follows (cf. Equation (3.35)):

$$\begin{aligned}
&\left(M_{\alpha\beta\gamma}(\mathbf{k})\int d^3j\right)^\dagger u^\dagger_\beta(\mathbf{k}-\mathbf{j},t)u^\dagger_\gamma(\mathbf{j},t)\\
&= e^{i\mathbf{k}.\mathbf{c}t}\,M_{\alpha\beta\gamma}(\mathbf{k})\int d^3j\, e^{-i(\mathbf{k}-\mathbf{j}).\mathbf{c}t}\,u^\dagger_\beta(\mathbf{k}-\mathbf{j},t)\times\\
&\quad e^{-i\mathbf{j}.\mathbf{c}t}\,u^\dagger_\gamma(\mathbf{j},t) \qquad (3.46)
\end{aligned}$$

The transformation of Equation (3.43) goes through exactly as the Navier-Stokes equation: multiplying Equation (3.43) by $e^{i\mathbf{k}.\mathbf{c}t}$ and averaging over the ensemble, with v written as the inverse GT of $v^\dagger$ and u written as the inverse GT of $u^\dagger$, we get, since the averaging and the transformation commute:

$$\begin{aligned}
&e^{i\mathbf{c}.\mathbf{k}t}\left(\frac{\partial}{\partial t}+\nu k^2\right)e^{-i\mathbf{c}.\mathbf{k}t}\,u^\dagger_\alpha(\mathbf{k},t)\\
&-2e^{i\mathbf{c}.\mathbf{k}t}\,M_{\alpha\beta\gamma}(\mathbf{k})\int d^3j\, e^{-i\mathbf{c}.(\mathbf{k}-\mathbf{j})t}\times\\
&\left[V^\dagger_\beta(\mathbf{k}-\mathbf{j},t)+c_\beta\delta^3(\mathbf{k}-\mathbf{j})\right]e^{-i\mathbf{c}.\mathbf{j}t}\,u^\dagger_\gamma(\mathbf{j},t)\\
&-e^{i\mathbf{c}.\mathbf{k}t}\,M_{\alpha\beta\gamma}(\mathbf{k})\int d^3j\, e^{-i\mathbf{c}.(\mathbf{k}-\mathbf{j})t}\,u^\dagger_\beta(\mathbf{k}-\mathbf{j},t)e^{-i\mathbf{c}.\mathbf{j}t}\,u^\dagger_\gamma(\mathbf{j},t)\\
&+e^{i\mathbf{c}.\mathbf{k}t}\,M_{\alpha\beta\gamma}(\mathbf{k})\int d^3j\,\langle e^{-i\mathbf{c}.(\mathbf{k}-\mathbf{j})t}\,u^\dagger_\beta(\mathbf{k}-\mathbf{j},t)e^{-i\mathbf{c}.\mathbf{j}t}\,u^\dagger_\gamma(\mathbf{j},t)\rangle\\
&\quad = e^{i\mathbf{c}.\mathbf{k}t}\,f_\alpha(\mathbf{k},t), \qquad (3.47)
\end{aligned}$$

i.e.:

$$\begin{aligned}
&\left(\frac{\partial}{\partial t}+\nu k^2\right)^\dagger u^\dagger_\alpha(\mathbf{k},t)\\
&-2\left(M_{\alpha\beta\gamma}(\mathbf{k})\int d^3j\right)^\dagger V^\dagger_\beta(\mathbf{k}-\mathbf{j},t)u^\dagger_\gamma(\mathbf{j},t)\\
&-\left(M_{\alpha\beta\gamma}(\mathbf{k})\int d^3j\right)^\dagger u^\dagger_\beta(\mathbf{k}-\mathbf{j},t)u^\dagger_\gamma(\mathbf{j},t)\\
&+\left(M_{\alpha\beta\gamma}(\mathbf{k})\int d^3j\right)^\dagger\langle u^\dagger_\beta(\mathbf{k}-\mathbf{j},t)u^\dagger_\gamma(\mathbf{j},t)\rangle\\
&\qquad = f^\dagger_\alpha(\mathbf{k},t). \qquad (3.48)
\end{aligned}$$

We can ignore the complications of arguments and subscripts and write symbolically:

$$Lu-2MVu-Muu+M\langle uu\rangle = f \qquad (3.49)$$

implies

$$L^\dagger u^\dagger - 2M^\dagger V^\dagger u^\dagger - M^\dagger u^\dagger u^\dagger + M^\dagger \langle u^\dagger u^\dagger \rangle \;=\; f^\dagger. \tag{3.50}$$

So the fluctuation equation is invariant under Galilean transformations.

The fluctuating moment equation

The equation for the 2nd moment of u, $\langle u_\alpha(\mathbf{k},t)u_\delta(\mathbf{k}',t')\rangle$, is obtained by multiplying Equation (3.43) by $u_\delta(\mathbf{k}',t')$ and averaging:

$$\begin{aligned}
&\left(\frac{\partial}{\partial t} + \nu k^2\right)\langle u_\alpha(\mathbf{k},t)u_\delta(\mathbf{k}',t')\rangle \\
-2M_{\alpha\beta\gamma}(\mathbf{k})&\int d^3j\, V_\beta(\mathbf{k}-\mathbf{j},t)\langle u_\gamma(\mathbf{j},t)u_\delta(\mathbf{k}',t')\rangle \\
-M_{\alpha\beta\gamma}(\mathbf{k})&\int d^3j\, \langle u_\beta(\mathbf{k}-\mathbf{j},t)u_\gamma(\mathbf{j},t)u_\delta(\mathbf{k}',t')\rangle \\
&= \langle f_\alpha(\mathbf{k},t)u_\delta(\mathbf{k}',t')\rangle.
\end{aligned} \tag{3.51}$$

This is easily shown to be Galilean invariant. Multiply Equation 3.51 by $e^{i\mathbf{k}.\mathbf{c}t}$ with V written as the inverse GT of $V^\dagger$ and u written as the inverse GT of $u^\dagger$, to get

$$\begin{aligned}
&e^{i\mathbf{c}.\mathbf{k}t}\left(\frac{\partial}{\partial t} + \nu k^2\right)\langle e^{-i\mathbf{c}.\mathbf{k}t}\, u^\dagger_\alpha(\mathbf{k},t)e^{-i\mathbf{c}.\mathbf{k}'t'}\, u^\dagger_\delta(\mathbf{k}',t')\rangle \\
&-2e^{i\mathbf{c}.\mathbf{k}t}\, M_{\alpha\beta\gamma}(\mathbf{k})\int d^3j\, e^{-i\mathbf{c}.(\mathbf{k}-\mathbf{j})t}\left[V^\dagger_\beta(\mathbf{k}-\mathbf{j},t) + c_\beta\delta^3(\mathbf{k}-\mathbf{j})\right]\times \\
&\langle e^{-i\mathbf{c}\mathbf{j}t}\, u^\dagger_\gamma(\mathbf{j},t)e^{-i\mathbf{c}.\mathbf{k}'t'}\, u^\dagger_\delta(\mathbf{k}',t')\rangle \\
&-e^{i\mathbf{c}.\mathbf{k}t}\, M_{\alpha\beta\gamma}(\mathbf{k})\int d^3j\,\times \\
&\langle e^{-i\mathbf{c}.(\mathbf{k}-\mathbf{j})t}\, u^\dagger_\beta(\mathbf{k}-\mathbf{j},t)e^{-i\mathbf{c}\mathbf{j}t}\, u^\dagger_\gamma(\mathbf{j},t)e^{-i\mathbf{c}.\mathbf{k}'t'}\, u_\delta(\mathbf{k}',t')\rangle \\
&\quad = \langle e^{i\mathbf{c}.\mathbf{k}t}\, f_\alpha(\mathbf{k},t)e^{-i\mathbf{c}.\mathbf{k}'t'}\, u_\delta(\mathbf{k}',t')\rangle.
\end{aligned} \tag{3.52}$$

Since $\mathbf{c}$ is not random (cf. RGTs, Section 3.5), the exponential factors can be pulled through the averages to give, after dividing by $e^{-i\mathbf{c}.\mathbf{k}'t'}$

$$e^{i\mathbf{c}.\mathbf{k}t}\left(\frac{\partial}{\partial t} + \nu k^2\right)e^{-i\mathbf{c}.\mathbf{k}t}\,\langle u^\dagger_\alpha(\mathbf{k},t)u^\dagger_\delta(\mathbf{k}',t')\rangle -$$

$$
\begin{aligned}
&-2e^{\mathbf{ic.kt}}\, M_{\alpha\beta\gamma}(\mathbf{k}) \int d^3j\, e^{-\mathbf{ic.(k-j)}t} \left[V^\dagger_\beta(\mathbf{k}-\mathbf{j},t) + c_\beta \delta^3(\mathbf{k}-\mathbf{j})\right] \times \\
&e^{-\mathbf{ic.j}t} \langle u^\dagger_\gamma(\mathbf{j},t) u^\dagger_\delta(\mathbf{k}',t')\rangle \\
&-e^{\mathbf{ic.kt}}\, M_{\alpha\beta\gamma}(\mathbf{k}) \int d^3j\, e^{-\mathbf{ic.(k-j)}t}\, e^{-\mathbf{ic.j}t} \times \\
&\langle u^\dagger_\beta(\mathbf{k}-\mathbf{j},t) u^\dagger_\gamma(\mathbf{j},t) u_\delta(\mathbf{k}',t')\rangle \\
&\qquad = \; e^{\mathbf{ic.kt}} \langle f_\alpha(\mathbf{k},t) u_\delta(\mathbf{k}',t')\rangle, \qquad (3.53)
\end{aligned}
$$

which is just the transformed equation

$$
\begin{aligned}
&\left(\frac{\partial}{\partial t} + \nu k^2\right)^\dagger \langle u^\dagger_\alpha(\mathbf{k},t) u^\dagger_\delta(\mathbf{k}',t')\rangle \\
&-2\left(M_{\alpha\beta\gamma}(\mathbf{k}) \int d^3j\right)^\dagger V^\dagger_\beta(\mathbf{k}-\mathbf{j},t) \langle u^\dagger_\gamma(\mathbf{j},t) u^\dagger_\delta(\mathbf{k}',t')\rangle \\
&-\left(M_{\alpha\beta\gamma}(\mathbf{k}) \int d^3j\right)^\dagger \langle u^\dagger_\beta(\mathbf{k}-\mathbf{j},t) u^\dagger_\gamma(\mathbf{j},t) u^\dagger_\delta(\mathbf{k}',t')\rangle \\
&\qquad = \; \langle f^\dagger_\alpha(\mathbf{k},t) u^\dagger_\delta(\mathbf{k}',t')\rangle. \qquad (3.54)
\end{aligned}
$$

Symbolically this is:

$$
L\langle uu\rangle - 2MV\langle uu\rangle - M\langle uuu\rangle \;=\; \langle fu\rangle \qquad (3.55)
$$

implies

$$
L^\dagger\langle u^\dagger u^\dagger\rangle - 2M^\dagger V^\dagger\langle u^\dagger u^\dagger\rangle - M^\dagger\langle u^\dagger u^\dagger u^\dagger\rangle \;=\; \langle f^\dagger u^\dagger\rangle \qquad (3.56)
$$

So the two time fluctuation moment equation is invariant under Galilean transformations and this result is easily extended to higher order moment equations.

Perturbation expansion

Details of the expansion of the fluctuating velocity field about the zero order field $\mathbf{u}^0$ are given in Section 2.3 and in this subsection we will show that this expansion, if done carefully, is Galilean invariant, *even* if the expansion parameter λ (see Equation 2.29) is not equal to 1. This result holds for any truncation of the series since the expansion is Galilean invariant term by term.

To clarify the treatment we assume homogeneity. We cannot assume isotropy since the transforming velocity $\mathbf{c}$ is in one direction for all realisations of the ensemble (compare this with Random Galilean Transformations later). Then the mean velocity is constant in space and time:

$$\langle v_\alpha(\mathbf{k},t)\rangle \;=\; V_\alpha \delta^3(\mathbf{k}) \tag{3.57}$$

and

$$\begin{aligned}\langle v^\dagger_\alpha(\mathbf{k},t)\rangle &= (V_\alpha - c_\alpha)\,\delta^3(\mathbf{k}) \\ &\equiv V^\dagger_\alpha \delta^3(\mathbf{k})\end{aligned} \tag{3.58}$$

One usually now assumes that $\mathbf{V} = 0$ and treats the fluctuation $\mathbf{u}$ only but here we do have to retain the possibility of $\mathbf{V}$ being non-zero since this is just what a Galilean transformation will give. We also assume that there is no average forcing at $\mathbf{k} = \mathbf{0}$, i.e. no 'rigid body' acceleration. Thus

$$\langle f_\alpha(\mathbf{k},t)\rangle \;=\; 0. \tag{3.59}$$

Then the averaged Navier Stokes equation (Equation 3.42) reduces for the case $V_\alpha(\mathbf{k},t) = V_\alpha \delta^3(\mathbf{k})$ to

$$\begin{aligned}&\left(\frac{\partial}{\partial t} + \nu k^2\right) V_\alpha \delta^3(\mathbf{k}) \\ &-M_{\alpha\beta\gamma}(\mathbf{k}) \int V_\beta \delta^3(\mathbf{k}-\mathbf{j}) V_\gamma \delta^3(\mathbf{j})\, d^3j \\ &-M_{\alpha\beta\gamma}(\mathbf{k}) \int \langle u_\beta(\mathbf{k}-\mathbf{j},t) u_\gamma(\mathbf{j},t)\rangle\, d^3j \;=\; 0\end{aligned} \tag{3.60}$$

which is just

$$M_{\alpha\beta\gamma}(\mathbf{k}) \int \langle u_\beta(\mathbf{k}-\mathbf{j},t) u_\gamma(\mathbf{j},t)\rangle\, d^3j \;=\; 0 \tag{3.61}$$

since V is constant in time and $\mathbf{k}\delta^3(\mathbf{k})$ and $M_{\alpha\beta\gamma}(\mathbf{k})\delta^3(\mathbf{k})$ are zero. Using Equa-

tion (3.61), Equation (3.43) becomes

$$\begin{aligned} &\left(\frac{\partial}{\partial t}+\nu k^2\right) u_\alpha(\mathbf{k},t) \\ -2M_{\alpha\beta\gamma}(\mathbf{k})&\int d^3j\, V_\beta \delta^3(\mathbf{k}-\mathbf{j}) u_\gamma(\mathbf{j},t) \\ -M_{\alpha\beta\gamma}(\mathbf{k})&\int d^3j\, u_\beta(\mathbf{k}-\mathbf{j},t) u_\gamma(\mathbf{j},t) \\ &= f_\alpha(\mathbf{k},t). \end{aligned} \tag{3.62}$$

Now,

$$2M_{\alpha\beta\gamma}(\mathbf{k})\int d^3j\, V_\beta \delta^3(\mathbf{k}-\mathbf{j}) u_\gamma(\mathbf{j},t) = 2M_{\alpha\beta\gamma}(\mathbf{k}) V_\beta u_\gamma(\mathbf{k},t) \tag{3.63}$$

using the δ-function. The RHS can be simplified as follows

$$\begin{aligned} 2M_{\alpha\beta\gamma}(\mathbf{k})V_\beta u_\gamma(\mathbf{k},t) &= -i\left[k_\beta D_{\alpha\gamma}(\mathbf{k}) + k_\gamma D_{\alpha\beta}(\mathbf{k})\right] V_\beta u_\gamma(\mathbf{k},t) \\ &= -i\mathbf{V}.\mathbf{k} u_\alpha(\mathbf{k},t) \end{aligned} \tag{3.64}$$

using the definition of M (Equation (2.8)) and incompressibility. Thus Equation (3.62) is

$$\begin{aligned} &\left(\frac{\partial}{\partial t}+\nu k^2 + i\mathbf{V}.\mathbf{k}\right) u_\alpha(\mathbf{k},t) \\ -M_{\alpha\beta\gamma}(\mathbf{k})&\int d^3j\, u_\beta(\mathbf{k}-\mathbf{j},t) u_\gamma(\mathbf{j},t) \\ &= f_\alpha(\mathbf{k},t) \end{aligned} \tag{3.65}$$

where all the terms linear in u are grouped together (cf. [29]). We now multiply the non-linear term by a parameter λ, which will be set to 1 eventually, to get

$$\begin{aligned} &\left(\frac{\partial}{\partial t}+\nu k^2 + i\mathbf{V}.\mathbf{k}\right) u_\alpha(\mathbf{k},t) \\ -\lambda M_{\alpha\beta\gamma}(\mathbf{k})&\int d^3j\, u_\beta(\mathbf{k}-\mathbf{j},t) u_\gamma(\mathbf{j},t) \\ &= f_\alpha(\mathbf{k},t) \end{aligned} \tag{3.66}$$

and proceed to develop a perturbation expansion as in Chapter 2. First expand

the velocity field $\mathbf{u}$ about $\mathbf{u}^{(0)}$, the solution of Equation (3.66) with $\lambda = 0$

$$\mathbf{u}(\mathbf{k},t) = \mathbf{u}^{(0)}(\mathbf{k},t) + \lambda \mathbf{u}^{(1)}(\mathbf{k},t) + \lambda^2 \mathbf{u}^{(2)}(\mathbf{k},t) + \ldots \tag{3.67}$$

where

$$\left(\frac{\partial}{\partial t} + \nu k^2 + i\mathbf{V}.\mathbf{k}\right) u_\alpha^{(0)}(\mathbf{k},t) = f_\alpha(\mathbf{k},t). \tag{3.68}$$

(Note the difference from Chapter 2 where there are no $\mathbf{V}$ terms since we assumed that the mean velocity was zero). This zero-order equation can be solved easily to give

$$u_\alpha^{(0)}(\mathbf{k},t) = \int_{-\infty}^{t} ds\, e^{-\nu k^2(t-s) - i\mathbf{V}.\mathbf{k}(t-s)}\, f_\alpha(\mathbf{k},s) \tag{3.69}$$

where the initial velocity at $t = -\infty$ has decayed to zero, noting that any zero-k $\mathbf{u}^{(0)}$ (or $\mathbf{u}$) is assumed to be zero. For $\mathbf{V} = \mathbf{0}$ we recover the 'usual' zero order solution. The first order correction is given by

$$\left(\frac{\partial}{\partial t} + \nu k^2 + i\mathbf{V}.\mathbf{k}\right) u_\alpha^{(1)}(\mathbf{k},t) = M_{\alpha\beta\gamma}(\mathbf{k}) \int d^3j\, u_\beta^{(0)}(\mathbf{k}-\mathbf{j},t) u_\gamma^{(0)}(\mathbf{j},t) \tag{3.70}$$

with solution

$$u_\alpha^{(1)}(\mathbf{k},t) = \int_{-\infty}^{t} ds\, e^{-\nu k^2(t-s) - i\mathbf{V}.\mathbf{k}(t-s)}\, M_{\alpha\beta\gamma}(\mathbf{k}) \int d^3j\, u_\beta^{(0)}(\mathbf{k}-\mathbf{j},s) u_\gamma^{(0)}(\mathbf{j},s). \tag{3.71}$$

The higher order corrections are formed similarly.

Now we do the same analysis in a Galilean transformed frame, with transformation velocity $\mathbf{c}$, using the transformed fields and operators and get the equations for the mean and fluctuating velocities, analogous to the untransformed equations:

$$\left(\frac{\partial}{\partial t} + \nu k^2\right)^\dagger V_\alpha^\dagger \delta^3(\mathbf{k}) -$$

$$
\begin{aligned}
&- \left(M_{\alpha\beta\gamma}(\mathbf{k}) \int d^3j \right)^\dagger V_\beta^\dagger \delta^3(\mathbf{k}-\mathbf{j}) V_\gamma^\dagger \delta^3(\mathbf{j}) \\
&- \left(M_{\alpha\beta\gamma}(\mathbf{k}) \int d^3j \right)^\dagger \langle u_\beta^\dagger(\mathbf{k}-\mathbf{j},t) u_\gamma^\dagger(\mathbf{j},t) \rangle \;=\; 0
\end{aligned} \tag{3.72}
$$

which is just

$$
\left(M_{\alpha\beta\gamma}(\mathbf{k}) \int d^3j \right)^\dagger \langle u_\beta^\dagger(\mathbf{k}-\mathbf{j},t) u_\gamma^\dagger(\mathbf{j},t) \rangle \;=\; 0 \tag{3.73}
$$

and

$$
\begin{aligned}
&\left(\frac{\partial}{\partial t} + \nu k^2 \right)^\dagger u_\alpha^\dagger(\mathbf{k},t) \\
&-2 \left(M_{\alpha\beta\gamma}(\mathbf{k}) \int d^3j \right)^\dagger V_\beta^\dagger \delta^3(\mathbf{k}-\mathbf{j}) u_\gamma^\dagger(\mathbf{j},t) \\
&- \left(M_{\alpha\beta\gamma}(\mathbf{k}) \int d^3j \right)^\dagger u_\beta^\dagger(\mathbf{k}-\mathbf{j},t) u_\gamma^\dagger(\mathbf{j},t) \\
&\qquad\qquad = \; f_\alpha^\dagger(\mathbf{k},t)
\end{aligned} \tag{3.74}
$$

which is just

$$
\begin{aligned}
&\left(\left(\frac{\partial}{\partial t} + \nu k^2 \right)^\dagger + i\mathbf{V}^\dagger.\mathbf{k} \right) u_\alpha^\dagger(\mathbf{k},t) \\
&- \left(M_{\alpha\beta\gamma}(\mathbf{k}) \int d^3j \right)^\dagger u_\beta^\dagger(\mathbf{k}-\mathbf{j},t) u_\gamma^\dagger(\mathbf{j},t) \\
&\qquad\qquad = \; f_\alpha^\dagger(\mathbf{k},t).
\end{aligned} \tag{3.75}
$$

We form a perturbation expansion in the transformed frame exactly as for the original frame

$$
\mathbf{u}^\dagger(\mathbf{k},t) \;=\; (\mathbf{u}^\dagger)^{(0)}(\mathbf{k},t) + \lambda(\mathbf{u}^\dagger)^{(1)}(\mathbf{k},t) + \lambda^2(\mathbf{u}^\dagger)^{(2)}(\mathbf{k},t) + \ldots \tag{3.76}
$$

where

$$
\left(\left(\frac{\partial}{\partial t} + \nu k^2 \right)^\dagger + i\mathbf{V}^\dagger.\mathbf{k} \right) (u^\dagger)_\alpha^{(0)}(\mathbf{k},t) \;=\; f_\alpha^\dagger(\mathbf{k},t). \tag{3.77}
$$

To invert this equation we express the operator in terms of untransformed quan-

tities:

$$\left(\left(\frac{\partial}{\partial t}+\nu k^2\right)^{\dagger}+i\mathbf{V}^{\dagger}.\mathbf{k}\right) = \left(\left(\frac{\partial}{\partial t}+\nu k^2\right)+i\mathbf{V}.\mathbf{k}\right)^{\dagger}, \quad (3.78)$$

$$\left(\left(\left(\frac{\partial}{\partial t}+\nu k^2\right)^{\dagger}+i\mathbf{V}^{\dagger}.\mathbf{k}\right)\right)^{-1} = \left(\left(\left(\frac{\partial}{\partial t}+\nu k^2\right)+i\mathbf{V}.\mathbf{k}\right)^{-1}\right)^{\dagger} \quad (3.79)$$

$$= e^{i\mathbf{c}.\mathbf{k}t} \times \left(\int_{-\infty}^{t} ds\, e^{-\nu k^2(t-s)-i\mathbf{V}.\mathbf{k}(t-s)}\right) \times e^{-i\mathbf{c}.\mathbf{k}t}. \quad (3.80)$$

So the zero-order solution of Equation 3.75 is

$$(u^{\dagger})^{(0)}_{\alpha}(\mathbf{k},t) = e^{i\mathbf{c}.\mathbf{k}t}\left(\int_{-\infty}^{t} ds\, e^{-\nu k^2(t-s)-i\mathbf{V}.\mathbf{k}(t-s)}\right) e^{-i\mathbf{c}.\mathbf{k}s}\, f^{\dagger}_{\alpha}(\mathbf{k},s). \quad (3.81)$$

The first order correction is given by

$$(u^{\dagger})^{(1)}_{\alpha}(\mathbf{k},t) = e^{i\mathbf{c}.\mathbf{k}t}\left(\int_{-\infty}^{t} ds\, e^{-\nu k^2(t-s)-i\mathbf{V}.\mathbf{k}(t-s)}\right) e^{-i\mathbf{c}.\mathbf{k}s} \times \left(M_{\alpha\beta\gamma}(\mathbf{k})\int d^3j\right)^{\dagger}(u^{\dagger})^{(0)}_{\beta}(\mathbf{k}-\mathbf{j},s)(u^{\dagger})^{(0)}_{\gamma}(\mathbf{j},s). \quad (3.82)$$

The higher order corrections are formed similarly.

In order to show that the perturbation expansion is Galilean invariant, we have to show that each term $(\mathbf{u}^{\dagger})^{(n)}$ is the Galilean transformation of $\mathbf{u}^{(n)}$:

$$(u^{\dagger})^{(n)}_{\alpha}(\mathbf{k},t) = (u^{(n)})^{\dagger}_{\alpha}(\mathbf{k},t) \quad (3.83)$$

and thus that

$$\begin{aligned}\mathbf{u}(\mathbf{k},t) &= \mathbf{u}^{(0)}(\mathbf{k},t)+\lambda\mathbf{u}^{(1)}(\mathbf{k},t)+\lambda^2\mathbf{u}^{(2)}(\mathbf{k},t)+\ldots \\ &\Updownarrow \\ \mathbf{u}^{\dagger}(\mathbf{k},t) &= (\mathbf{u}^{\dagger})^{(0)}(\mathbf{k},t)+\lambda(\mathbf{u}^{\dagger})^{(1)}(\mathbf{k},t)+\lambda^2(\mathbf{u}^{\dagger})^{(2)}(\mathbf{k},t)+\ldots \end{aligned} \quad (3.84)$$

We will see that the invariance holds term by term, and thus will hold even for $\lambda \neq 1$ and allow truncation of the perturbation expansion.

So, we show that $(\mathbf{u}^\dagger)^{(0)} = (\mathbf{u}^{(0)})^\dagger$ and then show that $\mathbf{u}^{(n)}$ transforms correctly by induction. First of all, what is $(\mathbf{u}^{(0)})^\dagger$? The definition of $\mathbf{u}^{(0)}$ is given by Equation (3.69), thus

$$\begin{aligned}(u^{(0)})^\dagger_\alpha(\mathbf{k},t) &= \left(\int_{-\infty}^{t} ds\, e^{-\nu k^2(t-s)-i\mathbf{V}.\mathbf{k}(t-s)}\right)^\dagger f^\dagger_\alpha(\mathbf{k},s) \\ &= e^{i\mathbf{c}.\mathbf{k}t}\, u^{(0)}_\alpha(\mathbf{k},t) \end{aligned} \tag{3.85}$$

using the transformation rules for the zero order propagator and the force. Thus, as expected, $\mathbf{u}^{(0)}$ transforms like a velocity difference. It is easily seen that this result extends to all $\mathbf{u}^{(n)}$:

$$(u^{(n)})^\dagger_\alpha(\mathbf{k},t) = e^{i\mathbf{c}.\mathbf{k}t}\, u^{(n)}_\alpha(\mathbf{k},t) \tag{3.86}$$

Equation 3.81 can be written as

$$(\mathbf{u}^\dagger)^{(0)}(\mathbf{k},t) = e^{i\mathbf{c}.\mathbf{k}t}\left(\int_{-\infty}^{t} ds\, e^{-\nu k^2(t-s)-i\mathbf{V}.\mathbf{k}(t-s)}\right)\mathbf{f}(\mathbf{k},s). \tag{3.87}$$

using the transformation rule for $\mathbf{f}$. This equation is just

$$(\mathbf{u}^\dagger)^{(0)}(\mathbf{k},t) = e^{i\mathbf{c}.\mathbf{k}t}\,\mathbf{u}^{(0)}(\mathbf{k},t). \tag{3.88}$$

Thus

$$(u^\dagger)^{(0)}_\alpha(\mathbf{k},t) = (u^{(0)})^\dagger_\alpha(\mathbf{k},t), \tag{3.89}$$

so $(\mathbf{u}^\dagger)^{(0)}$ *is* the Galilean transformation of $\mathbf{u}^{(0)}$.

Now consider $\mathbf{u}^{(1)}$ (Equations (3.70) and (3.82):

$$\begin{aligned}(u^\dagger)^{(1)}_\alpha(\mathbf{k},t) &= e^{i\mathbf{c}.\mathbf{k}t}\left(\int_{-\infty}^{t} ds\, e^{-\nu k^2(t-s)-i\mathbf{V}.\mathbf{k}(t-s)}\right)e^{-i\mathbf{c}.\mathbf{k}s}\times \\ &\quad \left(M_{\alpha\beta\gamma}(\mathbf{k})\int d^3j\right)^\dagger (u^\dagger)^{(0)}_\beta(\mathbf{k}-\mathbf{j},s)(u^\dagger)^{(0)}_\gamma(\mathbf{j},s) \\ &= e^{i\mathbf{c}.\mathbf{k}t}\left(\int_{-\infty}^{t} ds\, e^{-\nu k^2(t-s)-i\mathbf{V}.\mathbf{k}(t-s)}\right)e^{-i\mathbf{c}.\mathbf{k}s}\times \\ &\quad \left(M_{\alpha\beta\gamma}(\mathbf{k})\int d^3j\, u^{(0)}_\beta(\mathbf{k}-\mathbf{j},s)u^{(0)}_\gamma(\mathbf{j},s)\right)^\dagger \end{aligned}$$

$$
\begin{aligned}
&= e^{i\mathbf{c}.\mathbf{k}t}\left(\int_{-\infty}^{t} ds\, e^{-\nu k^2(t-s)-i\mathbf{V}.\mathbf{k}(t-s)}\right)\times \\
&\quad M_{\alpha\beta\gamma}(\mathbf{k})\int d^3j\, u_\beta^{(0)}(\mathbf{k}-\mathbf{j},s)u_\gamma^{(0)}(\mathbf{j},s) \\
&= e^{i\mathbf{c}.\mathbf{k}t}\, u_\alpha^{(1)}(\mathbf{k},t) \qquad (3.90)
\end{aligned}
$$

using the transformation rules for $M\mathbf{uu}$, $\mathbf{u}$ and the solution for the first order term $\mathbf{u}^{(1)}$ in the original frame. Thus

$$
(u^\dagger)_\alpha^{(1)}(\mathbf{k},t) = (u^{(1)})_\alpha^\dagger(\mathbf{k},t). \qquad (3.91)
$$

So $(\mathbf{u}^\dagger)^{(1)}$ is the Galilean transformation of $\mathbf{u}^{(1)}$.

In general, suppose we have shown that

$$
\begin{aligned}
(u^\dagger)_\alpha^{(0)}(\mathbf{k},t) &= (u^{(0)})_\alpha^\dagger(\mathbf{k},t) \\
&\vdots \\
(u^\dagger)_\alpha^{(n-1)}(\mathbf{k},t) &= (u^{(n-1)})_\alpha^\dagger(\mathbf{k},t), \qquad (3.92)
\end{aligned}
$$

that the nth term in the perturbation expansion in the original frame is given by an expression like

$$
\left(\left(\frac{\partial}{\partial t}+\nu k^2\right)+i\mathbf{V}.\mathbf{k}\right)(u)_\alpha^{(n)}(\mathbf{k},t) = X[(\mathbf{u})^{(0)},\ldots,(\mathbf{u})^{(n-1)}]_\alpha(\mathbf{k},t) \qquad (3.93)
$$

where X is some function of M and $((\partial/\partial t+\nu k^2)+i\mathbf{V}.\mathbf{k})^{-1}$ and the the nth term in the perturbation expansion in the transformed frame is given by an expression like

$$
\begin{aligned}
&\left(\left(\frac{\partial}{\partial t}+\nu k^2\right)^\dagger+i\mathbf{V}^\dagger.\mathbf{k}\right)(u^\dagger)_\alpha^{(n)}(\mathbf{k},t) \\
&\quad = X^\dagger[(\mathbf{u}^\dagger)^{(0)},\ldots,(\mathbf{u}^\dagger)^{(n-1)}]_\alpha(\mathbf{k},t) \qquad (3.94)
\end{aligned}
$$

where $X^\dagger$ is the same function of $M^\dagger$ and $\left((\partial/\partial t+\nu k^2)^\dagger+i\mathbf{V}^\dagger.\mathbf{k}\right)^{-1}$. Since $\mathbf{u}^{(0)},\ldots,u^{(n-1)}$ transform correctly, the right hand side of Equation (3.94) is just

the Galilean transformation of $X[\mathbf{u}^{(0)},\ldots,\mathbf{u}^{(n-1)}]_\alpha(\mathbf{k},t)$ and we have

$$\left(\left(\frac{\partial}{\partial t}+\nu k^2\right)^\dagger + i\mathbf{V}^\dagger.\mathbf{k}\right)(u^\dagger)^{(n)}_\alpha(\mathbf{k},t) \;=\; \left(X[\mathbf{u}^{(0)},\ldots,\mathbf{u}^{(n-1)}]_\alpha(\mathbf{k},t)\right)^\dagger \quad (3.95)$$

Inverting this, and expressing the linear operator in terms of untransformed quantities, we get

$$\begin{aligned}(u^\dagger)^{(n)}_\alpha(\mathbf{k},t) \;=\; & e^{i\mathbf{c}.\mathbf{k}t}\left(\int_{-\infty}^{t} ds\, e^{-\nu k^2(t-s)-i\mathbf{V}.\mathbf{k}(t-s)}\right)e^{-i\mathbf{c}.\mathbf{k}s}\times \\ & \left(X[\mathbf{u}^{(0)},\ldots,\mathbf{u}^{(n-1)}]_\alpha(\mathbf{k},t)\right)^\dagger. \end{aligned} \quad (3.96)$$

$\left(X[\mathbf{u}^{(0)},\ldots,\mathbf{u}^{(n-1)}]_\alpha(\mathbf{k},t)\right)$ is like a force, so its transformation rule will be

$$\left(X[\mathbf{u}^{(0)},\ldots,\mathbf{u}^{(n-1)}]_\alpha(\mathbf{k},t)\right)^\dagger \;=\; e^{i\mathbf{c}.\mathbf{k}t}\left(X[\mathbf{u}^{(0)},\ldots,\mathbf{u}^{(n-1)}]_\alpha(\mathbf{k},t)\right) \quad (3.97)$$

and thus the RHS of Equation 3.96 can be rewritten to give

$$\begin{aligned}(u^\dagger)^{(n)}_\alpha(\mathbf{k},t) \;=\; & e^{i\mathbf{c}.\mathbf{k}t}\left(\int_{-\infty}^{t} ds\, e^{-\nu k^2(t-s)-i\mathbf{V}.\mathbf{k}(t-s)}\right) \\ & X[\mathbf{u}^{(0)},\ldots,\mathbf{u}^{(n-1)}]_\alpha(\mathbf{k},t) \end{aligned} \quad (3.98)$$

which is

$$(u^\dagger)^{(n)}_\alpha(\mathbf{k},t) \;=\; e^{i\mathbf{c}.\mathbf{k}t}\,u^{(n)}_\alpha(\mathbf{k},t). \quad (3.99)$$

Since $u^{(n)}_\alpha(\mathbf{k},t)$ is a velocity difference, its Galilean transformation is

$$(u^{(n)})^\dagger_\alpha(\mathbf{k},t) \;=\; e^{i\mathbf{c}.\mathbf{k}t}\,u^{(n)}_\alpha(\mathbf{k},t) \quad (3.100)$$

and thus Equation 3.99 is just

$$(u^\dagger)^{(n)}_\alpha(\mathbf{k},t) \;=\; (u^{(n)})^\dagger_\alpha(\mathbf{k},t). \quad (3.101)$$

Thus the primitive perturbation expansion and each equation for $\mathbf{u}^{(n)}$ are Galilean invariant. In achieving this result the operators had to be transformed as well as

the fields and the average velocity had to be separated out correctly.

The properties of LET under a Galilean transformation

To show that LET is Galilean invariant we look at the LET equation for the two-time moment in homogeneous turbulence, $Q(\mathbf{k};t,t')$, derived in Section 2.3, and the equation for the propagator H. We generalise Equation (2.53) to include the effects of a mean velocity equal to $\mathbf{V}\delta^3(\mathbf{k})$, i.e. we start from Equation (3.65) rather than Equation (2.6):

$$\begin{aligned}
&\left(\left(\frac{\partial}{\partial t}+\nu k^2\right)+i\mathbf{V}.\mathbf{k}\right)Q_{\alpha\rho}(\mathbf{k};t,t') \\
&= M_{\alpha\beta\gamma}(\mathbf{k})\int d^3j\ \times \\
&\quad\left\{2\int_0^{t'} ds\, H_{\rho\sigma}(-\mathbf{k};t',s)M_{\sigma\omega\phi}(-\mathbf{k})Q_{\beta\omega}(\mathbf{j};t,s)Q_{\gamma\phi}(\mathbf{k}-\mathbf{j};t,s)\right. \\
&\quad\left.-4\int_0^{t} ds\, H_{\beta\sigma}(\mathbf{j};t,s)M_{\sigma\omega\phi}(\mathbf{j})Q_{\gamma\omega}(\mathbf{k}-\mathbf{j};t,s)Q_{\phi\rho}(\mathbf{k};s,t')\right\}. \qquad (3.102)
\end{aligned}$$

In this equation we have not yet specialised to isotropic turbulence, so the structure of the $M\int$ operator is still clear. Equation (2.20) for the propagator is

$$Q_{\alpha\beta}(\mathbf{k};t,t') = H_{\alpha\gamma}(\mathbf{k};t,t')Q_{\gamma\beta}(\mathbf{k};t',t'). \qquad (3.103)$$

The central point is that the transforming velocity $\mathbf{c}$ is not a random variable so transformations and averages commute, allowing us to write down the Galilean transformations of H and Q, which are averages, in terms of the transformation rules for operators and fields. As we will see later, under a Random Galilean Transformation transformations and averages do not commute. Q is the average of a $\mathbf{uu}$ product

$$Q_{\alpha\sigma}(\mathbf{k};t,t')\delta^3(\mathbf{k}+\mathbf{k}') = \langle u_\alpha(\mathbf{k},t)u_\sigma(\mathbf{k}',t')\rangle \qquad (3.104)$$

and the corresponding quantity in the transformed frame is given by

$$Q^\dagger_{\alpha\sigma}(\mathbf{k};t,t')\delta^3(\mathbf{k}+\mathbf{k}') = \langle u^\dagger_\alpha(\mathbf{k},t)u^\dagger_\sigma(\mathbf{k}',t')\rangle$$

$$= e^{i\mathbf{c}.\mathbf{k}t}\, e^{i\mathbf{c}.\mathbf{k}'t'} \langle u_\alpha(\mathbf{k},t) u_\sigma(\mathbf{k}',t') \rangle \tag{3.105}$$

using the transformation rule for $\mathbf{u}$ and pulling the exponential factors out of the average since $\mathbf{c}$ is not random. Rewriting the $\mathbf{uu}$ moment in terms of Q, we get

$$\begin{aligned} Q^\dagger_{\alpha\sigma}(\mathbf{k};t,t')\delta^3(\mathbf{k}+\mathbf{k}') &= e^{i\mathbf{c}.\mathbf{k}t}\, e^{i\mathbf{c}.\mathbf{k}'t'}\, Q_{\alpha\sigma}(\mathbf{k};t,t')\delta^3(\mathbf{k}+\mathbf{k}') \\ &= e^{i\mathbf{c}.\mathbf{k}t}\, e^{-i\mathbf{c}.\mathbf{k}t'}\, Q_{\alpha\sigma}(\mathbf{k};t,t')\delta^3(\mathbf{k}+\mathbf{k}') \end{aligned} \tag{3.106}$$

using the δ-function. Then integrating over $\mathbf{k}'$ gives us the transformation rule for Q

$$Q^\dagger_{\alpha\sigma}(\mathbf{k};t,t') = e^{i\mathbf{c}.\mathbf{k}(t-t')}\, Q_{\alpha\sigma}(\mathbf{k};t,t'). \tag{3.107}$$

From Equation (2.20) and the transformation rule for Q we can find the transformation rule for H:

$$Q^\dagger_{\alpha\beta}(\mathbf{k};t,t') = H^\dagger_{\alpha\gamma}(\mathbf{k};t,t') Q^\dagger_{\gamma\beta}(\mathbf{k};t',t') \tag{3.108}$$

can be written as

$$e^{i\mathbf{c}.\mathbf{k}(t-t')}\, Q_{\alpha\beta}(\mathbf{k};t,t') = H^\dagger_{\alpha\gamma}(\mathbf{k};t,t') e^{i\mathbf{c}.\mathbf{k}(t'-t')}\, Q_{\gamma\beta}(\mathbf{k};t',t'). \tag{3.109}$$

Thus

$$H_{\alpha\sigma}(\mathbf{k};t,s) = e^{-i\mathbf{c}.\mathbf{k}t}\, H^\dagger_{\alpha\sigma}(\mathbf{k};t,s) e^{i\mathbf{c}.\mathbf{k}s}. \tag{3.110}$$

and

$$H^\dagger_{\alpha\sigma}(\mathbf{k};t,s) = e^{i\mathbf{c}.\mathbf{k}t}\, H_{\alpha\sigma}(\mathbf{k};t,s) e^{-i\mathbf{c}.\mathbf{k}s}. \tag{3.111}$$

Rewriting Equation 3.102 with the operators and moments written in terms

of transformed quantities we get

$$
\begin{aligned}
& e^{-i\mathbf{c}.\mathbf{k}t}\left(\left(\frac{\partial}{\partial t}+\nu k^2\right)^{\dagger}+i\mathbf{V}^{\dagger}.\mathbf{k}\right)e^{i\mathbf{c}.\mathbf{k}t}\times \\
& e^{-i\mathbf{c}.\mathbf{k}t}\,Q^{\dagger}_{\alpha\rho}(\mathbf{k};t,t')e^{i\mathbf{c}.\mathbf{k}t'} \\
&\quad = \; e^{-i\mathbf{c}.\mathbf{k}t}\left(M_{\alpha\beta\gamma}(\mathbf{k})\int d^3j\right)^{\dagger}e^{i\mathbf{c}.(\mathbf{k}-\mathbf{j})t}\,e^{i\mathbf{c}.\mathbf{j}t}\times \\
&\qquad \left\{2\int_{(0)}^{t'} ds\, e^{-i\mathbf{c}.(-\mathbf{k})t'}\,H^{\dagger}_{\rho\sigma}(-\mathbf{k};t',s)e^{i\mathbf{c}.(-\mathbf{k})s}\times\right. \\
&\qquad e^{-i\mathbf{c}.(-\mathbf{k})s}\,M^{\dagger}_{\sigma\omega\phi}(-\mathbf{k})e^{i\mathbf{c}.(-\mathbf{k})s}\times \\
&\qquad e^{-i\mathbf{c}.\mathbf{j}t}\,Q^{\dagger}_{\beta\omega}(\mathbf{j};t,s)e^{i\mathbf{c}.\mathbf{j}s}\,e^{-i\mathbf{c}.(\mathbf{k}-\mathbf{j})t}\,Q^{\dagger}_{\gamma\phi}(\mathbf{k}-\mathbf{j};t,s)e^{i\mathbf{c}.(\mathbf{k}-\mathbf{j})s} \\
&\qquad -4\int_{(0)}^{t} ds\, e^{-i\mathbf{c}.\mathbf{j}t}\,H^{\dagger}_{\beta\sigma}(\mathbf{j};t,s)e^{i\mathbf{c}.\mathbf{j}s}\times \\
&\qquad e^{-i\mathbf{c}.\mathbf{j}s}\,M^{\dagger}_{\sigma\omega\phi}(\mathbf{j})e^{i\mathbf{c}.\mathbf{j}s}\times \\
&\qquad \left. e^{-i\mathbf{c}.(\mathbf{k}-\mathbf{j})t}\,Q^{\dagger}_{\gamma\omega}(\mathbf{k}-\mathbf{j};t,s)e^{i\mathbf{c}.(\mathbf{k}-\mathbf{j})s}\,e^{-i\mathbf{c}.\mathbf{k}s}\,Q^{\dagger}_{\phi\rho}(\mathbf{k};s,t')e^{i\mathbf{c}.\mathbf{k}t'}\right\}. \qquad (3.112)
\end{aligned}
$$

Rearranging and cancelling exponential factors we get the transformed version of Equation 3.102

$$
\begin{aligned}
& \left(\left(\frac{\partial}{\partial t}+\nu k^2\right)^{\dagger}+i\mathbf{V}^{\dagger}.\mathbf{k}\right)Q^{\dagger}_{\alpha\rho}(\mathbf{k};t,t') \\
&\quad = \; \left(M_{\alpha\beta\gamma}(\mathbf{k})\int d^3j\right)^{\dagger} \\
&\qquad \left\{2\int_{(0)}^{t'} ds\, H^{\dagger}_{\rho\sigma}(-\mathbf{k};t',s)M^{\dagger}_{\sigma\omega\phi}(-\mathbf{k})Q^{\dagger}_{\beta\omega}(\mathbf{j};t,s)Q^{\dagger}_{\gamma\phi}(\mathbf{k}-\mathbf{j};t,s)\right. \\
&\qquad \left. -\,4\int_{(0)}^{t} ds\, H^{\dagger}_{\beta\sigma}(\mathbf{j};t,s)M^{\dagger}_{\sigma\omega\phi}(\mathbf{j})Q^{\dagger}_{\gamma\omega}(\mathbf{k}-\mathbf{j};t,s)Q^{\dagger}_{\phi\rho}(\mathbf{k};s,t')\right\}. \qquad (3.113)
\end{aligned}
$$

So LET is Galilean invariant—symbolically we have

$$
L^{\dagger}Q^{\dagger} \;=\; 2M\int^{t'} HMQQ - 4M\int^{t} HMQQ \qquad (3.114)
$$

implies

$$
L^{\dagger}Q^{\dagger} \;=\; 2M^{\dagger}\int^{t'} H^{\dagger}M^{\dagger}Q^{\dagger}Q^{\dagger} - 4M^{\dagger}\int^{t} H^{\dagger}M^{\dagger}Q^{\dagger}Q^{\dagger}. \qquad (3.115)
$$

3.5 Random Galilean Transformations, Random Galilean Invariance and perturbation theory

Kraichnan's Random Galilean Transformation (RGT) can be defined in wavenumber space as follows:

> Consider an ensemble of N realisations of the velocity field $\mathbf{u}$, labelled $\mathbf{u}_1, \ldots, \mathbf{u}_N$ where for convenience we take $\langle \mathbf{u} \rangle = 0$ (the mean velocity is not central to the treatment of RGTs since $\mathbf{c}$ is a fluctuating quantity). Then to apply Kraichnan's RGT, Galilean transform the ith realisation using the transforming velocity $\mathbf{c}_{(i)}$, an instance of a random variable $\mathbf{c}$, i.e.
>
> $$\mathbf{u}^{\dagger}_{(i)}(\mathbf{k}, t) = e^{i\mathbf{k}.\mathbf{c}_{(i)}t}\, \mathbf{u}_{(i)}(\mathbf{k}, t) - \mathbf{c}_{(i)}\delta^3(\mathbf{k}). \qquad (3.116)$$
>
> $\mathbf{c}$ must be independent of $\mathbf{u}$ since the low wavenumber modes which $\mathbf{c}$ is meant to model are independent of the higher wavenumber modes (which are $\mathbf{u}$). $\mathbf{c}$ is chosen in [31] to be Gaussian with zero mean, but for our treatment we will not need this.

Thus the Random Galilean Transformed ensemble is a new *ensemble*, rather than a kinematical transformation. Under this ensemble/transformation the fields *and operators* transform into random variables, dependent on $\mathbf{c}$. Consider first one realisation. Then, the velocity field transforms as

$$\mathbf{u}^{\dagger}_{(i)}(\mathbf{k}, t) = e^{i\mathbf{k}.\mathbf{c}_{(i)}t}\, \mathbf{u}_{(i)}(\mathbf{k}, t) - \mathbf{c}_{(i)}\delta^3(\mathbf{k}). \qquad (3.117)$$

This is like the transformation rule for the total velocity under an ordinary Galilean transformation; here $\mathbf{c}$ is part of the fluctuating velocity while in the case of an ordinary Galilean transformation the transforming velocity is part of the mean velocity. Since $\mathbf{c}$ is included additively in the transformed $\mathbf{u}$ field, the transformation rules for the operators must reflect this, and so the operators

$\partial/\partial t + \nu k^2$ and M transform as

$$\left(\frac{\partial}{\partial t} + \nu k^2\right)^{\dagger}_{(i)} u^{\dagger}_{(i)\alpha}(\mathbf{k},t) = e^{i\mathbf{k}.\mathbf{c}_{(i)}t}\left(\frac{\partial}{\partial t} + \nu k^2\right)_{(i)} e^{-i\mathbf{k}.\mathbf{c}_{(i)}t} \times \left[u^{\dagger}_{(i)\alpha}(\mathbf{k},t) + c_{(i)\alpha}\delta^3(\mathbf{k})\right] \tag{3.118}$$

and

$$\begin{aligned}\left(M_{\alpha\beta\gamma}(\mathbf{k})\int d^3j\right)^{\dagger}_{(i)} & u^{\dagger}_{(i)\beta}(\mathbf{k}-\mathbf{j},t)u^{\dagger}_{(i)\gamma}(\mathbf{j},t) \\ = \; & e^{i\mathbf{k}.\mathbf{c}_{(i)}t}\left(M_{\alpha\beta\gamma}(\mathbf{k})\int d^3j\right)_{(i)} \\ & e^{-i(\mathbf{k}-\mathbf{j}).\mathbf{c}_{(i)}t}\left[u^{\dagger}_{(i)\beta}(\mathbf{k}-\mathbf{j},t) + c_{(i)\beta}\delta^3(\mathbf{k}-\mathbf{j})\right] \\ & \times e^{-i\mathbf{j}.\mathbf{c}_{(i)}t}\left[u^{\dagger}_{(i)\gamma}(\mathbf{j},t) + c_{(i)\gamma}\delta^3(\mathbf{j})\right], \end{aligned} \tag{3.119}$$

where

$$\begin{aligned}\left(\frac{\partial}{\partial t} + \nu k^2\right)_{(i)} &= \frac{\partial}{\partial t} + \nu k^2, \\ \left(M_{\alpha\beta\gamma}(\mathbf{k})\int d^3j\right)_{(i)} &= M_{\alpha\beta\gamma}(\mathbf{k})\int d^3j \end{aligned} \tag{3.120}$$

for all i, i.e. the original constant operators.

From these transformations in one realisation we can write down the corresponding transformations using random variables:

$$\begin{aligned}\mathbf{u}^{\ddagger}(\mathbf{k},t) &= e^{i\mathbf{k}.\mathbf{c}t}\,\mathbf{u}(\mathbf{k},t) - \mathbf{c}\delta^3(\mathbf{k}), \\ \left(\frac{\partial}{\partial t} + \nu k^2\right)^{\ddagger} u^{\ddagger}_{\alpha}(\mathbf{k},t) &= e^{i\mathbf{k}.\mathbf{c}t}\left(\frac{\partial}{\partial t} + \nu k^2\right) e^{-i\mathbf{k}.\mathbf{c}t} \\ & \quad \left[u^{\ddagger}_{\alpha}(\mathbf{k},t) + c_{\alpha}\delta^3(\mathbf{k})\right] \end{aligned} \tag{3.121}$$

and

$$\begin{aligned}\left(M_{\alpha\beta\gamma}(\mathbf{k})\int d^3j\right)^{\ddagger} & u^{\ddagger}_{\beta}(\mathbf{k}-\mathbf{j},t)u^{\ddagger}_{\gamma}(\mathbf{j},t) \\ = \; & e^{i\mathbf{k}.\mathbf{c}t}\left(M_{\alpha\beta\gamma}(\mathbf{k})\int d^3j\right) e^{-i(\mathbf{k}-\mathbf{j}).\mathbf{c}t}\left[u^{\ddagger}_{\beta}(\mathbf{k}-\mathbf{j},t) + c_{\beta}\delta^3(\mathbf{k}-\mathbf{j})\right] \\ & \times e^{-i\mathbf{j}.\mathbf{c}t}\left[u^{\ddagger}_{\gamma}(\mathbf{j},t) + c_{\gamma}\delta^3(\mathbf{j})\right], \end{aligned} \tag{3.122}$$

where ‡ is used to denote a Random Galilean Transformed quantity and $\mathbf{u}^{\ddagger}$,$L^{\ddagger}$ and $M^{\ddagger}$ are all random variables dependent on $\mathbf{c}$ ($\mathbf{u}$ is also a random variable, independent of $\mathbf{c}$).

Given these operator and field transformation rules, we can write down the Random Galilean Transformed Navier Stokes equations and moment equations and then delve into the problems with perturbation expansion and LET/DIA.

Navier Stokes Equations

The Navier Stokes equations are trivially invariant under a RGT since they are Galilean invariant in each realisation.

2nd Moment Equation

This equation,

$$\begin{aligned}
&\left(\frac{\partial}{\partial t}+\nu k^2\right)\langle u_\alpha(\mathbf{k},t)u_\delta(\mathbf{k}',t')\rangle \\
&-M_{\alpha\beta\gamma}(\mathbf{k})\int d^3j\,\langle u_\beta(\mathbf{k}-\mathbf{j},t)u_\gamma(\mathbf{j},t)u_\delta(\mathbf{k}',t')\rangle \\
&\quad=\ \langle f_\alpha(\mathbf{k},t)u_\delta(\mathbf{k}',t')\rangle
\end{aligned} \tag{3.123}$$

is in fact

$$\begin{aligned}
&\sum_{i=1}^{N}\left[\left(\frac{\partial}{\partial t}+\nu k^2\right)_{(i)} u_{(i)\alpha}(\mathbf{k},t)u_{(i)\delta}(\mathbf{k}',t')\right. \\
&\left.-\left(M_{\alpha\beta\gamma}(\mathbf{k})\int d^3j\right)_{(i)} u_{(i)\beta}(\mathbf{k}-\mathbf{j},t)u_{(i)\gamma}(\mathbf{j},t)u_{(i)\delta}(\mathbf{k}',t')\right] \\
&\quad=\ \sum_{i=1}^{N} f_{(i)\alpha}(\mathbf{k},t)u_{(i)\delta}(\mathbf{k}',t').
\end{aligned} \tag{3.124}$$

When the ensemble is Random Galilean Transformed each equation in Equation(s) (3.124) will become

$$\begin{aligned}
&\left(\frac{\partial}{\partial t}+\nu k^2\right)^{\dagger}_{(i)} u^{\dagger}_{(i)\alpha}(\mathbf{k},t)u^{\dagger}_{(i)\delta}(\mathbf{k}',t') \\
&-\left(M_{\alpha\beta\gamma}(\mathbf{k})\int d^3j\right)^{\dagger}_{(i)} u^{\dagger}_{(i)\beta}(\mathbf{k}-\mathbf{j},t)u^{\dagger}_{(i)\gamma}(\mathbf{j},t)u^{\dagger}_{(i)\delta}(\mathbf{k}',t')
\end{aligned}$$

$$= f^{\dagger}_{(i)\alpha}(\mathbf{k},t)u^{\dagger}_{(i)\delta}(\mathbf{k}',t'). \tag{3.125}$$

and we can average over the ensemble, now specified by $\mathbf{u}$ *and* $\mathbf{c}$ to get

$$\begin{aligned}
&\left\langle\left(\frac{\partial}{\partial t}+\nu k^2\right)^{\ddagger} u^{\ddagger}_{\alpha}(\mathbf{k},t)u^{\ddagger}_{\delta}(\mathbf{k}',t')\right\rangle \\
&-\left\langle\left(M_{\alpha\beta\gamma}(\mathbf{k})\int d^3j\right)^{\ddagger} u^{\ddagger}_{\beta}(\mathbf{k}-\mathbf{j},t)u^{\ddagger}_{\gamma}(\mathbf{j},t)u^{\ddagger}_{\delta}(\mathbf{k}',t')\right\rangle \\
&= \langle f^{\ddagger}_{\alpha}(\mathbf{k},t)u^{\ddagger}_{\delta}(\mathbf{k}',t')\rangle.
\end{aligned} \tag{3.126}$$

This equation cannot be simplified further since $L^{\ddagger}$ and $M^{\ddagger}$ are random variables through their $\mathbf{c}$ dependence and cannot be simply pulled out of the ensemble averages (compare this with deterministic Galilean transformations where the operators remain statistically sharp). This indicates the problems that lie ahead with the perturbation expansion and thus with renormalised perturbation theories. The operators have a special nature in the untransformed frame — they are *not* random variables — and this nature is destroyed by an RGT. *Because it is essentially an ensemble operation, not a general transformation, the RGT of any averaged equation requires the average to be analysed into the realisations, then a new average performed with the new random operators defined by the RGT.*

Perturbation Expansion and LET

We consider the LET equation for the two-time moment in homogeneous turbulence, $Q(\mathbf{k};t,t')$, Equation (2.53), (without any mean velocity $\mathbf{V}$, cf. Section 3.4)

$$\begin{aligned}
&\left(\frac{\partial}{\partial t}+\nu k^2\right) Q_{\alpha\rho}(\mathbf{k};t,t') \\
&= M_{\alpha\beta\gamma}(\mathbf{k})\int d^3j \\
&\quad\left\{2\int_{(0)}^{t'} ds\, H_{\rho\sigma}(-\mathbf{k};t',s)M_{\sigma\omega\phi}(-\mathbf{k})Q_{\beta\omega}(\mathbf{j};t,s)Q_{\gamma\phi}(\mathbf{k}-\mathbf{j};t,s)\right. \\
&\quad\left.-4\int_{(0)}^{t} ds\, H_{\beta\sigma}(\mathbf{j};t,s)M_{\sigma\omega\phi}(\mathbf{j})Q_{\gamma\omega}(\mathbf{k}-\mathbf{j};t,s)Q_{\phi\rho}(\mathbf{k};s,t')\right\}.
\end{aligned} \tag{3.127}$$

This equation is similar to the 2nd moment equation in that it *cannot* be Random Galilean Transformed directly. We must go back to the unaveraged equation

leading to Equation 3.127, change the ensemble using the RGT and then re-average — *that* is the RGT of the LET moment equation.

So, why do renormalised perturbation theories such as LET and DIA 'fail' the Random Galilean Invariance test? They 'fail' because the RGT ensemble no longer has the properties required for the derivation of the renormalised perturbation theory, in particular

1. The requirement that the propagator/response function (H in LET, G in DIA) be statistically sharp and thus can be brought outside averages (see Section 2.3).

2. The requirement that $\mathbf{u}^{(0)}$ be Gaussian so that a quadruple zero order velocity moment can be factored into a product of two double zero order velocity moments (see Section 2.3).

(Note that these properties have nothing to do with the question of renormalisation). To see that an Random Galilean Transformed ensemble no longer has these properties we look at the perturbation expansion in the RGT ensemble.

Assume that in the original ensemble we had a Gaussian zero order solution, i.e. $\mathbf{f}$ was Gaussian. The zero order Random Galilean Transformed velocity field (cf. Equation (3.81) for $\mathbf{u}^\dagger$) is given by

$$\left(\frac{\partial}{\partial t}+\nu k^2\right)^\ddagger (u^\ddagger)^{(0)}_\alpha(\mathbf{k},t) \;=\; e^{i\mathbf{k}.\mathbf{c}t}\, f^\ddagger_\alpha(\mathbf{k},t) \tag{3.128}$$

which is

$$\begin{aligned} e^{i\mathbf{k}.\mathbf{c}t}\left(\frac{\partial}{\partial t}+\nu k^2\right) e^{-i\mathbf{k}.\mathbf{c}t}\left[(u^\ddagger)^{(0)}_\alpha(\mathbf{k},t)+c_\alpha\delta^3(\mathbf{k})\right] \\ = \; e^{i\mathbf{k}.\mathbf{c}t}\, f_\alpha(\mathbf{k},t). \end{aligned} \tag{3.129}$$

This is easily simplified to give

$$(u^\ddagger)^{(0)}_\alpha(\mathbf{k},t) \;=\; e^{i\mathbf{k}.\mathbf{c}t}\, u^{(0)}_\alpha(\mathbf{k},t) - c_\alpha\delta^3(\mathbf{k}). \tag{3.130}$$

There is an element of choice in the RGT rules for $\mathbf{u}^{(0)}, \mathbf{u}^{(1)}, \ldots$ since the additive

term, $c_\alpha \delta^3(\mathbf{k})$, has to be included. We chose to add this when transforming $\mathbf{u}^{(0)}$ and to treat the $\mathbf{u}^{(n)}$, $n > 0$ as velocity differences. Other choices were tried but all led to difficulties in forming the perturbation expansion. So $\mathbf{u}^{(0)}$ transforms like $\mathbf{u}$,

$$(u^{(0)})^\ddagger_\alpha(\mathbf{k},t), \;=\; e^{i\mathbf{c}.\mathbf{k}t}\, u^{(0)}_\alpha(\mathbf{k},t) - c_\alpha \delta^3(\mathbf{k}). \tag{3.131}$$

Thus

$$(u^\ddagger)^{(0)}_\alpha(\mathbf{k},t) \;=\; (u^{(0)})^\ddagger_\alpha(\mathbf{k},t). \tag{3.132}$$

So $(\mathbf{u}^\ddagger)^{(0)}$ is the RGT of $\mathbf{u}^{(0)}$.

$(\mathbf{u}^\ddagger)^{(1)}$ is given by

$$\begin{aligned}
(u^\ddagger)^{(1)}_\alpha(\mathbf{k},t) \;&=\; e^{i\mathbf{c}.\mathbf{k}t}\left(\int_{-\infty}^{t} ds\, e^{-\nu k^2(t-s)}\right) e^{-i\mathbf{c}.\mathbf{k}s} \\
&\quad \left(M_{\alpha\beta\gamma}(\mathbf{k})\int d^3j\right)^\ddagger (u^\ddagger)^{(0)}_\beta(\mathbf{k}-\mathbf{j},s)(u^\ddagger)^{(0)}_\gamma(\mathbf{j},s) \\
&=\; e^{i\mathbf{c}.\mathbf{k}t}\left(\int_{-\infty}^{t} ds\, e^{-\nu k^2(t-s)}\right) \times \\
&\quad M_{\alpha\beta\gamma}(\mathbf{k})\int d^3j\, u^{(0)}_\beta(\mathbf{k}-\mathbf{j},s) u^{(0)}_\gamma(\mathbf{j},s) \\
&=\; e^{i\mathbf{c}.\mathbf{k}t}\, u^{(1)}_\alpha(\mathbf{k},t)
\end{aligned} \tag{3.133}$$

using the transformation rules for $M\mathbf{uu}$, $\mathbf{u}$ and the solution for the first order term $\mathbf{u}^{(1)}$ in the original frame. The transformation rule for $\mathbf{u}^{(1)}$ is

$$(u^{(1)})^\ddagger_\alpha(\mathbf{k},t), \;=\; e^{i\mathbf{c}.\mathbf{k}t}\, u^{(1)}_\alpha(\mathbf{k},t) \tag{3.134}$$

since $\mathbf{u}^{(1)}$ is treated as a fluctuating velocity difference. Thus

$$(u^\ddagger)^{(1)}_\alpha(\mathbf{k},t) \;=\; (u^{(1)})^\ddagger_\alpha(\mathbf{k},t). \tag{3.135}$$

So $(\mathbf{u}^\ddagger)^{(1)}$ is the RGT of $\mathbf{u}^{(1)}$.

Then, as in the case of ordinary Galilean transformations, the perturbation series can be shown to be invariant under RGTs order by order by induction.

To illustrate the problem with LET and DIA we now expand the 2nd moment equation (Equation (3.126)) about the zero order solution $\mathbf{u}^\ddagger$ to get the perturbation expansion in terms of λ. In the Random Galilean Transformed frame/ensemble this expanded equation is

$$\begin{aligned}
&\langle\left(\frac{\partial}{\partial t}+\nu k^2\right)^\ddagger u_\alpha^\ddagger(\mathbf{k},t)u_\rho^\ddagger(\mathbf{k}',t')\rangle \\
&= \lambda\langle\left(M_{\alpha\beta\gamma}(\mathbf{k})\int d^3j\right)^\ddagger (u^\dagger)_\beta^{(0)}(\mathbf{k}-\mathbf{j},t)(u^\dagger)_\gamma^{(0)}(\mathbf{j},t)(u^\dagger)_\rho^{(0)}(\mathbf{k}',t')\rangle + \\
&\quad \lambda^2\langle\left(M_{\alpha\beta\gamma}(\mathbf{k})\int d^3j\right)^\ddagger \times \\
&\quad \left(\int_{(0)}^{t'} ds\, D_{\rho\sigma}(\mathbf{k}')e^{-\nu k'^2(t'-s)}\right)^\ddagger \left(M_{\sigma\omega\phi}(\mathbf{k}')\int d^3l\right)^\ddagger \times \\
&\quad (u^\dagger)_\beta^{(0)}(\mathbf{j},t)(u^\dagger)_\gamma^{(0)}(\mathbf{k}-\mathbf{j},t)(u^\dagger)_\omega^{(0)}(\mathbf{l},s)(u^\dagger)_\phi^{(0)}(\mathbf{k}'-\mathbf{l},s)\rangle + \\
&\quad 2\lambda^2\langle\left(M_{\alpha\beta\gamma}(\mathbf{k})\int d^3j\right)^\ddagger \times \\
&\quad \left(\int_{(0)}^{t} ds\, D_{\beta\sigma}(\mathbf{j})e^{-\nu j^2(t-s)}\right)^\ddagger \left(M_{\sigma\omega\phi}(\mathbf{j})\int d^3l\right)^\ddagger \times \\
&\quad (u^\dagger)_\omega^{(0)}(\mathbf{l},s)(u^\dagger)_\phi^{(0)}(\mathbf{j}-\mathbf{l},s)(u^\dagger)_\gamma^{(0)}(\mathbf{k}-\mathbf{j},t)(u^\dagger)_\rho^{(0)}(\mathbf{k}',t')\rangle + \\
&\quad O(\lambda^3)
\end{aligned} \tag{3.136}$$

where we have stopped at $O(\lambda^2)$, which is enough to show the problems that occur (and is also where the renormalised expansions are truncated). In the original ensemble we could manipulate this as follows

1. on the LHS, $\partial/\partial t+\nu k^2$ could be pulled out of the average as it was statistically sharp;
2. on the RHS, $(\partial/\partial t+\nu k^2)^{-1}\equiv\int\exp(-\nu k^2\ldots)$ and M could be pulled out of the average as they were statistically sharp;
3. $\mathbf{u}^{(0)}$ was Gaussian, so the odd moments were zero and the even moments could be factored into products of double moments.

In the Random Galilean Transformed ensemble none of these manipulations are possible:

1. $(\partial/\partial t+\nu k^2)^\ddagger$ is a random variable and cannot be pulled out of the average

on the LHS (the 2nd moment equation shares this property);

2. $(\partial/\partial t + \nu k^2)^{-1})^\ddagger$ and $M^\ddagger$ are random variables and thus cannot be pulled out of the averages on the RHS;

3. even if they could be pulled out $(\mathbf{u}^\ddagger)^{(0)}$ is no longer Gaussian ($(\mathbf{u}^\ddagger)^{(0)} = e^{i\mathbf{c}.\mathbf{k}t}\, u^{(0)} - c\delta^3(\mathbf{k})$ with $\mathbf{u}^{(0)}$ and $\mathbf{c}$ Gaussian) and thus the even moments cannot be factored. (The triple moment is in fact zero from Gaussianity of $\mathbf{u}^{(0)}$ and homogeneity.

The *only* way out of this pass is to transform back to the original ensemble, where we *can* do the perturbation expansion of the averaged equations, renormalise and get LET or DIA.

So, the RGT is merely an unsuitable choice of ensemble on which to base a perturbation theory and only related to a real Galilean transformation at the level of a realisation in that ensemble. It is not the transformation rule for some fundamental physical symmetry.

Chapter 4

Energy Transfer

4.1 Introduction

The postulate of local (in wavenumber) energy transfer is basic to many phenomenological theories of turbulence. Energy transfers between various wavenumber bands have been calculated from a direct numerical simulation by Domaradzki and Rogallo [10], with the conclusion that energy transfer is local. In this chapter the LET results for the velocity field are analysed, using the same 'experimental' conditions as Domaradzki and Rogallo, with the conclusion that energy transfer in LET is local.

4.2 Background

The LET theory for the velocity field has been tested analytically and numerically at various Reynolds numbers [42, 45, 46] and compares very well with experiment. However, the detailed dynamics of the velocity field (in LET the basic field is in fact the two-time velocity correlation $Q(\mathbf{k};t,t') \sim \langle \mathbf{u}(\mathbf{k},t).\mathbf{u}(\mathbf{k},t') \rangle$) have not been studied, mainly because no directly comparable experimental results were available.

Domaradzki and Rogallo [10] have recently studied the detailed energy transfer in wavenumber space for three high resolution direct numerical simulations of decaying turbulent at Taylor microscale Reynolds numbers of 13, 20 and 46. Their

results allow a direct comparison with LET. They find that the energy transfer is local in wavenumber but is mediated through non-local triads, i.e. in the triple-correlation energy transfer term (see below) the wavenumber arguments $\mathbf{k}$, $\mathbf{j}$ and $\mathbf{k}-\mathbf{j}$ have the relation $|\mathbf{k}-\mathbf{j}| \ll k \sim j$. In the rest of this chapter we make a direct comparison between Domaradzki and Rogallo's results for $R_\lambda = 13.6$ and a LET calculation with similar integral parameters (total energy, dissipation, Reynolds number and skewness) and spectra (energy, dissipation, energy transfer and energy decay).

Dr. V. Shanmugasundaram developed the original code for the energy transfer calculation using a slightly different definition of the detailed energy transfer. He started doing energy transfer calculations at a range of Reynolds numbers from $R_\lambda = 5$ to $R_\lambda = 1000$ at the University of Edinburgh and is continuing the calculations at the Institute of Computational Fluid Dynamics, Tokyo. His results also support local energy transfer, at low Reynolds number mediated by non-local triads but at high Reynolds number the energy transfer appears to be due to triads with $k \sim j \sim |\mathbf{k}-\mathbf{j}|$ [54, 55]. The FORTRAN code used for the present work is Dr. Shanmugasundaram's program modified slightly to match Domaradzki and Rogallo's definitions of the detailed energy transfers.

Professor J.A. Domaradzki has very kindly supplied details of the numerical simulation with which we compare LET. This allows the 'experimental' conditions of the two calculations to be matched. He has also supplied further results not shown in [10], allowing a detailed comparison of the direct simulation and the LET calculation.

4.3 Detailed energy transfer

For the direct numerical simulation we follow Domaradzki and Rogallo's definitions and for LET we define analogous quantities.

In wavenumber space, for incompressible flow, the Navier-Stokes equations

are

$$\left(\frac{\partial}{\partial t}+\nu k^2\right)u_\alpha(\mathbf{k},t) \;=\; M_{\alpha\beta\gamma}(\mathbf{k})\int d^3j\, u_\beta(\mathbf{k}-\mathbf{j},t)u_\gamma(\mathbf{j},t) \qquad (4.1)$$

and

$$k_\alpha u_\alpha(\mathbf{k},t) \;=\; 0, \qquad (4.2)$$

where

$$M_{\alpha\beta\gamma}(\mathbf{k}) \;=\; (1/2i)\left[k_\beta D_{\alpha\gamma}(\mathbf{k})+k_\gamma D_{\alpha\beta}(\mathbf{k})\right] \qquad (4.3)$$

and the projection operator $D_{\alpha\beta}(\mathbf{k})$ is

$$D_{\alpha\beta}(\mathbf{k}) \;=\; \delta_{\alpha\beta}-\frac{k_\alpha k_\beta}{k^2}. \qquad (4.4)$$

(For the derivation of these equations from the Navier-Stokes equations and for general reference, see [43]). The energy amplitude is defined as

$$\begin{aligned}\frac{1}{2}\langle|\mathbf{u}(\mathbf{k},t)|^2\rangle &= \frac{1}{2}\langle u_\alpha(\mathbf{k},t)u^*_\alpha(\mathbf{k},t)\rangle \\ &= \frac{1}{2}\langle u_\alpha(\mathbf{k},t)u_\alpha(-\mathbf{k},t)\rangle, \end{aligned} \qquad (4.5)$$

where the last step follows since $\mathbf{u}(\mathbf{x},t)$ is real. The equation for $\frac{1}{2}\langle|\mathbf{u}(\mathbf{k},t)|^2\rangle$ is

$$\frac{\partial\frac{1}{2}\langle|\mathbf{u}(\mathbf{k},t)|^2\rangle}{\partial t} \;=\; -2\nu k^2\frac{1}{2}\langle|\mathbf{u}(\mathbf{k},t)|^2\rangle+T(\mathbf{k},t), \qquad (4.6)$$

where $T(\mathbf{k},t)$ is the non-linear energy transfer

$$\begin{aligned}T(\mathbf{k},t) \;=\; \langle&\frac{1}{2}u_\alpha(-\mathbf{k},t)M_{\alpha\beta\gamma}(\mathbf{k})\int d^3j\, u_\beta(\mathbf{k}-\mathbf{j},t)u_\gamma(\mathbf{j},t) \\ &+\frac{1}{2}u_\alpha(\mathbf{k},t)M_{\alpha\beta\gamma}(-\mathbf{k})\int d^3j\, u_\beta(-\mathbf{k}-\mathbf{j},t)u_\gamma(\mathbf{j},t)\rangle. \end{aligned} \qquad (4.7)$$

We see that $T(\mathbf{k},t)$ is an integral over triads of velocity field modes at wavenumbers $\mathbf{k}$, $\mathbf{j}$ and $\mathbf{k}-\mathbf{j}$. For isotropic turbulence we have the energy and the energy

transfer

$$E(k,t) = \int_{4\pi} \frac{1}{2}\langle|\mathbf{u}(\mathbf{k},t)|^2\rangle k^2\, d\Omega_{\mathbf{k}} \tag{4.8}$$

$$T(k,t) = \int_{4\pi} T(\mathbf{k},t) k^2\, d\Omega_{\mathbf{k}}\,. \tag{4.9}$$

The basic quantity defined by Domaradzki and Rogallo is the energy transfer between a mode at wavenumber $\mathbf{k}$ and all pairs of modes $\mathbf{j}$, $\mathbf{l} = \mathbf{k} - \mathbf{j}$ where $\mathbf{j} \in \mathcal{P}, \mathbf{l} \in \mathcal{Q}$ or $\mathbf{j} \in \mathcal{Q}, \mathbf{l} \in \mathcal{P}$ and $\mathcal{P}$ and $\mathcal{Q}$ are some prescribed regions of wavenumber space:

$$T_{\mathcal{P}\mathcal{Q}}(\mathbf{k},t) = \begin{cases} \langle \frac{1}{2}u_\alpha(-\mathbf{k},t) M_{\alpha\beta\gamma}(\mathbf{k}) \int d^3j\, u_\beta^{\mathcal{P}}(\mathbf{k}-\mathbf{j},t) u_\gamma^{\mathcal{Q}}(\mathbf{j},t) \\ +\frac{1}{2}u_\alpha(\mathbf{k},t) M_{\alpha\beta\gamma}(-\mathbf{k}) \int d^3j\, u_\beta^{\mathcal{P}}(-\mathbf{k}-\mathbf{j},t) u_\gamma^{\mathcal{Q}}(\mathbf{j},t)\rangle & \text{if } \mathcal{P} \not\equiv \mathcal{Q} \\ +\langle \frac{1}{2}u_\alpha(-\mathbf{k},t) M_{\alpha\beta\gamma}(\mathbf{k}) \int d^3j\, u_\beta^{\mathcal{Q}}(\mathbf{k}-\mathbf{j},t) u_\gamma^{\mathcal{P}}(\mathbf{j},t) \\ +\frac{1}{2}u_\alpha(\mathbf{k},t) M_{\alpha\beta\gamma}(-\mathbf{k}) \int d^3j\, u_\beta^{\mathcal{Q}}(-\mathbf{k}-\mathbf{j},t) u_\gamma^{\mathcal{P}}(\mathbf{j},t)\rangle & \\ \\ \langle \frac{1}{2}u_\alpha(-\mathbf{k},t) M_{\alpha\beta\gamma}(\mathbf{k}) \int d^3j\, u_\beta^{\mathcal{P}}(\mathbf{k}-\mathbf{j},t) u_\gamma^{\mathcal{P}}(\mathbf{j},t) & \text{if } \mathcal{P} \equiv \mathcal{Q} \\ +\frac{1}{2}u_\alpha(\mathbf{k},t) M_{\alpha\beta\gamma}(-\mathbf{k}) \int d^3j\, u_\beta^{\mathcal{P}}(-\mathbf{k}-\mathbf{j},t) u_\gamma^{\mathcal{P}}(\mathbf{j},t)\rangle & \end{cases} \tag{4.10}$$

where

$$u_\alpha^{\mathcal{P}}(\mathbf{m},t) = \begin{cases} u_\alpha(\mathbf{m},t) & \text{if } \mathbf{m} \in \mathcal{P} \\ 0 & \text{otherwise.} \end{cases} \tag{4.11}$$

If $T_{\mathcal{P}\mathcal{Q}}(\mathbf{k},t)$ is summed over all $\mathcal{Q}$ with $\mathcal{P}$ fixed, we obtain the energy transfer to the mode at $\mathbf{k}$ due to triads with at least one wavevector in the region $\mathcal{P}$

$$T_{\mathcal{P}}(\mathbf{k},t) = \sum_{\mathcal{Q}} T_{\mathcal{P}\mathcal{Q}}(\mathbf{k},t). \tag{4.12}$$

Note that

$$T(\mathbf{k},t) \neq \sum_{\mathcal{P}} T_{\mathcal{P}}(\mathbf{k},t) \tag{4.13}$$

since the sum over the $\mathcal{P}$ and $\mathcal{Q}$ regions counts the contributions to the total

energy transfer twice for each $\mathcal{P}$ and $\mathcal{Q}$, i.e. once for $\mathbf{j} \in \mathcal{P}$ and once for $\mathbf{j} \in \mathcal{Q}$.

For the case of isotropic, homogeneous turbulence we want to look at the energy transfer between different scales, i.e. at different $|\mathbf{k}|$. So Domaradzki and Rogallo choose $\mathcal{P}$ and $\mathcal{Q}$ as spherical shells $p - \frac{1}{2}\Delta p < k < p + \frac{1}{2}\Delta p$ and $q - \frac{1}{2}\Delta q < k < q + \frac{1}{2}\Delta q$ and define

$$T(k|p,q) = \int_{4\pi} T_{\mathcal{P}\mathcal{Q}}(\mathbf{k},t) k^2 \, d\Omega_{\mathbf{k}} \tag{4.14}$$

which gives the $E(k)$ transfer into k due to modes in the bands centred on wavenumbers p and q. Similarly they define

$$P(k|p) = \int_{4\pi} T_{\mathcal{P}}(\mathbf{k},t) k^2 \, d\Omega_{\mathbf{k}} \tag{4.15}$$

The LET equations are derived in Chapter 2 and we have the energy equation (Equation (2.58)) for isotropic, homogeneous turbulence,

$$\begin{aligned} &\left(\frac{\partial}{\partial t} + 2\nu k^2\right) Q(k;t,t) \\ &= 2 \int d^3j \, L(\mathbf{k},\mathbf{j}) \int_{t_0}^{t} ds \, [H(k;t,s)Q(j;t,s)Q(|k-j|;t,s) \\ &\quad - H(j;t,s)Q(|k-j|;t,s)Q(k;s,t)], \end{aligned} \tag{4.16}$$

where

$$Q(k;t,t') = \frac{1}{2}\langle u_\alpha(\mathbf{k},t) u_\alpha(-\mathbf{k},t')\rangle \tag{4.17}$$

and

$$Q(k;t,t') = H(k;t,t')Q(k;t',t'). \tag{4.18}$$

Defining

$$Q^p(k;t,t') = \begin{cases} Q(k;t,t') & \text{if } p - \frac{1}{2}\Delta p < k < p + \frac{1}{2}\Delta p \\ 0 & \text{otherwise,} \end{cases} \tag{4.19}$$

and similar quantities H^p, Q^q and H^q, we define for LET

$$T(k|p,q) = \begin{cases} 2\int d^3j\, L(\mathbf{k},\mathbf{j}) \int_{t_0}^{t} ds \times \\ [H(k;t,s)Q^p(j;t,s)Q^q(|k-j|;t,s) \\ -H^p(j;t,s)Q^q(|k-j|;t,s)Q(k;s,t)] & \text{if } p \neq q \\ +2\int d^3j\, L(\mathbf{k},\mathbf{j}) \int_{t_0}^{t} ds \times \\ [H(k;t,s)Q^q(j;t,s)Q^p(|k-j|;t,s) \\ -H^q(j;t,s)Q^p(|k-j|;t,s)Q(k;s,t)], & \\ \\ 2\int d^3j\, L(\mathbf{k},\mathbf{j}) \int_{t_0}^{t} ds \times \\ [H(k;t,s)Q^p(j;t,s)Q^p(|k-j|;t,s) & \text{if } p = q. \\ -H^p(j;t,s)Q^p(|k-j|;t,s)Q(k;s,t)] \end{cases} \tag{4.20}$$

We can then sum over the q bands to get

$$P(k|p) = \sum_{q \text{ bands}} T(k|p,q). \tag{4.21}$$

These definitions differ from Domaradzki and Rogallo's in that the scales are defined effectively by the correlation field $Q(\mathbf{k};t,t')$ rather than the velocity field $\mathbf{u}(\mathbf{k},t)$. However, for homogeneous turbulence Equation (4.17) shows that the scales $|\mathbf{k}|$ are the same.

We mention here a numerical problem with the LET energy transfer calculations. The integral over $\mathbf{j}$ is calculated as

$$\int d^3j = \int j^2\, dj \int_{-1}^{1} d\mu \tag{4.22}$$

where μ is the cosine of the angle between wavevectors $\mathbf{k}$ and $\mathbf{j}$ and the equations are discretised on a (k,μ) mesh. $l = |\mathbf{k}-\mathbf{j}|$ is related to j and μ by

$$l^2 = k^2 + j^2 - 2kj\mu. \tag{4.23}$$

When $k = j$ and μ is near 1 we have

$$l^2 \simeq 2j^2\epsilon, \tag{4.24}$$

where $\epsilon = 1 - \mu$. Thus, for a chosen μ resolution, the l resolution depends on j and is quite coarse at large j,

$$l_{step} \simeq \sqrt{2}j\sqrt{\Delta\mu} \tag{4.25}$$

and when we calculate $T(k|p,q)$ we will not be able to resolve the contributions of q bands with $q \lesssim \sqrt{2}p\sqrt{\Delta\mu}$. We chose a relatively fine resolution for μ in the LET calculations to allow energy transfer calculations at high p wavenumber.

4.4 The calculation of the velocity field

Domaradzki and Rogallo used the velocity fields computed in three direct numerical simulations to provide the detail required to compute $T(k|p,q)$ and $P(k|p)$. We use the results for their simulation LH which is based on the self-similar energy spectrum found by Ling and Huang [41] between $R_\lambda = 3$ and $R_\lambda = 30$. When the energy spectrum and the wavenumber are normalised using the Taylor microscale as follows

$$\tilde{E}(\tilde{k}) = \frac{E}{2\lambda u^2}, \tag{4.26}$$

$$\tilde{k} = \sqrt{2}\lambda k, \tag{4.27}$$

the normalised energy spectrum has the form

$$\tilde{E}(\tilde{k}) = \frac{1}{2\sqrt{2}}\tilde{k}(1+\tilde{k})e^{\tilde{k}}. \tag{4.28}$$

(NB. This is 3/2 times the formula in Domaradzki and Rogallo which is based on Ling and Huang's definition of $E(k)$ which is 2/3 our definition and that of Domaradzki and Rogallo. Our unnormalised energy spectra and u_{rms} *do* match those of Domaradzki and Rogallo). In the direct numerical simulation a velocity

field with this initial spectrum was relaxed to build up non-linear correlations and then rescaled to be used as the initial condition for the simulation [9]. The energy transfer results were obtained after the simulation had run for a sufficiently long time: the energy, dissipation and transfer spectra were all well resolved and approach zero at the largest wavenumbers and the energy spectra at different times collapsed onto the same curve when scaled using Equations (4.26) and (4.27). Table 4.1 summarises the computational and integral parameters of the simulation.

For the LET calculations we start with an initial spectrum of the Ling and Huang form with $\lambda(0) = 0.161$ and $u(0) = 6.05$ and run the computation until the integral parameters and spectra are close to those of Domaradzki and Rogallo. The details of the velocity calculation are given in [45] and are almost exactly the same as for the passive scalar LET calculations (see Chapter 2).

Table 4.2 gives the computational and integral parameters for the LET calculation. The wavenumber resolution was chosen to match Domaradzki and Rogallo's and the timestep throughout the calculation was the lesser of the convective $(1/u(t)k_{max})$ and viscous $(1/\nu k_{max}^2)$ time-scales for the largest wavenumber. With the μ resolution chosen (μ mesh at $-0.99, -0.97, \ldots, 0.99$) and p and q band width $\Delta p = \Delta q = 5$ for all bands, we can calculate $T(k|p,q)$ correctly for $0 < q < 5$ up to $p \simeq 25$. Beyond this some, or all, of the transfer from/to $0 < q < 5$ will appear to be transfer from/to $5 < q < 10$.

The spectra (energy, dissipation, transfer and energy decay) were closest to Domaradzki and Rogallo's at timestep 15, which was 0.78 eddy turnover times (based on the initial rms velocity $u(0)$ and the initial integral scale $L(0)$). The integral parameters at $tu(0)/L(0) = 0$ and $tu(0)/L(0) = 0.78$ are shown in Table 4.2; they are fairly close to the parameters of the direct numerical simulation.

The LET calculations are well developed at 0.78 eddy turnover times, as can be seen in Figure 4.1 which shows the development of the integral parameters in time, and in Figure 4.2 which shows the self-similarity of the energy spectrum using Ling and Huang's scaling (Equations (4.26) and (4.27)). The scaled spectra collapse onto one curve, but this is not precisely that given by Equation (4.28).

In Figures 4.3 and 4.4 we compare the energy, transfer, dissipation and energy decay spectra from the LET calculation with those from Domaradzki and Rogallo's simulation. The agreement is very good, except at low wavenumbers, where the direct numerical simulation has large variation, probably due to the small sample size for wavenumber shell averaging at these wavenumbers. Thus the 'experimental conditions' of the LET calculation and the direct numerical simulation are very close, allowing a direct comparison of results.

4.5 Results

We compare, where possible, the LET results with the results reported by Domaradzki and Rogallo in [10], i.e. their Figures 4, 5, 7, 8(a) and 10.

Localness of energy transfer: $P(k|p)$

The function $P(k|p)$ gives a measure of the localness of the energy transfer and we compare our LET results with Domaradzki and Rogallo's direct numerical simulation results in Figures 4.5, 4.6 and 4.7. At wavenumbers well above the peak in the energy spectrum (see Figure 4.5 where $23 < p < 25$) the behaviour of $P(k|p)$ indicates that energy transfer is local: $P(k|p)$ is negligible outside the range $\frac{1}{2}p < k < 2p$. At low wavenumbers, near the energy peak (see Figure 4.6 where $6 < p < 9$) the energy transfer is not negligible for $k > 2p$ but this is due to the effects of a cascade of local transfers rather than non-local transfer (see the discussion below).

In Figure 4.7 we divide the wavenumber space into logarithmic p bands labelled $n = 1, \ldots, 6$, with boundaries $[2^{n-1}, 2^n]$. For bands 4, 5 and 6 we see an energy cascade, with the energy transfer into k due to band $n-1$ balanced by the transfer out of k due to band n.

In all the Figures, the qualitative agreement (position and shape of the curves) between LET and the simulation is excellent but LET generally underestimates the magnitude of $P(k|p)$ compared with this numerical simulation.

Detailed energy transfer: $T(k|p,q)$

$T(k|p,q)$ provides the most detailed description of the energy transfer process.

The wavenumber space $0 < k < 65$ (strictly $0 < k < 61$ since both the simulation and LET computation have $k_{max} = 61$) is split up into 13 p,q bands labelled $n = 1,\ldots,13$ with boundaries $[5(n-1), 5n]$ and width $\Delta k = 5$. With this choice of bands, the LET results for $T(k|p,q)$ are correct up to $p \simeq 25$; above this the μ discretisation affects the transfer due to q in band 1 ($0 < q < 5$).

In Figures 4.8 and 4.9 we compare LET with the simulation for p in band 5, $20 < p < 25$. The qualitative agreement is excellent but the magnitude of $T(k|p,q)$ and $P(k|p)$ is lower in the LET calculation. This is generally true for p in each band $1,\ldots,13$, with the the relative magnitude of the LET results decreasing with increasing p wavenumber. The transfer $P(k|p)$ is mostly local, with the peaks of $P(k|p)$ occurring at $k = 18$ and $k = 25$. The $T(k|p,q)$ curves show, however, that this local energy transfer is mediated by non-local interactions with q in bands 1, 2 and 3. This behaviour is typical for all the p bands with p above the energy spectral peak (near $k = 5$) both in the simulation and in the LET calculation (except that in the LET calculation for p bands 7 and above the $T(k|p,q)$ curve for $0 < q < 5$ is absorbed into the $5 < q < 10$ curve because of the limited μ resolution). The LET results agree with Domaradzki and Rogallo's conclusion that, for bands above the energy spectrum peak, energy transfer is local in wavenumber but is due to non-local wavevector triad interactions.

At the energy peak LET and the simulation are again in excellent agreement, with the magnitude difference now small, see Figures 4.10 and 4.11. The form of $P(k|p)$ and the decomposition of $P(k|p)$ into $T(k|p,q)$ is very different from Figures 4.8 and 4.9.

For q in bands 1, 2 and 3, i.e. close to p (band 2), we do see local energy transfer due to local triads, because of geometrical constraints. At larger k the form of the $P(k|p)$ curve may suggest non-local energy transfer but the $T(k|p,q)$ curves show that this is due to a cascade of local energy transfers. Note that the curve $T(k|p,q)$ with p in band m and q in band n is just the same as the curve $T(k|p,q)$ with p in band n and q in band m—compare the curves labelled 5 in

Figures 4.10 and 4.11 with the curves labelled 2 in Figures 4.8 and 4.9 respectively, taking into account the different vertical scales.

Table 4.1: Computational and integral parameters for Domaradzki and Rogallo's direct numerical simulation, case LH.

Computational grid size	k_{min}	k_{max}	ν
128^3	0	60.35	0.065

Time	u_{rms}	λ	R_λ	Velocity derivative skewness, $-S$
0	6.05	0.161	15	—
?	4.07	0.218	13.6	0.480

Table 4.2: Computational and integral parameters for the LET calculation, with initial spectrum of Ling and Huang form

k_{min}	k_{max}	Δk	$\Delta\mu$	timestep at $t = 0$	ν
0.0	61.0	1.0	0.02	0.0027	0.065

$tu(0)/L(0)$	u_{rms}	λ	E	ϵ	R_λ	$-S$
0	6.05	0.161	54.9	1370	15.0	—
0.78	4.06	0.227	24.8	312	14.2	0.418

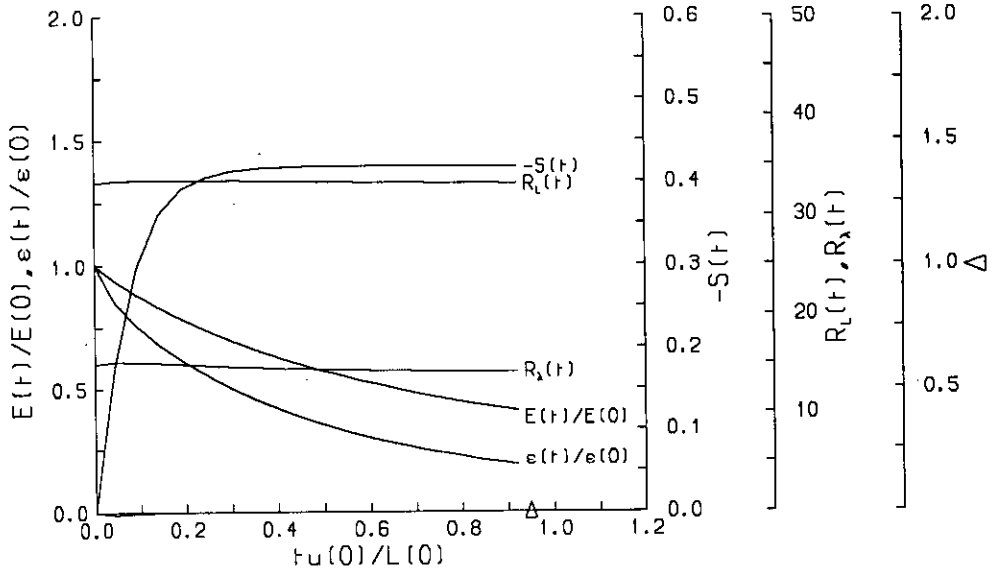

Figure 4.1: Evolution of the integral parameters for the LET calculation.

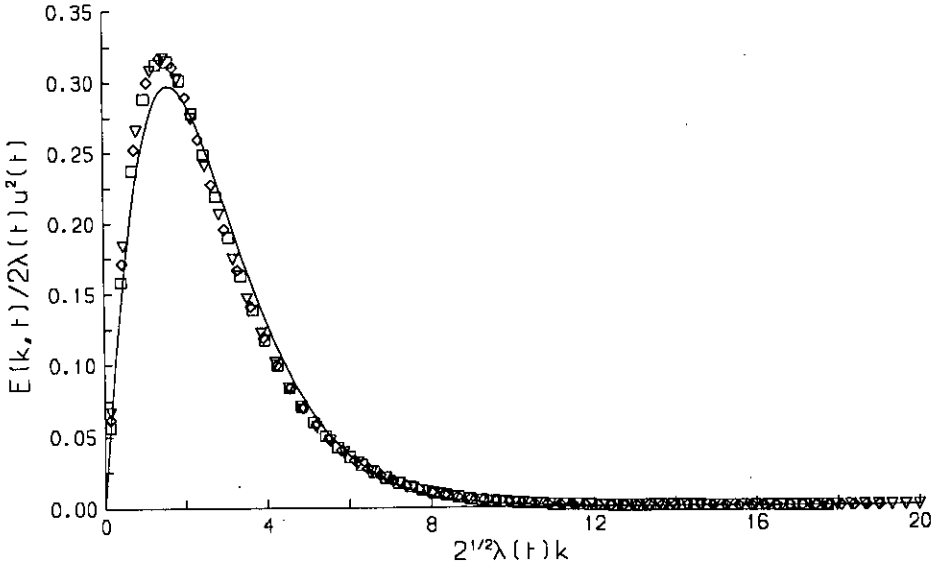

Figure 4.2: LET calculation: self similarity of the energy spectrum under Ling and Huang's scaling (Equations (4.26) and (4.27)). □, $tu(0)/L(0) = 0.5$; ◇, $tu(0)/L(0) = 0.7$; ▽, $tu(0)/L(0) = 0.9$; ————, Equation (4.28).

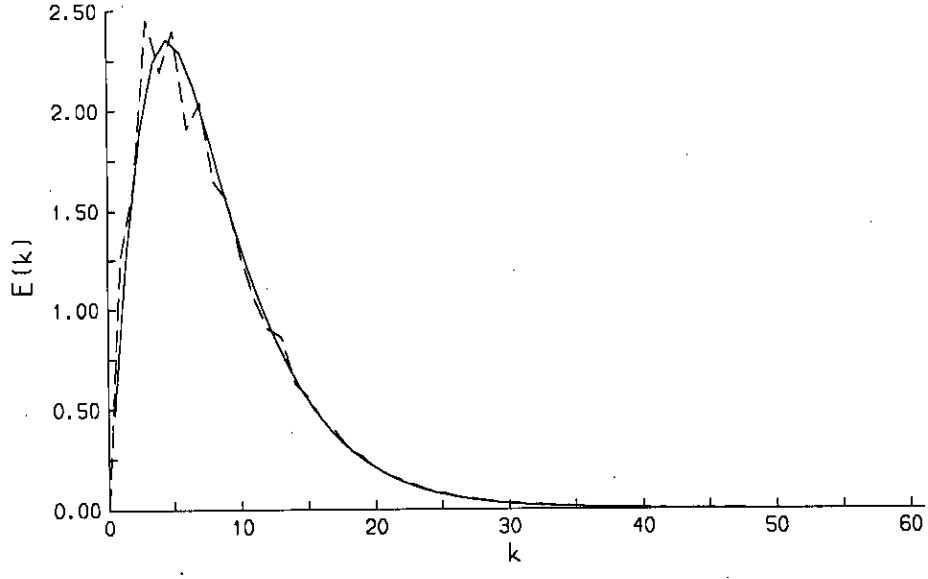

Figure 4.3: Comparison of the unscaled energy spectrum from the LET calculation and Domaradzki and Rogallo's direct numerical simulation ————, LET; – – – –, Domaradzki and Rogallo.

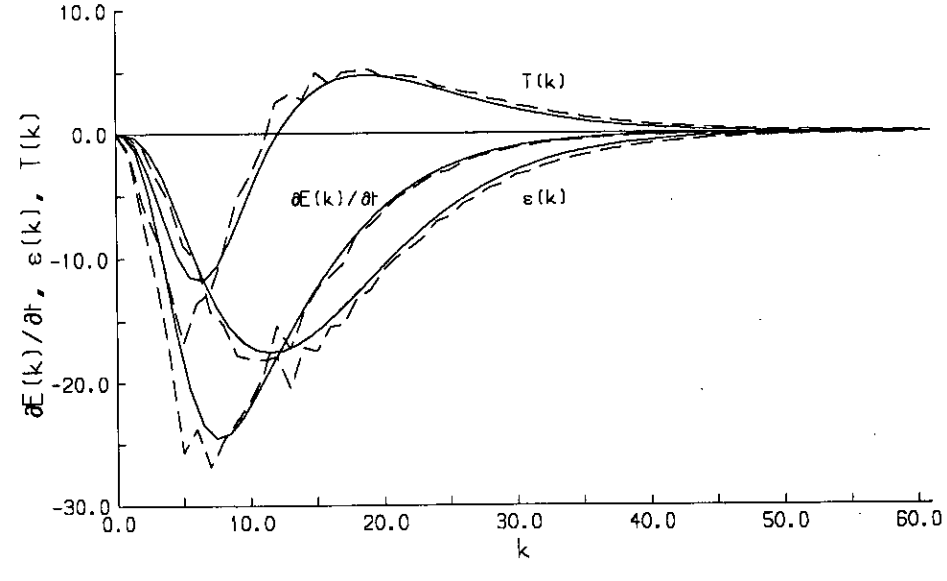

Figure 4.4: Comparison of the unscaled transfer, dissipation and $\partial E(k,t)/\partial t$ spectra from the LET calculation and Domaradzki and Rogallo's direct numerical simulation ————, LET; – – – –, Domaradzki and Rogallo.

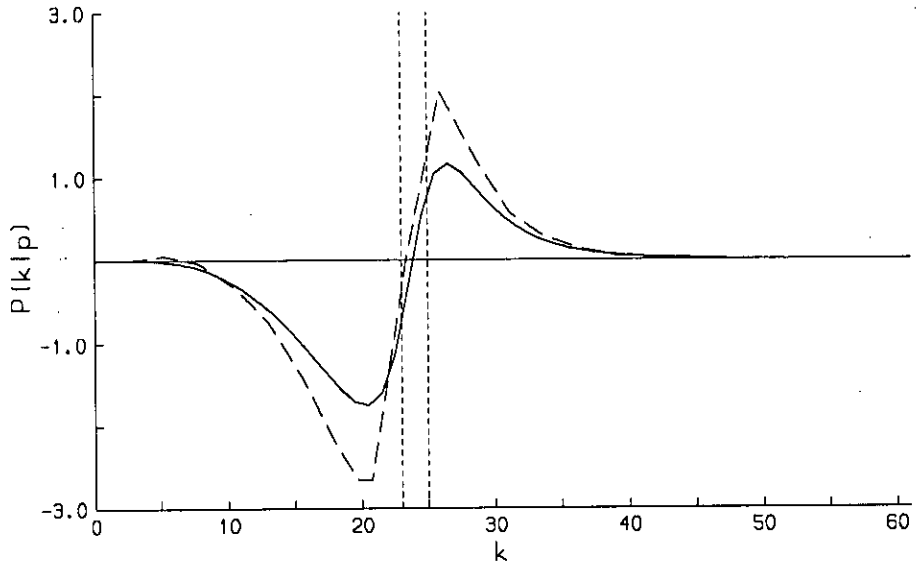

Figure 4.5: $P(k|p)$ for $23 < p < 25$; the vertical dashed lines are at $k = 23$ and $k = 25$. ————, LET; — — — —, Domaradzki and Rogallo.

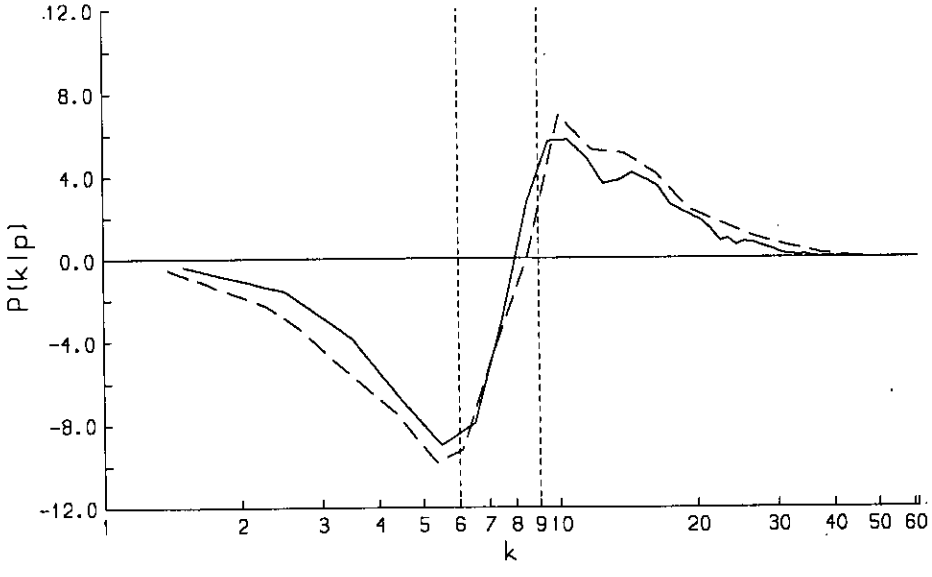

Figure 4.6: $P(k|p)$ for $6 < p < 9$; the vertical dashed lines are at $k = 6$ and $k = 9$. ————, LET; — — — —, Domaradzki and Rogallo.

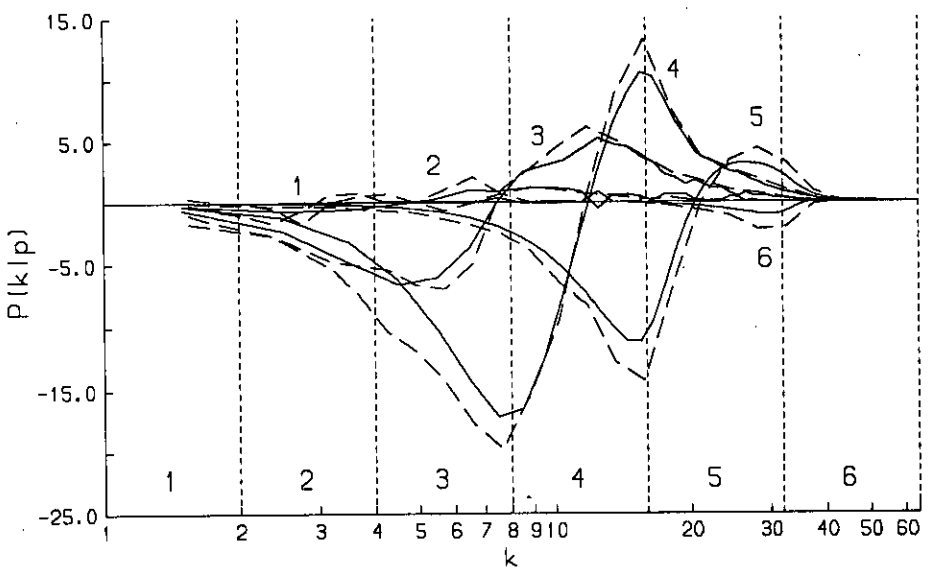

Figure 4.7: $P(k|p)$ for p in different logarithmic bands $2^{n-1} < p < 2^n$. The boundaries of the bands are shown by the vertical dashed lines and the curves are labelled with the relevant p band. ———, LET; — — — —, Domaradzki and Rogallo.

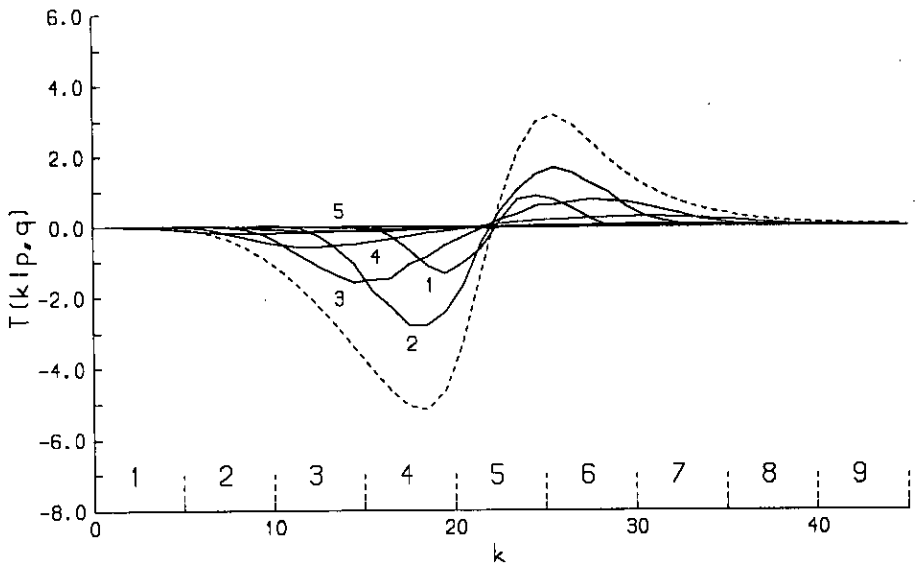

Figure 4.8: LET calculation: decomposition of $P(k|p)$ (----------) into $T(k|p,q)$ for p in band 5 ($20 < p < 25$), q in bands $1,\ldots,13$. The boundaries of the bands are shown by the vertical dashed lines and the curves are labelled with the relevant q band.

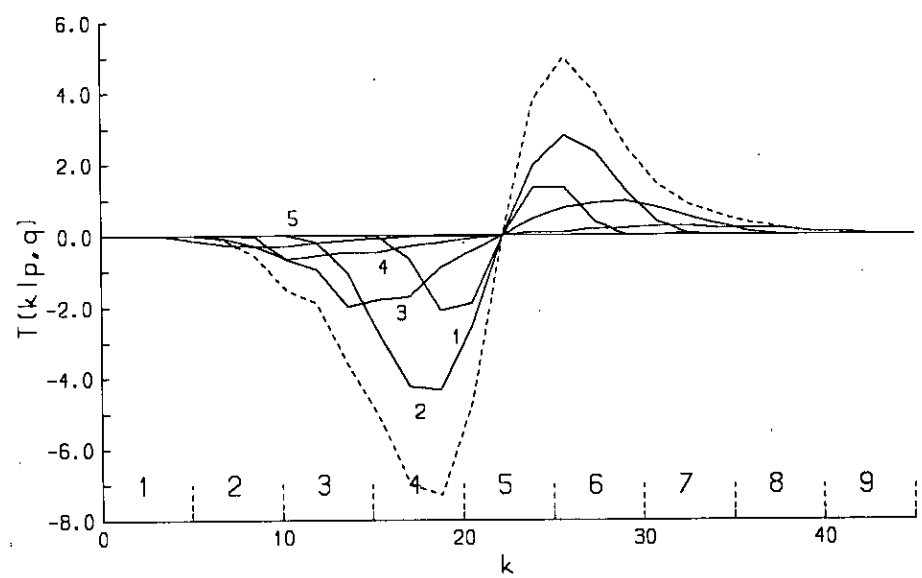

Figure 4.9: Domaradzki and Rogallo's direct numerical simulation: decomposition of $P(k|p)$ (----------) into $T(k|p,q)$ for p in band 5 ($20 < p < 25$), q in bands $1,\ldots,13$. The boundaries of the bands are shown by the vertical dashed lines and the curves are labelled with the relevant q band.

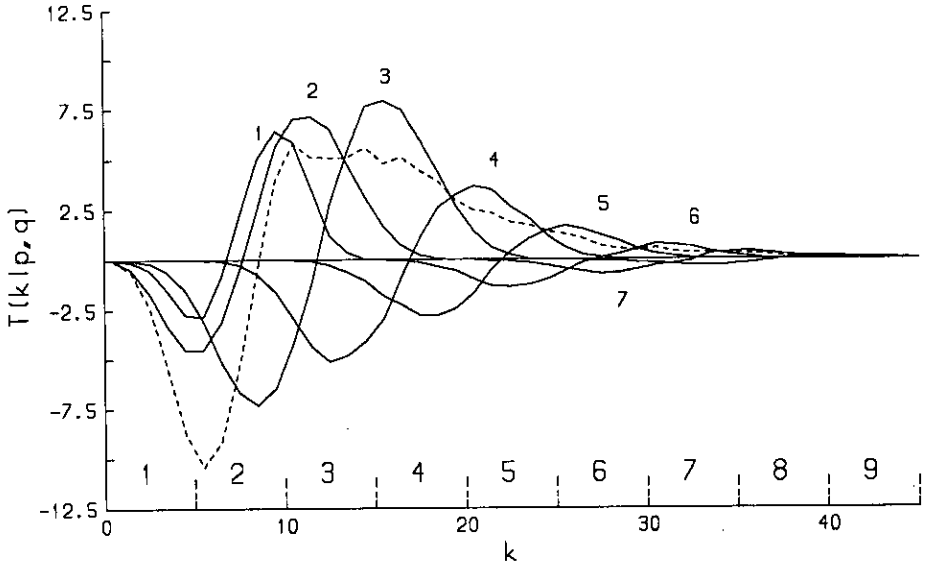

Figure 4.10: LET calculation: decomposition of $P(k|p)$ (----------) into $T(k|p,q)$ for p in band 2 ($5 < p < 10$), q in bands $1,\ldots,13$. The boundaries of the bands are shown by the vertical dashed lines and the curves are labelled with the relevant q band.

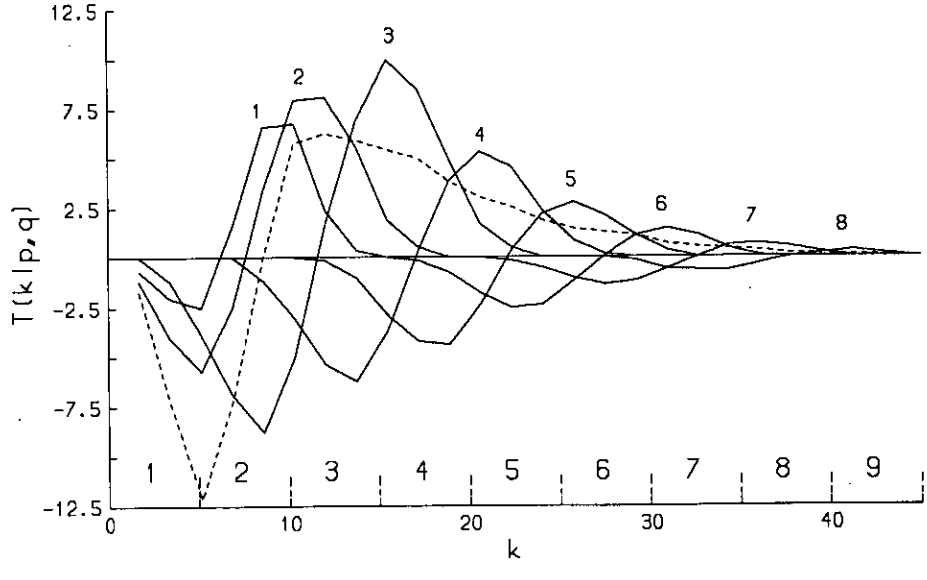

Figure 4.11: Domaradzki and Rogallo's direct numerical simulation: decomposition of $P(k|p)$ (----------) into $T(k|p,q)$ for p in band 2 ($5 < p < 10$), q in bands $1,\ldots,13$. The boundaries of the bands are shown by the vertical dashed lines and the curves are labelled with the relevant q band.

Chapter 5

Conclusion

This thesis has addressed three aspects of the LET theory

1. LET has been extended to treat passive scalar transport and is found to give consistent results, in fair to good agreement with experiment, at a range of Reynolds numbers and Prandtl numbers.

2. The 'fundamental' argument against Eulerian renormalised perturbation theories (including LET), that they are not invariant under a Random Galilean Transformation, has been countered by an analysis of the concept of a Random Galilean Transformation (RGT). This analysis shows that an RGT is not a physical symmetry operation, like the 'deterministic' Galilean transformation, but is a new choice of the ensemble of flows which defines the averaging operation and this new choice of ensemble is not suitable for developing a perturbation theory (for instance, transformed zero order velocity fields are no longer Gaussian). Therefore Eulerian renormalised perturbation theories should be re-examined.

3. Finally, the detailed energy dynamics of LET follow those of the Navier-Stokes equations very closely (at least at low Reynolds number), indicating that LET is a very good approximation for turbulent flows.

Bibliography

[1] Antonia, R.A. and van Atta, C.W. *J. Fluid Mech.* **84**, 561 (1978)

[2] Antonia, R.A. and Chambers, A.J. *Boundary Layer Met.* **18**, 399 (1980)

[3] Antonopoulos-Domis, M. *J. Fluid Mech.* **104**, 55 (1981)

[4] Batchelor, G.K. *J. Fluid Mech.* **5**, 113 (1959)

[5] Batchelor, G.K. *An introduction to fluid dynamics.* CUP, Cambridge. (1967)

[6] Batchelor, G.K., Howells, I.D. and Townsend, A.A. *J. Fluid Mech.* **5**, 134 (1959)

[7] Boston, N.E.J. and Burling, R.W. *J. Fluid Mech.* **55**, 473 (1972)

[8] Champagne, F.H., Friehe, C.A. and LaRue, J.C. *J. Atm. Sci.* **34**, 515 (1977)

[9] Domaradzki, J.A. *Private communication* (1991)

[10] Domaradzki, J.A. and Rogallo, R.S. *Phys. Fluids A,* **2**, 413 (1990)

[11] Eswaran, V. and Pope, S.B. *Phys. Fluids* **31**, 506 (1988)

[12] Gibson, C.H. *Phys. Fluids* **11**, 2316 (1968)

[13] Gibson, C.H. and Schwarz, W.H. *J. Fluid Mech.* **16**, 365 (1963)

[14] Gibson, C.H., Stegen, G.R. and Williams, R.B. *J. Fluid Mech.* **41**, 153 (1970)

[15] Grant, H.L., Hughes, B.A., Vogel, W.M. and Moilliet, A. *J. Fluid Mech.* **34**, 423 (1968)

[16] Grant, H.L., Stewart, R.W. and Moilliet, A. *J. Fluid Mech.* **12**, 241 (1962)

[17] Herring, J.R. and Kraichnan, R.H. *in Lecture Notes in Physics, Volume 12, 'Statistical models and turbulence'*, Springer (1972)

[18] Herring, J.R. and Kerr, R.M. *J. Fluid Mech.* **118**, 205 (1982)

[19] Herring, J.R., Schertzer, D., Lesieur, M., Newman, G.R., Chollet, J.P. and Larcheveque, M. *J. Fluid Mech.* **124**, 411 (1982)

[20] Hill, R.J. *J. Fluid Mech.* **88**, 541, (1978)

[21] Hinze, J.O. *Turbulence (Second edition).* McGraw-Hill, New York. (1975)

[22] Kaneda, Y. *Phys. Fluids* **29**, 701 (1986)

[23] Kerr, R.M. *NASA Technical Memo* **84407** (1983)

[24] Kerr, R.M. *J. Fluid Mech.* **153**, 31 (1985)

[25] Kerr, R.M. *J. Fluid Mech.* **211**, 309 (1990)

[26] Kerr, R.M. *Private communication* (1991)

[27] Kraichnan, R.H. *J. Fluid Mech.* **5**, 497 (1959)

[28] Kraichnan, R.H. *Phys. Fluids* **7**, 1030 (1964)

[29] Kraichnan, R.H. *Phys. Fluids* **7**, 1048 (1964)

[30] Kraichnan, R.H. *Phys. Fluids* **7**, 1723 (1964)

[31] Kraichnan, R.H. *Phys. Fluids* **8**, 575 (1965)

[32] Kraichnan, R.H. *Phys. Fluids* **11**, 945 (1968)

[33] Kraichnan, R.H. *Phys. Fluids* **9**, 1937 (1966)

[34] Kraichnan, R.H. and Herring, J.R. *J. Fluid Mech.* **88**, 355 (1978)

[35] Larcheveque, M., Chollet, J.P., Herring, J.R., Newman, G.R. and Schertzer, D. *Turbulent Shear Flows 2*, ed. Bradbury, L.J.S. Springer, Heidelberg (1980)

[36] Lee, J. *Phys. Fluids* **8**, 1647 (1965)

[37] Lee, L.L. *Ann. Phys (New York)* **32**, 292 (1965)

[38] Lesieur, M., Montmory, C. and Chollet, J-P. *Phys. Fluids* **30**, 1278 (1987)

[39] Leslie, D.C. *Developments in the theory of turbulence.* Clarendon Press, Oxford (1973)

[40] Lin, S.C. and Lin, S.C. *Phys. Fluids* **16**, 1587, (1977)

[41] Ling, S.C. and Huang, T.T. *Phys. Fluids* **13**, 2912 (1970)

[42] McComb, W.D. *J. Phys. A: Math. Gen.* **9**, 179 (1978)

[43] McComb, W.D. *The physics of fluid turbulence.* Clarendon Press, Oxford. (1990)

[44] McComb, W.D., Filipiak, M.J. and Shanmugasundaram, V. *Submitted to J. Fluid Mech.* (1991)

[45] McComb, W.D. and Shanmugasundaram, V. *J. Fluid Mech.* **143**, 95 (1984)

[46] McComb, W.D., Shanmugasundaram, V. and Hutchinson, P. *J. Fluid Mech.* **208**, 91 (1989)

[47] Moeng, C-H. and Wyngaard, J.C. *J. Atm. Sci.* **45**, 3573, (1988)

[48] Newman, G.R. and Herring, J.R. *J. Fluid Mech.* **94**, 163 (1979)

[49] Newman, G.R., Launder, B.E. and Lumley, J.L. *J. Fluid Mech.* **111**, 217 (1981)

[50] Pao, Y-H. *Phys. Fluids* **8**, 1063 (1965)

[51] Paquin, J.E. and Pond, S. *J. Fluid Mech.* **50**, 257 (1971)

[52] Roberts, P.H. *J. Fluid Mech.* **11**, 257 (1961)

[53] Sepri, P. *Phys. Fluids* **19**, 1876 (1976)

[54] Shanmugasundaram, V. *Private communications.* (1990,1991)

[55] Shanmugasundaram, V. *Internal report*, ISAS, Tokyo (1991)

[56] Shirani, E., Ferziger, J.H. and Reynolds, W.C. *Dept. of Mech. Eng., Stanford University, Report No. TF-15.* (1981)

[57] Sreenivasan, K.R., Tavoularis, S., Henry, R. and Corrsin, S. *J. Fluid Mech.* **100**, 597 (1980)

[58] Warhaft, Z. and Lumley, J.L. *J. Fluid Mech.* **88**, 659 (1978)

[59] Williams, R.M. and Paulson, C.A. *J. Fluid Mech.* **83**, 547 (1977)

[60] Wyld, H.W. *Ann. Phys. (New York)* **14**, 143 (1961)

[61] Yeh, T.T. and van Atta, C.W. *J. Fluid Mech.* **58**, 233 (1973)